Acta Biomaterialia 9 (2013) 4457–4486

Contents lists available at SciVerse ScienceDirect

Acta Biomaterialia

journal homepage: www.elsevier.com/locate/actabiomat

Review

Review of bioactive glass: From Hench to hybrids

Julian R. Jones *

Department of Materials, Imperial College London, South Kensington Campus, London SW7 2AZ, UK

ARTICLE INFO

Article history:
Received 20 May 2012
Received in revised form 10 August 2012
Accepted 14 August 2012
Available online 21 August 2012

Keywords:
Bioactive glass
Bioglass
Bioactive scaffolds
Hybrids
Synthetic bone grafts

ABSTRACT

Bioactive glasses are reported to be able to stimulate more bone regeneration than other bioactive ceramics but they lag behind other bioactive ceramics in terms of commercial success. Bioactive glass has not yet reached its potential but research activity is growing. This paper reviews the current state of the art, starting with current products and moving onto recent developments. Larry Hench's 45S5 Bioglass® was the first artificial material that was found to form a chemical bond with bone, launching the field of bioactive ceramics. In vivo studies have shown that bioactive glasses bond with bone more rapidly than other bioceramics, and in vitro studies indicate that their osteogenic properties are due to their dissolution products stimulating osteoprogenitor cells at the genetic level. However, calcium phosphates such as tricalcium phosphate and synthetic hydroxyapatite are more widely used in the clinic. Some of the reasons are commercial, but others are due to the scientific limitations of the original Bioglass 45S5. An example is that it is difficult to produce porous bioactive glass templates (scaffolds) for bone regeneration from Bioglass 45S5 because it crystallizes during sintering. Recently, this has been overcome by understanding how the glass composition can be tailored to prevent crystallization. The sintering problems can also be avoided by synthesizing sol–gel glass, where the silica network is assembled at room temperature. Process developments in foaming, solid freeform fabrication and nanofibre spinning have now allowed the production of porous bioactive glass scaffolds from both melt- and sol–gel-derived glasses. An ideal scaffold for bone regeneration would share load with bone. Bioceramics cannot do this when the bone defect is subjected to cyclic loads, as they are brittle. To overcome this, bioactive glass polymer hybrids are being synthesized that have the potential to be tough, with congruent degradation of the bioactive inorganic and the polymer components. Key to this is creating nanoscale interpenetrating networks, the organic and inorganic components of which have covalent coupling between them, which involves careful control of the chemistry of the sol–gel process. Bioactive nanoparticles can also now be synthesized and their fate tracked as they are internalized in cells. This paper reviews the main developments in the field of bioactive glass and its variants, covering the importance of control of hierarchical structure, synthesis, processing and cellular response in the quest for new regenerative synthetic bone grafts. The paper takes the reader from Hench's Bioglass 45S5 to new hybrid materials that have tailorable mechanical properties and degradation rates.

1. Introduction and scope

Many of the best inventions have been made by accident. That was not quite the case for bioactive glass, but it was nonetheless a curious set of events. The first bioactive glass was invented by Larry Hench at the University of Florida in 1969. Professor Hench began his work on finding a material that could bond to bone following a bus ride conversation with a US Army colonel. The colonel, having just returned from the Vietnam war, asked him if materials could be developed that could survive the aggressive environment of the human body. The problem was that all implant materials available at the time, e.g. metals and polymers that were designed to be bioinert, triggered fibrous encapsulation after implantation, rather than forming a stable interface or bond with tissues. Professor Hench decided to make a degradable glass in the Na_2O–CaO–SiO_2–P_2O_5 system, high in calcium content and with a composition close to a ternary eutectic in the Na_2O–CaO–SiO_2 diagram [1]. The main discovery was that a glass of the composition 46.1 mol.% SiO_2, 24.4 mol.% Na_2O, 26.9 mol.% CaO and 2.6 mol.% P_2O_5, later termed 45S5 and Bioglass®, formed a bond with bone so strong that it could not be removed without breaking the bone [2]. This launched the field of bioactive ceramics, with many new materials and products being formed from variations on bioactive glasses [1] and also glass–ceramics [3] and ceramics such as synthetic hydroxyapatite (HA) and other calcium phosphates [4]. Herein, a bioactive material is defined as a material

* Tel.: +44 2075946749.
E-mail address: julian.r.jones@imperial.ac.uk

1742-7061/$ - see front matter © 2012 Acta Materialia Inc. Published by Elsevier Ltd. All rights reserved.
http://dx.doi.org/10.1016/j.actbio.2012.08.023

that stimulates a beneficial response from the body, particularly bonding to host tissue (usually bone). The term "bioceramic" is a general term used to cover glasses, glass–ceramics and ceramics that are used as implant materials. The name "Bioglass®" was trademarked by the University of Florida as a name for the original 45S5 composition. It should therefore only be used in reference to the 45S5 composition and not as a general term for bioactive glasses.

Bioglass 45S5 bonds with bone rapidly and also stimulates bone growth away from the bone–implant interface. The mechanism for bone bonding is attributed to a hydroxycarbonate apatite (HCA) layer on the surface of the glass, following initial glass dissolution [2]. HCA is similar to bone mineral and is thought to interact with collagen fibrils to integrate (bond) with the host bone. Section 6.1 describes the mechanism of HCA formation. The osteogenic properties (often termed osteoinduction) of the glass are thought to be due to the dissolution products of the glass, i.e. soluble silica and calcium ions, that stimulate osteogenic cells to produce bone matrix [5]. Section 6.2 provides more detail.

There are now several types of bioactive glass: the conventional silicates, such as Bioglass 45S5; phosphate-based glasses; and borate-based glasses. Recently, interest has increased in borate glasses [6], largely due to very encouraging clinical results of healing of chronic wounds, such as diabetic ulcers, that would not heal under conventional treatment [7]. The soft tissue response may be due to their fast dissolution, which is more rapid than that for silica-based glasses. The benefits of phosphate glasses are also likely to be related to their very rapid solubility rather than bioactivity [8]. This review will focus on silicates made by both the conventional melt-quenching route, and on glasses and hybrids made by the low-temperature chemistry-based sol–gel process.

Surprisingly, after 40 years of research on bioactive glasses by numerous research groups, no other bioactive glass composition has been found to have better biological properties than the original Bioglass 45S5 composition. While reviewing the literature on bioactive glasses, this paper will explain the reasons why. Answers to the question of why calcium phosphates are the market leaders for artificial bone graft materials will also be sought, considering the apparent potential benefits of Bioglass 45S5 over synthetic HA and other calcium phosphates. The paper will explain why the original Bioglass 45S5 is so difficult to process into fibres, scaffolds and coatings, and why it has not been such a commercial success as perhaps it should have been. It will then review the recent developments in bioactive glasses and processing methods, such as: the first amorphous bioactive glass scaffolds with pore sizes suitable for bone regeneration; bioactive glass nanoparticles and nanofibres; and bioactive inorganic–organic hybrids that impart toughness to bioactive glasses while maintaining their bioactive properties. The paper focuses on the most recent developments.

2. Synthetic bone grafts, scaffolds and bone regeneration

The most important applications for bioactive bioceramics is the healing of bone defects, which can arise due to trauma, congenital defects or disease, e.g. osteoporosis or tumour removal. Another common procedure is spinal fusion, where the cartilage intervertebral disc has badly herniated (slipped disc). The disc is replaced with a titanium or poly(ether ether ketone) (PEEK) cage filled with bone graft. The bone grows through the cage and bone, fusing the vertebrae. Currently, autografts are favoured by surgeons for defect repair and spinal fusion. Autografting involves transplanting bone from another part of the patient, usually the pelvis, to the defect site [9]. Bone is one of the most commonly transplanted tissues, second only to blood. The disadvantages of autografts are that the bone is limited in supply, and a large proportion of patients suffer severe pain at the donor site. A synthetic alternative is needed for the one million bone graft operations that are carried out worldwide each year. When not enough autograft is available, granules of a bone graft extender material, usually a calcium phosphate, are mixed with the autograft. Surgeons tend to mix graft granules with blood from the patient to create a putty-like material, which is pressed into the defect. The blood improves handling of the material and the hope is that the natural growth factors and cells that it contains will help bone repair.

The concept of bone regeneration is to use a scaffold that can act as a three-dimensional (3-D) temporary template to guide bone repair. Ideally the scaffold will stimulate the natural regenerative mechanisms of the human body. The scaffold must therefore recruit cells, such as bone marrow stem cells, and stimulate them to form new bone. Blood vessels must also penetrate if the new bone is to survive. Over time, the scaffold should degrade, leaving the bone to remodel naturally. Another way to look at it is that a scaffold that mimics autograft cancellous bone is needed. Fig. 1 shows a photograph of a femur with a piece of bone removed and an X-ray microtomography (μCT) image of the removed cancellous bone. From a materials science perspective, bone is a nanocomposite of collagen and bone mineral, with a hierarchical structure. Cancellous bone has an open interconnected porous network with pores in excess of 500 μm and large interconnects between the pores (Fig. 1, inset).

From an engineer's standpoint, an ideal scaffold would be a bioactive and tough material that could be made into an open porous structure similar to cancellous bone. However, a surgeon's list of criteria does not always match that of an engineer. Surgeons would like a porous material that matches the mechanical properties of cortical bone, that can be cut to shape in theatre, and that can either be pressed into a bone defect, such that it then expands to fill the defect, or be injected into the defect (Fig. 2).

An ideal future application would be the development of an osteochondral implant that could bond to bone and regenerate cartilage, reducing the number of total joint replacement operations that are needed. Currently, more than 600,000 hip and a million knee replacements are performed annually worldwide. Although a total joint replacement involves replacement of cartilage and bone, it is usually damage to the articular cartilage that is the source of the problem, but pain is only felt when damage to the bone occurs. An osteochondral device that can regenerate cartilage while anchoring into and regenerating the underlying bone is a massive challenge [10].

3. Bioactive glass products and clinical trials

The original Bioglass 45S5 has been used in more than a million patients to repair bone defects in the jaw and in orthopaedics [11]. Used in this way, it dissolves and stimulates natural bone repair (bone regeneration). Considering its potential, age and properties, perhaps this figure is lower than it should be, and bioactive glass has not reached its full potential it terms of bone regeneration. Its major commercial success is as an active repair agent in toothpaste, under the name NovaMin® (GlaxoSmithKline, UK). Clinical studies show that the dentifrice can mineralize tiny holes in dentine, reducing tooth sensitivity (Section 3.3).

3.1. Monolithic medical devices

Hearing was restored to a previously deaf patient using the first Bioglass 45S5 clinical product in 1984 [12]. The patient was deaf from an infection that caused degradation of two of the three bones of her middle ear. The implant was designed to replace the

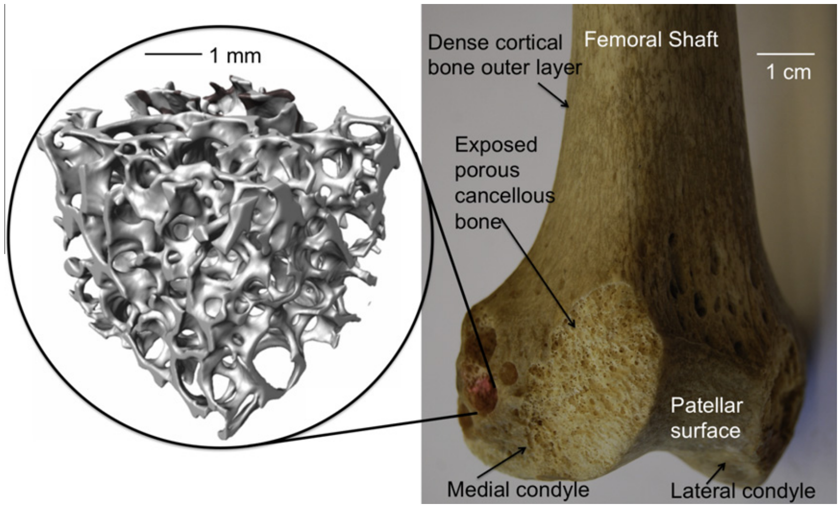

Fig. 1. Photograph of a human femur with a core-drilled piece removed. Inset: X-ray microtomography (μCT) image of the cancellous bone removed from the femur proximal to the knee joint.

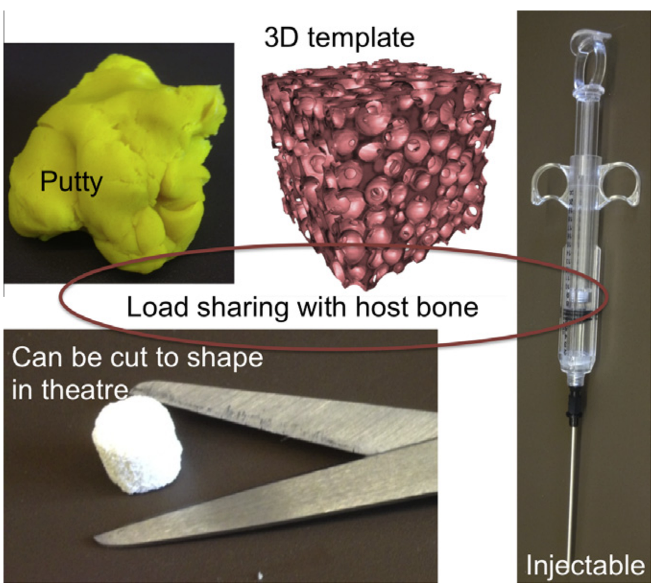

Fig. 2. An illustration of the design criteria of a synthetic bone graft from the point of view of orthopaedic surgeons.

bones and to transmit sound from the eardrum to the cochlea, restoring hearing. Previous materials used for this indication were metals and plastics, selected because they were inert in the body. However, they failed because fibrous tissue formed around them after implantation. The Bioglass 45S5 middle ear prosthesis (MEP®) was cast into shape from the melt. Early prototypes were cast to shape to fit each patient's indication. After 10-year follow-up studies, four out of 21 had failed due to fracture, but the others retained function, improving on polymeric, metallic and ceramic implants [12]. The four that failed were all the same shape. Custom design of each implant was not commercially viable, so the device was remodelled to cone shapes of three sizes (Douek-MED™) for optimal mechanical properties.

The second commercial Bioglass 45S5 device was the Endosseous Ridge Maintenance Implant (ERMI®) in 1988, which was also a simple cone of Bioglass 45S5. The devices were inserted into fresh tooth extraction sites to repair tooth roots and to provide a stable ridge for dentures. They proved to be extremely stable, and a 5-year study quantified improvements over HA tooth root implants [13].

None of these products is in widespread clinical use, as surgeons needed to be able to cut the implant to shape rather than be limited to cones of fixed size, which prevented commercial success. Monolithic Bioglass 45S5 is more suited to implants that are custom made for the patient's need. Thompson et al. performed clinical trials on 30 trauma patients with orbital floors that were so badly damaged that their vision was blurred. Traditional methods of repair (e.g. autograft) failed and patients were likely to become blind due to kinking of the optical nerve [14]. Using computed axial tomography (CAT) scans of the defect site, a rapid prototyping (or "additive manufacturing") machine was used to produce moulds for casting the Bioglass 45S5 implants, which were then sutured into place (Fig. 3). At 5-year follow-up, patients regained full movement of their eyes; their vision was no longer blurred and the cosmetic appearance of the face was much improved. Separate similar studies were carried out with glasses of the S53P4 (53.8 mol.% SiO_2, 21.8 mol.% CaO, 22.7 mol.% Na_2O, 1.7 mol.% P_2O_5) composition, except that implants were supplied with three sizes of 1 mm thick, round, heart- or kidney-shaped plates [15]. The glass implants were successful, and performed as well as the more traditional procedure of cartilage harvested from the patient's ear. This may not be a business model for commercial success, but results so far suggest that the technique is helping patients. Products that are in commercial use internationally are those based on particles rather than monolithic shapes.

3.2. Bioactive glass particulates for bone regeneration

Orthopaedic surgeons and dentists often like to use particles or granules (granules are large particles), as they can be pressed easily into a defect. The first particulate Bioglass 45S5 product was PerioGlas® (now sold by NovaBone Products LLC, Alachua, FL), which was released in 1993 as a synthetic bone graft for repair of defects in the jaw that result from periodontal disease. It is now sold in over 35 countries. PerioGlas has a particle size range of 90–710 μm and can be used to regenerate bone around the root of a healthy tooth to save the tooth, or can be used to repair bone in the jaw so that the quality of bone becomes sufficient for anchoring titanium implants.

Early success was supported by in vivo studies [16–18] and clinical studies [19–31], which all showed that defects treated with

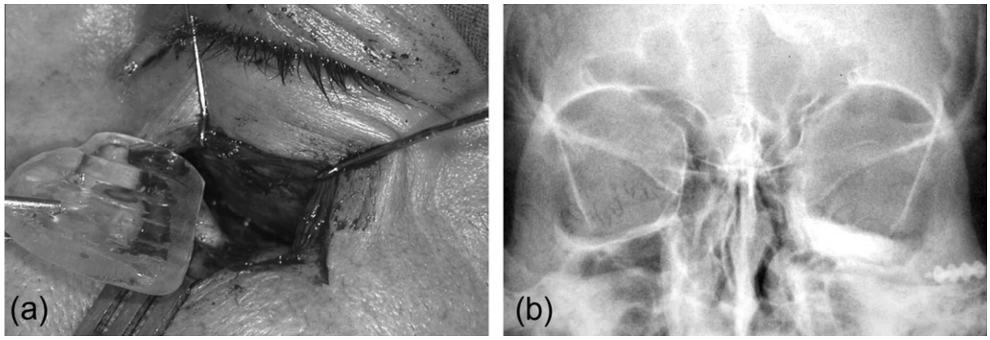

Fig. 3. Using cast bioactive glass monoliths for repair of orbital floors. (a) Inserting the glass implant beneath the eye. (b) Post-operative X-ray, showing that the bioactive glass implant has repaired the orbital floor and the eyes are now the same height. Modified from Thompson et al. [14].

PerioGlas were ~70% filled with new bone compared to ~35% for controls. For infra-bony defects, which are between the roots of molars, clinical trials showed that its regenerative properties were further enhanced with low-level laser therapy post-operatively [32]. The product has also been used with polymeric membranes, termed "guided tissue regeneration" [33]. Bioactive glass slurry can also be used as a root canal sterilization tool, prior to insertion of implants. Conventionally, calcium hydroxide is used to raise pH to bactericidal levels, but a Bioglass 45S5 slurry is a possible alternative, as fine particles in high concentration can trigger high pH in addition to its bioactive properties [34].

Owing to the success of bioactive glass particles in dental bone regeneration, a particulate for orthopaedic bone grafting of non-load-bearing sites was released in 1999, named NovaBone (NovaBone Products LLC). Surgeons usually mix it with blood from the defect site and work it into a putty-like consistency as the blood starts to clot, before pushing it into the defect. The particles have a similar distribution to PerioGlas (90–710 μm), so packing of the particles in the defect is random. Gaps between the particles are thought to increase the rate of bone ingrowth. Fig. 4 shows the NovaBone packaging with a scanning electron micrography (SEM) image of the particles.

NovaBone was compared to autograft in posterior spinal fusion operations for treatment of adolescent idiopathic scoliosis (curvature of the spine). In a group of 88 patients, 40 received iliac crest autograft and 48 received NovaBone. The NovaBone (15 cm^3) was mixed with the patient's blood and secured in place by compressing the neighbouring vertebrae with metal screws and hooks [35]. The NovaBone performed as well as autograft over the follow-up period of 4 years but with fewer infections (2% vs. 5%) and fewer mechanical failures (2% vs. 7.5%) and with the main benefit that a donor site was not needed with NovaBone.

The Bioglass 45S5 is not the only product on the market. Biogran® (BIOMET 3i, Palm Beach Gardens, FL) is another synthetic bone graft used in jaw bone defect regeneration. It has the Bioglass 45S5 composition, but with a narrower (300–360 μm) particle size range. The significant bioactive glass research programme in Finland led to the commercialization of particulates of the S53P4 composition, now known as BonAlive® (BonAlive Biomaterials, Turku, Finland). BonAlive received European approval for orthopaedic use as a bone graft substitute in 2006.

While the mandible (lower jaw) consists mainly of compact cortical bone that can be easily grafted, the maxilla (upper jaw) consists of porous cancellous bone that resorbs rapidly in periodontitis and is therefore more difficult to graft. Treatment is usually maxillary sinus floor lifting, where bone grows partially into the sinus cavity. Implantation of a mixture of BonAlive granules with autologous bone allowed the implantation of titanium roots in the porous maxilla and showed more rapid bone repair with thicker trabeculae compared to autograft alone [36].

Sinus obliteration is a procedure that eliminates the frontal sinuses in order to prevent chronic infection or in response to trauma or tumour removal. Traditionally, the defect is filled with fat, but this leads to up to 25% of patients experiencing complications. Trials with S53P4 and 13–93 (54.6 mol.% SiO_2, 22.1 mol.% CaO, 6.0 mol.% Na_2O, 1.7 mol.% P_2O_5, 7.9 mol.% K_2O, 7.7 mol.% MgO) glass particles (0.5–1 mm size range) showed improved bone repair, in terms of quantity and quality, compared to synthetic HA [37]. Bone growth was also faster for BonAlive than for 13–93, which is likely to be due to the magnesium content of the glass reducing the bioactivity of 13–93 (Section 8.1).

Clinical trials for cases of severe spondylolisthesis (displacement of the vertebral column) used BonAlive granules of 1–2 mm. The glass (20–40 g, depending on the amount needed) and autograft

Fig. 4. NovaBone® packaging, with an SEM image of the particles. Scale bar is 200 μm.

were implanted in the same site in each patient. The implants were held in position between vertebrae by compression of the vertebrae assisted by a metal screw system (Fig. 5). After 11 years, the fusion rate for the glass was 88% compared to 100% for autograft [38]. Similar results were seen for treatment of osteomyelitis, where the bone quality of the vertebrae is reduced due to bacterial infection [39]. BonAlive was also compared to autograft in the same patient in spondylodesis procedures for treatment of spine burst fractures. At 10 years follow-up, five out of 10 implants had full fusion compared to all 10 autografts [40].

The same glass, in the form of particles (0.83–3.15 mm), was compared to autograft in procedures used to treat trauma-induced tibial fractures that also caused compression of subchondral cancellous bone [41]. Surgery was required to restore joint alignment. The grafts were placed inside the subchondral bone defects and were supported by metal condylar plates and casts. Full weight-bearing was allowed when radiographs indicated that healing had occurred, so the implants were loaded. 11-year follow-up showed similar bone regeneration and no difference in articular depression. Some glass particles were still present, even at 11 years post-operation [42]. The lack of resorption of S53P4 may be due to glass composition, which has higher silica content than 45S5. Section 7 explains the relationship between composition, atomic structure and bioactivity.

Glass granules (1–4 mm) were also observed after 14 years when BonAlive was used in trials for repairing bone defects (1–30 cm^3) left by benign bone-tumour surgery in hands, tibia and humerus [43]. The cortical bone was twice as thick as it was when autograft was used. In shorter-term studies, the glass was observed to begin to decrease in size (degrade) between 12 and 36 months, and this stimulated remodelling of the bone [44]. However, remodelling was slower than it was for autograft (12 months) and the glass particles were still present at 3-year follow-up [45]. BonAlive has also been used successfully in trials for filling cavities in the middle ear created by surgeons removing mastoid air cells and mucous membranes that were damaged by chronic infection [46].

There seems to be more clinical data available for BonAlive (S53P4) than for Bioglass 45S5, at least in journal articles. Its clinical results are good, but its degradation rate may be slower than ideal. A disadvantage of Bioglass 45S5 and BonAlive over other bioceramics, as synthetic regenerative bone grafts, is that they cannot be made into amorphous bioactive glass scaffolds because they crystallize during sintering. Section 8 discusses the new developments in porous glasses, but these have not yet reached clinical trials. However, the particulates have found commercial success in the consumer dental market.

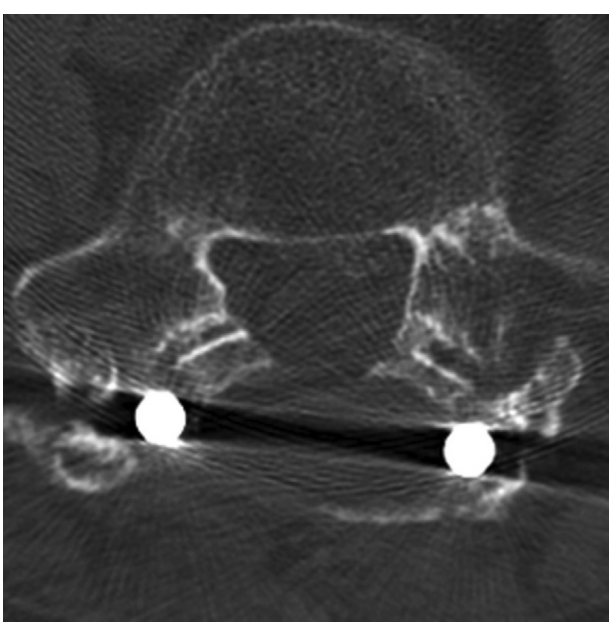

Fig. 5. X-ray image showing the position of S53P4 glass rods compressed between vertebrae in 11-year follow-up clinical trials. Courtesy of Dr. Janek Frantzén, Turku University Hospital.

3.3. Oral care for treatment of hypersensitivity

Since 2004, a very fine Bioglass 45S5 particulate called NovaMin® (NovaMin Technology, FL; now owned by GlaxoSmithKline, UK), with a particle size (D_{50} value) of ~18 μm is used in toothpaste for treating tooth hypersensitivity, which affects up to 35% of people. NovaMin was first available in the USA in fluoride-free toothpastes, but the technology was acquired by GlaxoSmithKline in 2010. This has led to a NovaMin- and fluoride-containing toothpaste being made available in more than 20 countries (Fig. 6a). The common abrasive additive in toothpaste is alumina particles, which can be replaced by Bioglass 45S5. Tooth hypersensitivity occurs when dentine becomes exposed around the gum line. The dentine contains tubules that link to the pulp chamber, which contains nerve endings. Change in fluid flow (hydraulic conductance) through the tubules, e.g. volume of fluid, ion concentration or temperature, can cause pain. Traditional speciality toothpastes contain chemicals (e.g. potassium nitrate) that temporarily anaesthetize the nerves and prevent pain. Clinical studies show that the Bioglass 45S5 particles adhere to the dentine and form an HCA layer that is similar in composition to tooth enamel and blocks the tubules, which are ~1 μm in diameter, relieving the pain for longer periods [47]. A randomized, double-blind clinical trial of 100 volunteers found 58.8% reduction in gingival bleeding and 16.4% reduction in plaque growth for those who brushed twice daily with a NovaMin-containing toothpaste (5 wt.% glass, no fluoride) over the 6-week period, with no change in those using control toothpaste [48]. Another trial (more than 100 participants) showed improved pain relief when brushing with a NovaMin-containing toothpaste compared to that achieved with a toothpaste containing potassium nitrate (a conventional anaesthetic additive in toothpastes). The improvement was significant at 2 and 6 weeks of brushing using cold air and cold water as measures of sensitivity [49].

In vitro trials showed that the Bioglass 45S5 particles seem to attach to the dentine [50]. This may explain how the particles stimulate long-term repair even though brushing may only be for a few minutes a day. Fig. 6b shows the fine NovaMin particles. In preparation for in vitro trials, human dentine is lightly etched to remove the smearing of the surface caused by machining. This process is necessary to reveal the tubules. Fig. 6c shows the NovaMin immediately after it was brushed onto the dentine. The particles attach and within 24 h the surface was almost completely covered by an HCA layer (Fig. 6c and d). This indicates that NovaMin seems to work by stimulating mineralization (calcium phosphate deposition over the dentine tubules). It is likely that the glass dissolution products stimulate the mineralization. HCA deposition is promoted by a pH rise, and dissolution of the glass in the mouth would also cause a pH rise. Saliva naturally contains mineralization inhibitors, so a burst of calcium and phosphate from the glass and a pH rise may enhance mineralization.

The success of NovaMin has led to trials with sol–gel-derived bioactive particles (<30 μm). Toothpaste containing the sol–gel particles reduced hydraulic conductance compared to a toothpaste containing bioinert silica [51]. The trials also showed that the tubules remained occluded after 24 h and after washing with cola, juice, coffee and further brushing, which was attributed to the glass particles bonding to the dentine [51]. In vitro trials also

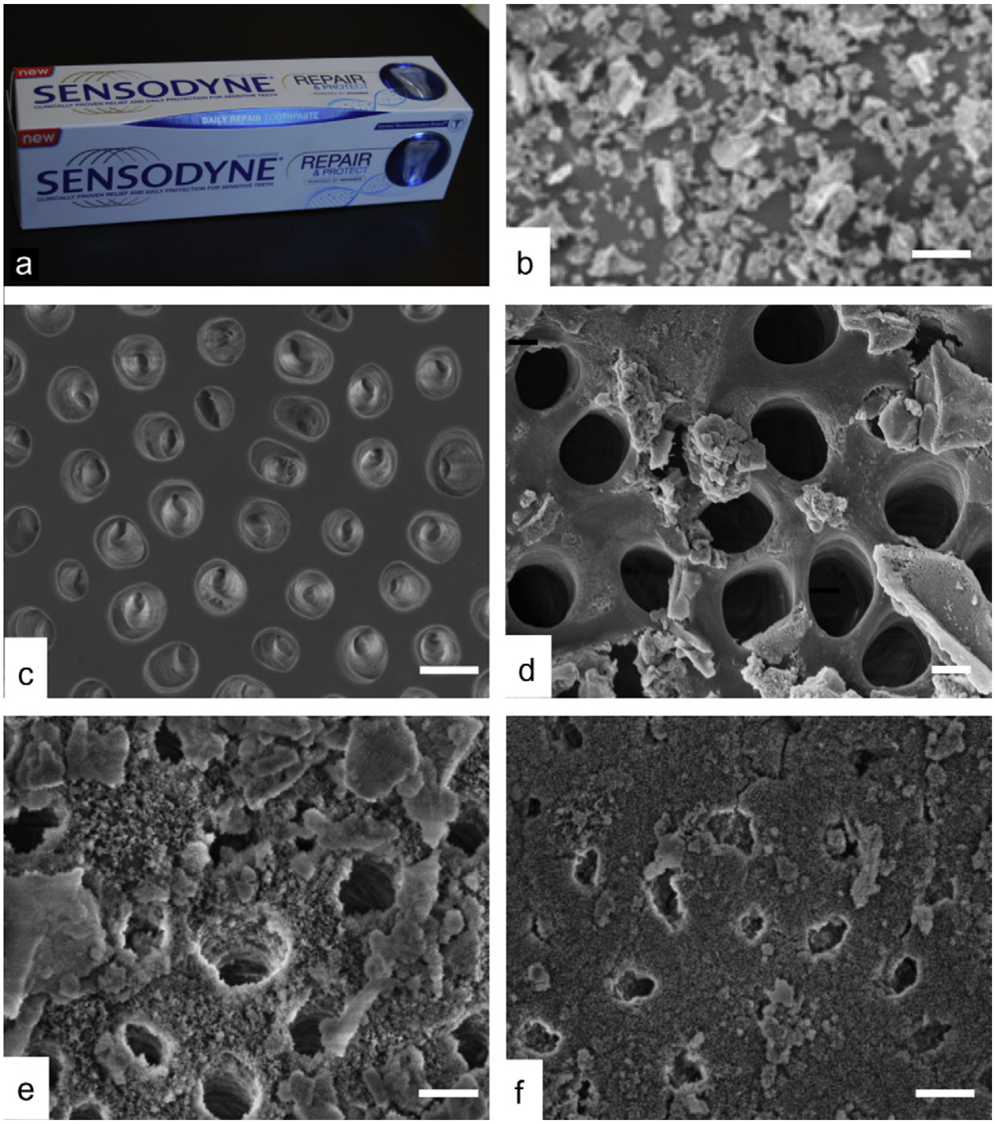

Fig. 6. (a) Photograph of Sensodyne Repair and Protect toothpaste, which contains NovaMin®, a fine particulate of Bioglass 45S5®. (b) SEM image of NovaMin particles (bar = 20 μm). (c–f) SEM micrographs of human dentine (bar = 1 μm): (c) untreated, (d) immediately after application of NovaMin in artificial saliva (AS); (e) 24 h after application of NovaMin in AS; (f) 5 days after application. SEM images modified from Earl et al. [50].

showed that Bioglass 45S5 and sol–gel particles can remineralize acid-etched enamel after 3 min of brushing with aqueous pastes containing 1.0 ml g^{-1} of glass particles (<50 μm in size). The success has led to the development of more complex glass compositions, such as those designed to stimulate the formation of fluoroapatite on the dentine, which is more resistant to acid attack than HCA. An example composition that incorporates CaF_2 in the composition is 36.41 mol.% SiO_2, 28.28 mol.% Na_2O, 24.74 mol.% CaO, 6.04 mol.% P_2O_5 and 4.53 mol.% CaF_2 [52]. Increasing CaF_2 at the expense of CaO increases glass dissolution [53]. Keeping the phosphate content high (e.g. 6 mol.%) seems to favour fluoroapatite formation rather than fluorite [52,54].

Dental care with Bioglass 45S5 is not limited to toothpaste. Bleaching treatments of teeth, which usually use hydrogen peroxide, can damage enamel by demineralization. In vitro trials indicate that NovaMin can repair the enamel though remineralization to pre-bleaching levels (5 min exposure and brushing) [50]. Dentists often use air polishing to whiten teeth, which is a technique that uses ceramic particles (traditionally sodium bicarbonate) as abrasives to remove stains, but they are reluctant to do the operation on patients suffering from hypersensitivity. Use of Bioglass 45S5 powder in the polishing procedure aims to stimulate mineralization of dentine tubules in a similar mechanism to that of NovaMin-containing toothpaste. Air polishing with Bioglass 45S5 (Sylc, OSspray Ltd, UK) was clinically compared to sodium bicarbonate (Prophy-Jet, Dentsply, UK) [55]. Patients reported that the Bioglass 45S5 polishing resulted in a 44% reduction in tooth sensitivity according to their subjective scoring. Teeth treated with the Bioglass 45S5 were also whiter than those treated with sodium bicarbonate.

3.4. Bioactive glass coatings

Bioactive coatings are important for metallic implants such as hip prostheses and periodontal implants because the metals alone are bioinert, which means they are encapsulated with fibrous tissue after implantation. Bioactive coatings have the potential to improve the stability of implants by bonding them to the host bone; however, the HCA layer forms on bioactive glass as a result of dissolution. Bioactive glasses are by nature biodegradable, and therefore a highly bioactive coating may degrade over time, causing instability of the metallic implant in the long term. Bioactive glass coating applications may therefore be limited. Perhaps the dental field is their best application, e.g. on titanium implants with screw threads. When glass coatings are applied, the thermal expansion coefficient of the glass must match that of the metal to prevent the glass pulling away from the metal during processing [56]. This is a challenge for bioactive glasses, and the thermal expansion coefficient of the original 45S5 composition does not match that of titanium or similar metals. An added problem for Bioglass 45S5 is that it crystallizes on sintering, and sintering is needed for a good coating. In order to match the thermal expansion coefficient of the glass to that of the titanium alloy, glasses in the SiO_2–CaO–MgO–Na_2O–K_2O–P_2O_5 system have been investigated [56–62]. Replacement (substitution) of some of the Na_2O and CaO with K_2O and MgO, respectively, is key to tailoring the thermal expansion coefficient [56]. The role of Mg in the glass network is discussed in Section 8.1. There is a narrow range of glass compositions in this compositional system that produce good coatings and that also form HCA, and multiple layers of different compositions may be needed for optimal dissolution and bone integration [56]. An example is the dip-coating of titanium implants with glass of the 1–98 composition (53 wt.% SiO_2, 6 wt.% Na_2O, 22 wt.% CaO, 11 wt.% K_2O, 5 wt.% MgO, 2 wt.% P_2O_5, 1 wt.% B_2O_3), which were tested in rabbit femurs [63]. More bone grew on the coated implants and in regions 250 μm from the implant compared to non-coated implants. A borosilicate containing small amounts of titania was applied to titanium implants for a clinical trial, and the glass-coated implants behaved as well as HA-coated implants at 12 months. In both these cases, the time points may be too early to assess their long-term success in relation to long-term glass degradation [64].

In summary, bioactive glass particles have been successful in regenerating bone defects, but the compositions that have regulatory approval as particulate synthetic bone grafts are not suitable for making fibres, scaffolds or coatings. New compositions are needed for scaffold production, or sol–gel glasses should be used and taken through regulatory approval (Section 8).

4. Bioactive sol–gel glass

Glass can be made using two processing methods: the traditional melt-quenching route and the sol–gel route. Bioglass 45S5 and other commercial bioactive glasses are made by melt-quenching, where oxides are melted together at high temperatures (above 1300 °C) in a platinum crucible and quenched in a graphite mould (for rods or monoliths) or in water (frit). The sol–gel route essentially forms and assembles nanoparticles of silica at room temperature. It is a chemistry-based synthesis route where a solution containing the compositional precursors undergoes polymer-type reactions at room temperature to form a gel [65]. The gel is a wet inorganic network of covalently bonded silica, which can then be dried and heated, e.g. to 600 °C, to become a glass. Typical bioactive compositions are in the ternary system [66], e.g. 58S (60 mol.% SiO_2, 36 mol.% CaO, 4 mol.% P_2O_5) and 77S (80 mol.% SiO_2, 16 mol.% CaO, 4 mol.% P_2O_5), or binary system [67,68], e.g. 70S30C (70 mol.% SiO_2, 30 mol.% CaO). The physical differences in melt- and sol–gel-derived glasses are that sol–gel glasses tend to have an inherent nanoporosity (*a*) whereas melt-quenched glasses are dense [69]. The nanoporosity can result in improved cellular response due to the nanotopography [70] and a specific surface area two orders of magnitude higher than for similar compositions of melt-derived glass [69]. Sol–gel compositions usually have fewer components than bioactive melt-quenched glasses. This is because the primary role of Na_2O in melt-quenched bioactive glass is to lower the melting point, improving processability. It also increases the solubility of the glass, which is important for bioactivity. The high surface area of sol–gel glasses results in high dissolution rates and, as there is no melting involved, sodium is not required in the composition. Nonetheless, sol–gel glasses have been produced close to the 45S5 composition, e.g. 49.15 mol.% SiO_2, 25.80 mol.% CaO, 23.33 mol.% Na_2O, 1.72 mol.% P_2O_5 [71], although the gels must not be heated above 600 °C if the glasses are to remain amorphous.

The sol–gel process has great versatility: bioactive glasses can be made as nanoporous powders or monoliths or as nanoparticles (Fig. 7) simply by changing the pH of the process [68].

A typical silicate precursor is tetraethyl orthosilicate (TEOS), $Si(OC_2H_5)$, which reacts with water (hydrolysis) under acidic or basic conditions to form a solution (sol) containing nanoparticles (Fig. 8). If synthesis is carried out under basic conditions (Stöber process [72]), spherical bioactive nanoparticles and submicrometre particles can be formed (Fig. 7b and Section 11.1) [73].

More commonly, microparticles, monoliths or foams are produced using acidic catalysis. Under acidic catalysis the primary nanoparticles (diameters ~2 nm) that form in the sol (Fig. 8) coalesce and condensation (polymerization) occurs, forming Si–O–Si bonds. The nanoparticles coarsen, coalesce and bond together, forming a gel network of assembled nanoparticles (Fig. 9) [74]. The gel is wet due to excess water in the reagents and the water and ethanol produced during the condensation reactions. Thermal processing is used to age (continued condensation in sealed conditions), dry and stabilize the gel to produce a nanoporous glass. As the water and alcohol evaporate during drying, they leave behind an interconnected pore network. The pores are the interstices between the coalesced nanoparticles [74] and their size depends on

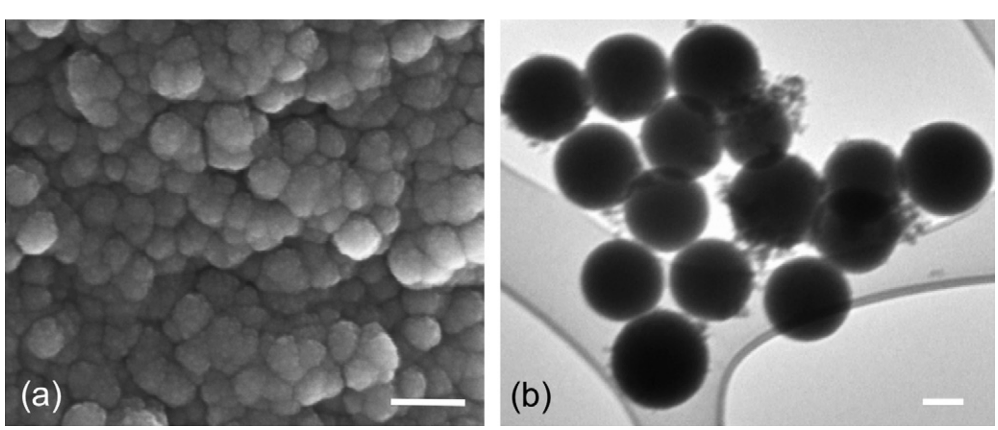

Fig. 7. (a) Scanning electron micrograph of a bioactive sol–gel glass monolith made under acid catalysis (courtesy of Sen Lin). (b) Transmission electron microscope image of bioactive glass nanoparticles (courtesy of Sheyda Labbaf). Bars are 100 nm.

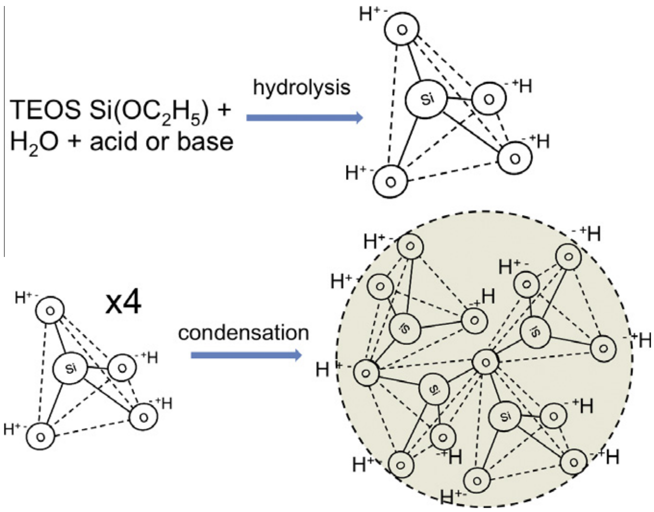

Fig. 8. Schematic of reactions in the sol–gel process: formation of silica tetrahedra and nanoparticles at room temperature.

the precursors used, the glass composition and the pH of the reaction [66,75]. Pore diameters are typically in the range 1–30 nm. The usual method is to heat the dried gel to temperatures above 700 °C to produce a nanoporous bioactive glass. Typical 58S and 70S30C glasses have nanopore sizes of 6–17 nm [69,76], and particles with a size range of 1–32 μm have specific surface areas of 70–130 $m^2\,g^{-1}$, compared to 2.7 $m^2\,g^{-1}$ for Bioglass 45S5 particles of similar size [69]. Common precursors for introducing calcium and phosphate into the sol–gel are calcium nitrate tetrahydrate and triethylphosphate, respectively. The thermal process also removes by-products of the non-alkoxide precursors, such as nitrates from calcium nitrate. The low-temperature process provides opportunities to make porous scaffolds (Section 8.2) and allow incorporation of polymers and organic molecules to make less brittle hybrid materials (Section 10).

Ordered mesopores can also be created by introducing surfactants that act as templates [77]. Ordered mesoporous silicates are of great interest in drug delivery applications, as the drug can be stored within the mesoporous network. These materials are beyond the scope of this paper and have been reviewed recently [78].

Disadvantages of sol–gel synthesis over the melt process is that it is difficult to obtain crack-free bioactive glass monoliths with diameters in excess of 1 cm, because larger monoliths crack during drying. The cracking is due to two reasons: the large shrinkage that occurs during drying; and the evaporation of the liquid by-products of the condensation reaction. When pore liquor is removed from the gels, the vapour must travel from within the gel to the surface via the interconnected pore network. This can cause capillary stresses within the pore network and therefore cracking. For small cross-sections, such as in powders, coatings or fibres, drying stresses are small, as the path of evaporation is short and the stresses can be accommodated by the material. For monolithic objects, the path from the centre of the monolith to the surface is long and tortuous, and the drying stresses can introduce catastrophic fracture. Increasing pore size and obtaining pores with a narrow distribution reduce tortuosity.

5. Bioactive glasses in vivo

A problem with clinical trials is that every patient is different, and multiple implants cannot be directly compared in the same patient. Results are often only based on non-invasive assessment methods, such as X-rays or patients giving scores on how they feel or how they can move. In vivo animal studies can be compared if the same models are used.

The first in vivo studies for Bioglass 45S5 were on monoliths (1 mm × 2 mm × 2 mm) in rat femurs and showed that the interfacial shear strength of the bond between the glass and cortical bone at 6 weeks was equal to or greater than the strength of the host bone [2,79]. Control implants (e.g. 99% SiO_2) did not bond. Subsequent in vivo studies on particulates (100–300 μm) showed that after 1 week there was 17 times more bone in the defects filled with Bioglass 45S5 and twice as much bone 24 weeks after surgery

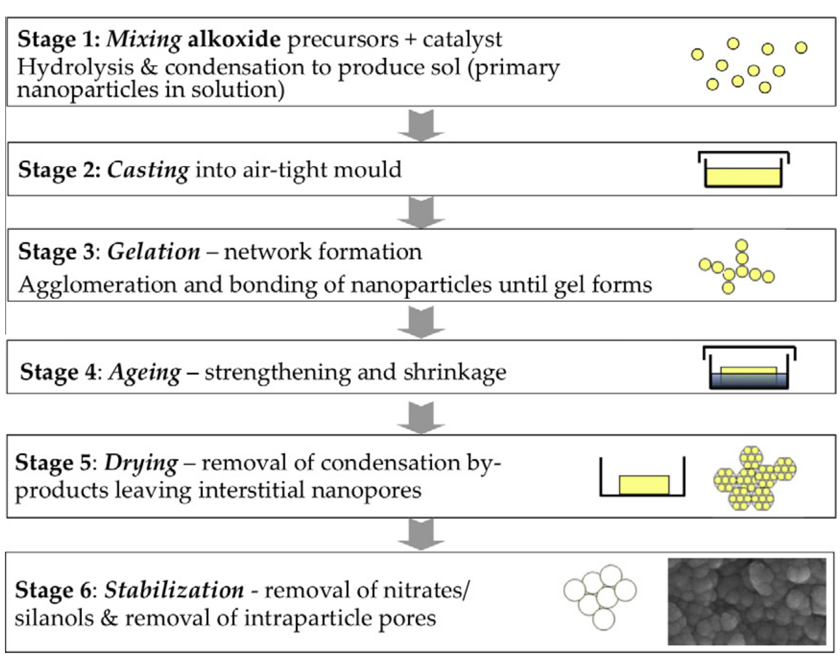

Fig. 9. A flow chart of the acid-catalysed sol–gel process of synthesis of a bioactive glass with schematics of the evolution of the gel and its nanoporosity.

compared to defects filled with HA [80]. The Bioglass 45S5 was also seen to degrade more rapidly than HA and the degradation was attributed to solution-mediated dissolution (rather than cellular/enzyme action) [80–83]. These studies indicate that Bioglass 45S5 regenerates bone better than the more commercially successful bioceramics. The model used, which later became known as the "Oonishi model", involved drilling 6 mm diameter critical-sized defects into the femoral condyle of rabbits. Bleeding was stopped prior to insertion of the particles. Schepers et al. [18] also found Bioglass 45S5 (mixed with blood) to stimulate more bone growth than HA in the jaw of Beagle dogs. They observed that particles with diameters in the narrow range of 300–355 μm (essentially the Biogran product) hollowed out within 4 weeks of implantation. The HCA layer formed and grew and all the silica dissolved, leaving a hollow particle. Phagocytic cells were thought to have assisted silica degradation, but the evidence for this occurring rather than solution-mediated dissolution is unclear. More recently, Bioglass 45S5 nanofibres reacted in vitro to form tubes of HCA in acellular conditions [84], so the hollowing could be simply solution-mediated. In the in vivo study on the Biogran particles, bone grew into the particles that were in contact with the host bone, but new bone also formed inside isolated particles within 2 months of implantation, indicating that the particles triggered stem cell differentiation into osteoblasts [18]. The glass particles were mixed with blood prior to implantation to create a putty-like material that surgeons prefer to handle. The hollowing out is not specific to the Biogran particles. PerioGlas (Bioglass 45S5 particles 90–710 μm) and Biogran (300–355 μm) particles implanted in the Oonishi model [85] both hollowed out after 4 weeks of implantation. The broad particle size distribution of the PerioGlas (which is equivalent to NovaBone) produced a higher bone-to-graft ratio than the Biogran particles.

As surgeons prefer a putty, NovaBone developed NovaBone Putty, which is Bioglass 45S5 particles (69%) in a polyethylene glycol and glycerine binder (31%). 6 weeks after implantation into 10 mm diameter critical-sized defects in sheep spine, the defect filled with the putty was filled with 42% bone, compared to 20% bone in the defect filled with NovaBone particulate and 5% bone in the empty control defect [86]. The putty matrix may separate the particles to allow more new bone to grow between them than the tightly packed particles allowed. An alternative explanation is that the pH environment created by the putty was more suitable for bone ingrowth than that produced by the tightly packed particles. The results are in contrast to a previous study in a similar model, where acute inflammation was observed, which was attributed to migration of the particles [87]. The use of a 3-D scaffold rather than particles would reduce this problem.

The Oonishi model was also used to test phosphate-free ternary glass particles (100–300 μm) in the SiO_2–CaO–Na_2O system of five compositions with 50–70 mol.% SiO_2 and equal proportions of Na_2O and CaO [88]. An example is a glass of composition 50 mol.% SiO_2, 25 mol.% Na_2O and 25 mol.% CaO, which stimulated a similar amount of bone ingrowth to Bioglass 45S5, although bone formation at the centre of the defect took 2 weeks, compared to 1 week for Bioglass 45S5 [80]. The rate of bone ingrowth decreased dramatically as SiO_2 content increased. Glass with higher silica content (55 mol.% and above) only stimulated bone ingrowth after 2 weeks, and those with an SiO_2 content of 60 mol.% or above did not bond to the bone. The glasses with 50 mol.% SiO_2 became HCA shells after 6 weeks and were fully integrated into new bone filling the defect. In defects containing the glass with 55 mol.% SiO_2, the observation was similar at the periphery, but bone did not grow into the centre of the defect and bone ingrowth did not progress after 3 weeks' post-implantation. The retardation of bone ingrowth was attributed to the presence of multinuclear giant cells in the core of the bone defects when bone ingrowth was initially slow [89,90]. The giant cells were not found in the core of the defects filled with the highly bioactive 50 mol.% SiO_2 glass.

Bioglass 45S5 (e.g. NovaBone) and S53P4 (BonAlive) have only been compared simultaneously in very few studies. Bioglass 45S5 reacts more rapidly than S53P4, so, when cones were implanted in rat femur and soft tissue, HCA layer thickness was higher for 45S5 than for S53P4 [91]. Both glasses showed good contact with the bone.

Wheeler et al. [83] compared Bioglass 45S5 with sol–gel glass particles of the 77S and 58S in the Oonishi model. Up until 8 weeks after implantation, bone defects filled with Bioglass 45S5 contained more bone than those filled with 77S or 58S, but within 12 weeks the amounts were equivalent. Each of the glasses formed a bond to the bone via HCA formation. However, resorption of 77S and 58S particles was more rapid than the 45S5 particles. This is due to the nanoporosity and enhanced specific surface area of the sol–gel glasses. Between 4 and 24 weeks after implantation, the area covered by Bioglass 45S5 particles in histological slices decreased by a mean of 15%, compared to 34% and 70% for 77S and 58S particles, respectively. The degradation of the 58S was continuous but 77S seemed to stop degrading at 12 weeks. No silicon was detected in the 58S particles after 12 weeks. The 58S degrades more rapidly than 77S due to its lower silica content – in fact, the degradation of the 58S particles may be too rapid for good-quality bone regeneration. The slower rate of initial bone ingrowth into the sol–gel glass-filled defects compared to the Bioglass 45S5 defects was not discussed, but it could be that the initial pH increase in the defects containing the sol–gel particles was higher than it was for the Bioglass 45S5. If this were the case, it would be due to the calcium in the sol–gel glasses releasing rapidly initially, due to the nanoporosity and high surface area. The compressive strengths of the filled defects were equivalent to normal bone at all time points.

As bioactive glasses are degradable, questions are often asked as to how long the glass is present in a bone defect and what happens to the degradation products. These are important question for surgeons, who would like to see regeneration of large bone defects over a period of ~12 months. Of course, an ideal bone scaffold would degrade at the rate at which the bone regenerates. Bioglass 45S5 degradation rate depends on morphology, surface area and the implantation site. Bioglass 45S5 particles smaller than 300 μm in maximum diameter are likely to become shells of HCA within 4 weeks, initially by solution-mediated dissolution and then perhaps by osteoclast action [18,85,89,90]. Larger particles may remain longer. Degradation rate is also dependent on glass composition and type.

As natural levels of Si in the human body are low (0.6 $\mu g\ ml^{-1}$ for serum and 41 $\mu g\ ml^{-1}$ for muscle), it is important to be sure of the route of excretion of the dissolution products. Harmless Si excretion in urine was observed in rabbits up to 7 months after implantation of Bioglass 45S5 particles (300–355 μm) in the tibia [92] and muscle [93]. For 750 mg of Bioglass 45S5 implanted in the tibia, Si levels in the urine were 2.4 mg day^{-1}, which is below saturation, and histology of the brain, heart, kidney, liver, lung, lymph nodes, spleen and thymus showed no elevation of Si levels.

Bioactive glasses are also being tested in applications where good interfaces are needed between soft and hard tissue. An example is 58S-coated polyethylene terephthalate (PET) ligaments, which showed reduced scar tissue and bone formation at the interface between the graft and the host bone, in the tibial tunnel, compared with the uncoated controls at 6 and 12 weeks after surgery [94]. However, as the Wheeler study showed that the 58S particles degraded in 12 weeks in the Oonishi model, the concept of coating a permanent ligament may be flawed. A PET ligament may need a longer-lasting or permanent bioactive coating to ensure long-term stability.

Synthetic bone grafts are often used as bone graft extending materials when the amount of autograft available is insufficient. A combination of NovaBone with 60% glass and 40% autologous bone stimulated more rapid bone regeneration than 80% glass and 20% bone in rabbit crania [95]. This indicates that natural bone is still the best scaffold for bone regeneration. A closer mimic to natural bone incorporating the properties of bioactive glass is needed.

6. Why do bioactive glasses bond with bone and stimulate new bone growth?

There are two mechanisms of bioactivity for bioactive glasses. Bone bonding is attributed to the formation of an HCA layer, which interacts with collagen fibrils of damaged bone to form a bond [96]. Formation of the HCA layer is now quite well understood, but the biological interactions at the HCA–host bone interface are less well understood. Bone bonding to the HCA layer is thought to involve protein adsorption, incorporation of collagen fibrils, attachment of bone progenitor cells, cell differentiation and the excretion of bone extracellular matrix, followed by its mineralization [5]. However, evidence for each of these steps is sparse.

Osteogenesis is related to the action of dissolution products of the glasses on osteoprogenitor cells, stimulating new bone growth [5]. However, the HCA layer also provides a surface suitable for osteogenic cell attachment and proliferation. The ideal surface chemistry and topography of a surface are yet to be identified. Another unanswered question is what role osteoclasts play in remodelling the glass once osteogenesis begins. Some authors suggest that osteoclasts only remodel the HCA layer [90], whereas others suggest that they can break down the silica network [18].

6.1. Mechanism of HCA layer formation on bioactive glasses

The HCA layer forms following solution-mediated dissolution of the glass with a mechanism very similar to conventional glass corrosion [97]. Accumulation of dissolution products causes both the chemical composition and the pH of the solution to change, providing surface sites and a pH conducive to HCA nucleation. There are five proposed stages for HCA formation in body fluid in vivo or in simulated body fluid (SBF) in vitro [98,99].

1. Rapid cation exchange of Na^+ and/or Ca^{2+} with H^+ from solution, creating silanol bonds (Si–OH) on the glass surface:

   $$Si - O^{-}Na^{+} + H^{+} + OH^{-} \rightarrow Si - OH^{+} + Na^{+}(aq) + OH^{-}$$

   The pH of the solution increases and a silica-rich (cation-depleted) region forms near the glass surface. Phosphate is also lost from the glass if present in the composition.
2. High local pH leads to attack of the silica glass network by OH^-, breaking Si–O–Si bonds. Soluble silica is lost in the form of $Si(OH)_4$ to the solution, leaving more Si–OH (silanols) at the glass–solution interface:

   $$Si - O - Si + H_2O \rightarrow Si - OH + OH - Si$$

3. Condensation of Si–OH groups near the glass surface: repolymerization of the silica-rich layer.
4. Migration of Ca^{2+} and PO_4^{3-} groups to the surface through the silica-rich layer and from the solution, forming a film rich in amorphous $CaO–P_2O_5$ on the silica-rich layer.
5. Incorporation of hydroxyls and carbonate from solution and crystallization of the $CaO–P_2O_5$ film to HCA.

Although these stages were proposed many years ago, characterization techniques have been pushed to the limit to prove that they occur. Repolymerization of Si–OH groups in the silica-rich layer was confirmed by an increase in the proportion of bridging oxygen bonds during leaching, shown by ^{17}O solid-state nuclear magnetic resonance (NMR) [100]. Surface-sensitive shallow-angle X-ray diffraction (XRD) confirmed the formation of amorphous calcium phosphate prior to HCA on polished Bioglass 45S5 [101]. Calcium phosphate was found to nucleate on the Si–OH groups, which have a negative charge in solution [102,103] and the separation of the Si–OH groups is thought to dictate the orientation of the apatite crystals [104], which grow with a preferred orientation in the 001 plane on Bioglass 45S5 [105]. Real-time studies on 70S30C sol–gel glass in SBF using synchrotron-source XRD showed that octacalcium phosphate (OCP) crystallites formed within 1 h, but by 10 h the crystallites were replaced by an amorphous calcium phosphate, which continued to grow. After 25 h, poorly crystalline HCA had formed [106].

Glass composition is the variable that has the greatest influence on rate of HCA layer formation and bone bonding. Essentially, lower silica content means a less connected silica network, which is more prone to dissolution, and therefore the stages listed above happen more rapidly. Bioactivity has been shown to be directly related to the activation energy of silica dissolution in the glass [107]. However, the connectivity of the network is key and depends on silica content and what other cations modify the glass. For example, adding sodium at the expense of silicon increases dissolution rate, but replacing cations such as sodium and calcium with multivalent ions such as Al^{3+}, Ti^{4+} or Ta^{5+} reduces bioactivity by reducing solubility [108,109]. As a rule of thumb, melt-derived glasses with compositions containing more than 60% SiO_2 do not bond and are bioinert. Sol–gel-derived glasses can, however, be bioactive with up to 90 mol.% SiO_2 [110]. Section 7 discusses the importance of understanding glass structure and network connectivity in terms of the properties of bioactive glasses.

6.2. Ionic dissolution products and osteogenesis

Once the HCA layer has formed, the next stages are less clear. What is clear is that proteins adsorb to the HCA layer, and cells attach, differentiate and produce bone matrix. The exact mechanism is difficult to follow as in vivo and in vitro experiments do not tell the full story. An important property for bioactive glasses is that new bone can form on the glass away from the implant–bone interface, termed "osteoproduction" by Wilson [17]. The use of the term osteoproduction was coined to distinguish between it and "osteoinduction". An osteoinductive material stimulates bone growth in ectopic (non-bone) sites. A common model to test for it is implantation of a material in muscle. In bioactive ceramics that are only osteoconductive, bone grows along the material surface from the bone–implant interface. In vitro experiments have given clues as to why bioactive glass has such good osteogenic properties [111].

Human osteoblasts cultured on bioactive glasses produce collagenous extracellular matrix (ECM) that mineralizes to form bone nodules without the usual supplements of hormones present in the culture [112–114], even when phosphate was not in the glass composition [115]. The dissolution of calcium ions and soluble silica from bioactive glass was shown to stimulate osteoblast cell division, production of growth factors and ECM proteins. Other bioceramics need osteogenic supplements added to the media, such as dexamethasone and β-glycerophosphate, for bone nodule formation to occur.

In vitro culture of primary human osteoblasts with only the ionic dissolution products of Bioglass 45S5 increased intracellular calcium levels [116] and showed that seven families of genes were up-regulated within 48 h [117]. An example is insulin-like growth factor II (IGF-II), which increased by more than 3-fold. IGF is the most abundant growth factor in bone and induces osteoblast proliferation. There was also induction of transcription of at least five ECM components (2- to 3.7-fold). Extracellular matrix secretion was also increased, which mineralized without addition of supplements [118,119]. The dose of the dissolution products is important, as too many ions can be toxic. The gene expression was dose-dependent, with the highest gene expression observed at $\sim$20 $\mu g\ ml^{-1}$ of soluble silica, accompanied by 60–90 $\mu g\ ml^{-1}$ of calcium ions [120]. The dissolution products seem also to affect the cell cycle of osteoblasts, because the transition of osteoblasts from the G0 stage (resting) to the G1 stage (first growth stage involving amino acid synthesis) is regulated by the transcription factors that were up-regulated by the dissolution products. The number of cells dying by programmed cell death (apoptosis) increased on exposure to the dissolution products, but the remaining cells exhibited enhanced synthesis and mitosis [121]. This correlated with the 1.6- to 4.5-fold up-regulation of apoptosis regulators, the 2- to 5-fold up-regulation of cell cycle regulators and the 2- to 3-fold up-regulation of DNA synthesis [117]. As these studies all used the dissolution products of Bioglass 45S5, the media contained soluble silica, phosphate species and sodium and calcium ions. Understanding the role of individual ions is also important for the design of new materials. Extracellular calcium ions alone have been found to increase IGF-II up-regulation [122,123] and glutamate production by osteoblasts [124]. Silica is thought to be released from the glass in the form of silicic acid ($Si(OH)_4$), which has been shown to stimulate collagen I production by human osteoblast cells at a concentration of 10 mmol [125]. More detail on cellular response to individual ions is given in Hoppe et al. [126].

The studies reported above were all on mature human osteoblasts. Ideally, bioactive glass implants would recruit osteoprogenitor cells in vivo and send them down a bone differentiation pathway. When human foetal osteoblasts were exposed to Bioglass 45S5 dissolution products, genes associated with osteoblast differentiation were up-regulated [127]. A similar dose-dependent response was observed to the mature osteoblasts, with 15–20 $\mu g\ ml^{-1}$ of soluble silica promoting highest metabolic activity, with expression of the core-binding factor alpha 1 (Cbfa1) and enhanced formation of mineralized bone nodules [128].

Bioglass 45S5 and sol–gel-derived bioactive glass particles induced osteogenic differentiation of bone-marrow-derived adult stem cells (mesenchymal stem cells, MSCs) into osteoblast-like cells, and the resulting cells produced mineralized matrix [114]. However, it is not quite clear how the culture was performed in terms of how the cells were seeded on the particles. A separate study on 45S5 Bioglass 45S5 discs showed no significant difference on differentiation of human-bone-marrow-derived MSCs compared to those cultured on tissue culture plastic (with or without bone morphogenetic protein 2, BMP-2) [129]. When bone marrow MSCs were cultured on bioactive sol–gel coatings with low silica content (40 mol.% SiO_2, 54 mol.% CaO, 6 mol.% P_2O_5), the MSCs differentiated into osteoblasts and osteoclasts (with or without BMP-2 added to the culture) [130], which seems an ideal result for bone regeneration (bone production and remodelling). When the cells were cultured on glass coatings of high silica composition (80 mol.% SiO_2, 54 mol.% CaO, 6 mol.% P_2O_5), the MSCs differentiated into osteoblasts but not osteoclasts. When osteogenic media (containing dexamethasone and β-glycerophosphate) supplemented with sol–gel glass dissolution products was administered to mouse embryonic stem cells, the number of mineralized bone nodules increased in a dose-dependent manner, but there was little evidence for stem cell differentiation without the supplements [131]. Human adipose stem cells have also been shown to differentiate into osteogenic cells when cultured on bioactive glasses in the presence of osteogenic supplements [132]. Interestingly, differentiation was delayed when the HCA layer was formed on the glass prior to cell seeding. Whether the cells differentiated on the glasses without osteogenic supplements was unfortunately not reported.

In terms of osteoclast action on bioactive glasses in vitro, results are also mixed. Osteoclasts cultured on S53P4 did not erode the surface of the biomaterial [133]. However, osteoclast response to three other bioactive glass powders was compared and a significant increase in the number of multinucleated osteoclasts was observed on melt-derived 45S5 and sol–gel-derived 58S bioactive glass powders and relatively few osteoclasts were observed on sol–gel-derived 77S [114]. The higher activity on the 45S5 and 58S glasses could be due to higher calcium content on the glass surface. This does not agree with an in vivo study that suggested that 58S and 77S sol–gel particulates have demonstrated an improvement in the bone remodelling potential of these sol–gel products when compared to melt-derived Bioglass 45S5 in vivo [134]. But dissolution-mediated dissolution was not distinguishable from osteoclast action in the in vivo study.

In summary, the bioactivity and ability for a bioactive glass to stimulate bone regeneration at a cellular level is dependent on rate of dissolution and formation of the HCA layer, which can be controlled by the composition and atomic structure of the glass.

7. Atomic structure of bioactive glass and its relation to dissolution and HCA formation

The properties of glass, e.g. dissolution rate and therefore the rate of formation of the HCA layer on bioactive glasses, are a direct result of atomic structure. Understanding the structure of glass is important but not trivial. Advanced characterization techniques are required to understand their complex amorphous structure [135].

Silicate glasses are a collection of silica tetrahedra connected by –Si–O–Si– bridging oxygen bonds (see Fig. 8). Silicon is therefore the glass network-forming atom. Sodium and calcium are network modifiers that disrupt the network by forming non-bridging oxy-

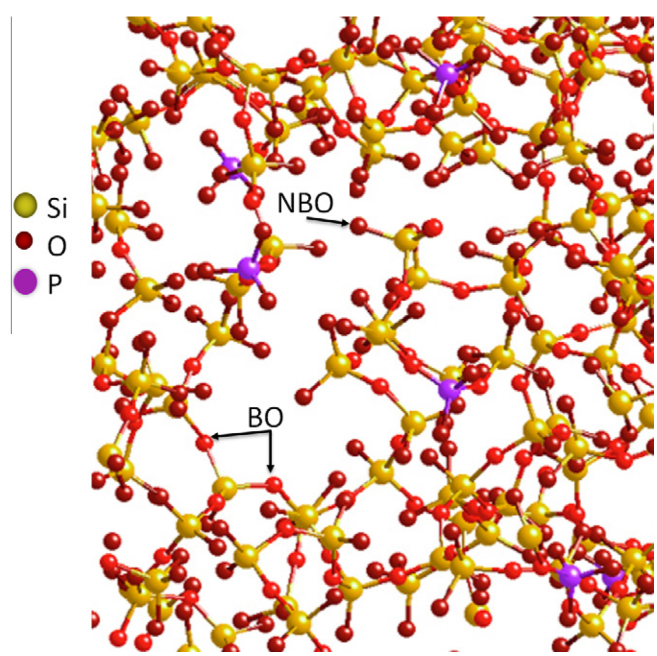

Fig. 10. Section of a model of Bioglass® 45S5, with the Na and Ca ions removed for clarity. NBO = non-bridging oxygen, BO = bridging oxygen. Modified from Cormack et al. [136].

gen bonds such as $Si–O^{-}$ ^{+}Na bonds [136]. Fig. 10 shows a snapshot of a molecular dynamics model of Bioglass 45S5. The silica tetrahedron and its associated bonds can be described by Q^n notation, where n is the number of bridging oxygen bonds. A ^{29}Si solid-state NMR study showed that Bioglass 45S5 primarily consists of 69% chains and rings of Q^2, with 31% of Q^3 units providing some cross-linking [137]. According to NMR, the phosphorus is present in an orthophosphate environment (Q^0), with charge balanced by sodium and/or calcium (^{31}P and ^{17}O NMR) [138,139] without any P–O–Si bonds [137,140]. The phosphorus is therefore isolated from the silica network and removes sodium and calcium cations from their network-modifying role [139]. This explains why phosphate is rapidly lost from the glass on exposure to aqueous environments [141]. The presence of the orthophosphate in a bioactive glass was first found in $CaO–SiO_2–P_2O_5–CaF_2$ [142] and is effectively phase separation. Its presence is the reason why two glass transition temperatures (T_g) are often observed in melt-quenched bioactive glasses containing high (>6 mol.%) phosphate [143]. This is not to say that P–O–Si bonds are impossible: they have been observed in glasses with >50 mol.% phosphate [144]. Molecular dynamics models [145] and XRD data [137] suggest that the distribution of Ca in the glass is non-uniform and suggest the presence of calcium-rich Ca–O regions.

Understanding of the atomic structure is important when it comes to designing alternative glass compositions. The connectivity of the silica network is dictated by the composition and method of glass synthesis. High silica content results in a highly connected network containing a large proportion of bridging oxygen bonds and low dissolution and low bioactivity. Connectivity is lowered by adding more network-modifying cations such as sodium and calcium. As phosphate content increases, the network connectivity increases as the cations charge-balance the orthophosphate as monophosphate with or without diphosphate complexes [146].

Network connectivity can be quantified (N_c, mean number of bridging oxygen bonds per silicon atom) and used to predict the bioactivity of a glass [143,147]. In melt-derived glasses, the composition can be used to calculate N_c. The knowledge that the phosphate is in the form of orthophosphate (Q^0 $[PO_4]^{3-}$ units) and not part of the silica network (i.e. no Si–O–P bonds are present) was important for accurate derivation of the equation [143]:

$$N_c = \frac{4[SiO_2] - 2[M^I_2O + M^{II}O] + 6[P_2O_5]}{[SiO_2]} \quad (1)$$

This calculates Bioglass 45S5 to have an N_c of 2.12. Table 1 summarizes the properties of Bioglass 45S5 [60,148]. Glasses that have N_c greater than 2.6 are likely not to be bioactive due to their resistance to dissolution [149].

In sol–gel glasses, the network connectivity is lower than that calculated from the nominal composition. This is because H^+ acts a network modifier, disrupting the silica network and reducing network connectivity [74,150], and increasing dissolution rate and bioactivity (Section 6). Although the drying process removes water, hydroxyl (OH) groups are left on the pore walls. Thermal stabilization drives off many of the –OH groups, causing further formation of O–Si–O bonds [74], but some remain, so the glass composition also contains –OH groups. This reduction in network connectivity in combination with their inherent nanoporosity is why sol–gel glasses can be bioactive with up to 90 mol.% silica, whereas melt-derived glasses are limited to 60 mol.% [151]. The OH content in the sol–gel glass depends on the conditions used in synthesis, e.g. the final stabilization or sintering temperature. Sintering sol–gel glasses above their T_g causes a reduction in the porosity and densification of the silica network. The sintering temperature should be kept below the crystallization temperature ($T_{c,onset}$) for the glass to prevent the formation of a glass–ceramic [74].

Table 1
Selected properties of melt-derived Bioglass 45S5 [60,148].

Property	Value
Density	$2.7\ g\ cm^{-3}$
Network connectivity	2.12
Glass transition temperature	538 °C
Onset of crystallization	677 °C
Thermal expansion coefficient	$15.1 \times 10^{-6}\ °C^{-1}$
Young's modulus (stiffness)	35 MPa

Results from solid-state proton NMR show that, for 70S30C stabilized at 700 °C, there are 0.38 −OH per silicon atom, so that every 2.6 silica tetrahedra has an Si–OH bond, reducing network connectivity [74]. Results from ^{29}Si NMR also showed that sol–gel-derived bioactive glasses have a broad distribution of Q units, e.g. a 70S30C glass contains Q^4, Q^3 and Q^2 units when stabilized at 700 °C [74]. When phosphate is present (usually using the precursor triethylphosphate) in a silica sol–gel glass, it is present as orthophosphate, as it is in the melt-derived glasses [152]. Replacing calcium with magnesium can also reduce the dissolution rate of the glass and therefore its bioactivity, perhaps due to the magnesium behaving as a network intermediate [153–155].

The high water content of sol–gel glass complicates the modelling of the structure. Currently there is not sufficient computing power to carry out ab initio models over the timescales required. Molecular dynamics simulations have been carried out based on a classic model for melt-quenched glass but with the composition $(CaO)_x(SiO_2)_{1-x}(H_2O)_y$ to take into account OH content. The models suggest that the calcium distribution becomes more homogeneous with increasing OH content [156].

8. Bioactive glass scaffolds

Particulate systems lack some dimensional stability when first placed into the surgical site. A bone defect cavity may hold the particles in place until they are integrated with the host bone, but in some clinical cases bone repair is needed where there is no bony chamber and additional fixation materials are needed. An ideal synthetic bone graft is a porous material that can act as a temporary template (scaffold) for bone growth in three dimensions. It should:

1. be biocompatible and bioactive, promoting osteogenic cell attachment and osteogenesis;
2. bond to the host bone without fibrous tissue sealing it off from the body;
3. have an interconnected porous structure that can allow fluid flow, cell migration, bone ingrowth and vascularization;
4. be able to be cut to shape in theatre so that it can fit the defect (for some applications, clinicians may prefer porous granules to a single block);
5. degrade at a specified rate and eventually be remodelled by osteoclast action;
6. share mechanical load with the host bone and maintain an appropriate level of mechanical properties during degradation and remodelling;
7. be made by a fabrication process that can be up-scalable for mass production;
8. be sterilizable and meet regulatory requirements for clinical use.

An ideal synthetic scaffold is expected to mimic porous cancellous bone (autograft), which fulfils most of the listed criteria. Bioactive glass cannot fulfil all of the criteria, but porous bioactive glass scaffolds have the potential to improve on current market-leading commercial porous synthetic bone grafts such as Actifuse®, which are porous granules (1–3 mm) of silicon-doped hydroxyapatite, and to improve on the commercially available bioactive glass products, which are particulates. The reason that there are not yet porous bioactive glasses on the market is that the commercially available particulates that have regulatory approval are compositions such as Bioglass 45S5 and BonAlive S53P4. Porous scaffolds that are made from glass particles must be sintered to fuse the glass particles together, and when the 45S5 and S53P4 glass particles are sintered they crystallize, or partially crystallize, forming a glass–ceramic [157–160]. Glass–ceramic scaffolds have been produced from 45S5 particles with 90% porosity and open pores [160]. However, full crystallization reduces bioactivity whereas partial crystallization can lead to instability, as the residual amorphous regions degrade preferentially [161]. This was evident in Ceravital®, a glass–ceramic synthesized by crystallizing glass of the 45S5 composition with small additions of K_2O and MgO. Although Ceravital bonded to bone [109], implants failed due to long-term instability of crystal phase boundaries [1].

8.1. Melt-derived bioactive glass scaffolds

Production of porous melt-derived glasses involves starting with particles and sintering them, often around a template, or after a foaming process, or after solid freeform fabrication (also termed "additive manufacturing"). Sintering involves heating the particles above their T_g, which causes local flow of the glass, fusing the particles at their points of contact. However, to maintain the amorphous glass structure and properties, the temperature must not be raised above $T_{c,onset}$. The temperature difference between T_g and $T_{c,onset}$ is termed the "sintering window". The size of the sintering window is dependent on the structure of the silica network and therefore on composition. For currently commercially available glasses such as Bioglass 45S5 (Table 1) and S53P4, the sintering window is too small, so they cannot be sintered without crystallization. The efficiency of sintering and the temperature at which crystallization occurs also depend on particle size. There is a greater driving force for sintering as particle size decreases and specific surface area increases; therefore, particles must be small enough to sinter efficiently without leaving defects in the struts. However, crystallization is surface-nucleating and therefore the propensity for crystallization also increases [160,162]. A balance is needed.

It is quite a challenge to design a glass composition that can be sintered without crystallizing but also remains bioactive. Only recently has understanding the relationship between sintering window, composition and bioactivity become sufficient. The network connectivity should be ~2 (as it is for Bioglass 45S5) for a glass to be bioactive, but conventional four-component glasses with network connectivity of ~2 have small sintering windows. Increasing the silica content reduces the tendency of a glass to crystallize, but this increases network connectivity and reduces degradation rate and bioactivity. The sintering window can be widened by introducing a variety of network modifiers, e.g. K_2O, MgO, B_2O_3 and Al_2O_3, which increases the activation energy for crystallization [163–165]. Key is to substitute for calcium and sodium in mol.%, to keep network connectivity constant. Replacing just 0.1 wt.% of Na_2O with ZnO increased the sintering window by 5 °C [166]. Magnesium is particularly effective at widening the sintering window, but also affects bioactivity.

One of the first compositions designed not to crystallize on sintering was 13–93, which contained 7.7 mol.% MgO (54.6 mol.% SiO_2, 6 mol.% Na_2O, 22.1 mol.% CaO, 1.7 mol.% P_2O_5, 7.9 mol.% K_2O, 7.7 mol.% MgO) [163]. It takes 7 days to form an HCA layer in simulated body fluid tests, whereas Bioglass 45S5 particles of similar size formed the layer within 8 h. This is because the network connectivity is higher in glass composition 13–93 (N_c = 2.6) compared to Bioglass 45S5 (N_c = 2.12) due to the increased silica content. However, the effective N_c of 13–93 is likely to be even higher, as the N_c of 2.6 was calculated assuming that magnesium is a network modifier, but magnesium has been found to switch its role as its content is increased. Using solid-state NMR, the change in role of magnesium was monitored as it was substituted for calcium, becoming a network intermediate. While 86% of magnesium oxide behaved as a network modifier, like calcium, 14% of the magnesium oxide was found to form tetrahedral MgO_4, which removes other network-modifying ions (e.g. Na^+ and Ca^{2+}) for charge compensation, resulting in increased network connectivity of the silica network [167]. This was observed by an increase in relative numbers of Q^3 units at the expense of Q^2 as the amount of magnesium increased. This is why magnesium is an excellent additive for expanding the sintering window, but it reduces bioactivity. Having said that, scaffolds with 50% porosity made from 13–93 fibres (75 µm thick, 3 mm long) completely degraded within 6 months after implantation in rabbit tibia [168].

In order to obtain a similar result without compromising bioactivity, ICIE16 (49.46 mol.% SiO_2, 36.27 mol.% CaO, 6.6 mol.% Na_2O, 1.07 mol.% P_2O_5 and 6.6 mol.% K_2O) was developed, as it maintains an N_c = 2.12 [138]. A more straightforward approach was recently taken by Sola et al., who simply replaced all the Na_2O in Bioglass 45S5 with K_2O [169,170], maintaining N_c and naming the glass BioK. However, the change in composition was not sufficient, as some crystallization still occurred at the minimum sintering temperature (>600 °C). They also replaced sodium with calcium

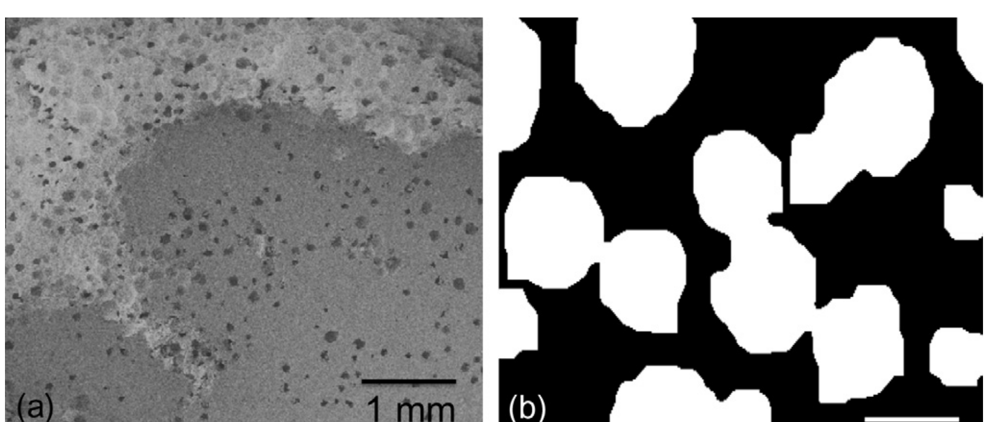

Fig. 11. Porous bioactive glasses (ICIE16 composition) produced by the space-holder method, using PMMA microspheres (diameter ~500 µm) with glass/polymer ratio of 50/50: (a) SEM image showing isolated spherical pores (courtesy of Zoe Wu); (b) 2D µCT projection showing isolated pores (courtesy of Sheng Yue).

(47.3 mol.% SiO_2, 45.6 mol.% CaO, 4.6 mol.% Na_2O and 2.6 mol.% P_2O_5), which increased the onset of crystallization but also increased T_g [171], as shown previously [172]. The more complicated compositions such as 13–93 or ICIE16 must therefore be used.

When processing glass particles, the aim is to create large pores with interconnects greater than 100 μm, while having highly sintered struts that provide as much strength as possible. The most common method for making porous ceramics is to pack the glass particles around a sacrificial polymer template. The particles will fuse together during sintering. The template can either be particles or a foam that is burnt out during the sintering process, leaving pores. The pore size and interconnectivity depend on the template.

The space-holder or porogen method is the most common, for which sacrificial particles are used, e.g. polymethyl methacrylate (PMMA) microbeads. Combustible polymers are usually used for glass synthesis. However, if not enough oxygen reaches the combustible polymer, a black carbon residue will be left behind (coring), reducing the sintering efficiency. Using PMMA reduces coring because it leaves little residue as it burns. The space-holder technique is simple and can be easily up-scaled for commercial production, but pore size is largely determined by the particle size of the sacrificial polymer, and it is difficult to maintain a homogeneous distribution of the polymer spheres. Therefore, pore interconnectivity is low and poorly controlled (Fig. 11).

Interconnectivity can be improved through using sacrificial polyurethane foams rather than spheres [157]. Fig. 12a shows an SEM image of a polyurethane foam with large and well-connected pores. To create a porous glass, the foam is immersed in a slurry of glass so that the particles coat the foam struts. The aim is that, after sintering, the glass will take the shape of the foam. The challenge in the process is to ensure that the polymer is well coated but excess particles must be removed prior to sintering. The common way to remove excess powder is to squeeze it out of the foam. After the excess powder is removed, the foams are heated to 250 °C, to pyrolyse the polyurethane foam, and then sintered for 3 h. Fig. 12b shows an SEM image of the resulting glass scaffold of the ICIE16 composition. In this example, the struts had a thin coating of glass prior to sintering, resulting in thin struts. This technique has been used to create scaffolds from the 45S5 composition, which became glass–ceramics during sintering (Fig. 12c) [157]. The nature of the process means that polymer removal leaves hollow foam struts (Fig. 12d), which means that mechanical properties can be lower than might be expected; for example, the 45S5 glass–ceramic foams had a compressive strength of 0.4 MPa (90% porosity). However, by choosing an optimal polymer foam and by optimizing the amount of glass particles (<10 μm) used in the slurry (35 vol.%), compressive strengths of 11 MPa were obtained with 13–93 scaffolds, with 85% porosity and pore sizes ranging from 100 to 500 μm [173].

Instead of using a polymer template, ice crystals can be used [174]. By controlling the direction of freezing and the cooling rate, orientation can be given to the pores in a technique termed "freeze casting". The ice is removed by sublimation to avoid cracking prior to sintering. Glass scaffolds of the 13–93 composition have been prepared using the technique with particles <5 μm (Fig. 13). When water alone was used as a solvent, a lamellar pore structure was formed that had maximum pore widths of 40 μm. The pore width was increased by adding 60 wt.% dioxane [175] to the water, which resulted in wider columnar-like pores. Percentage porosity depended closely on the glass loading of the slurry, e.g. 15 vol.% glass

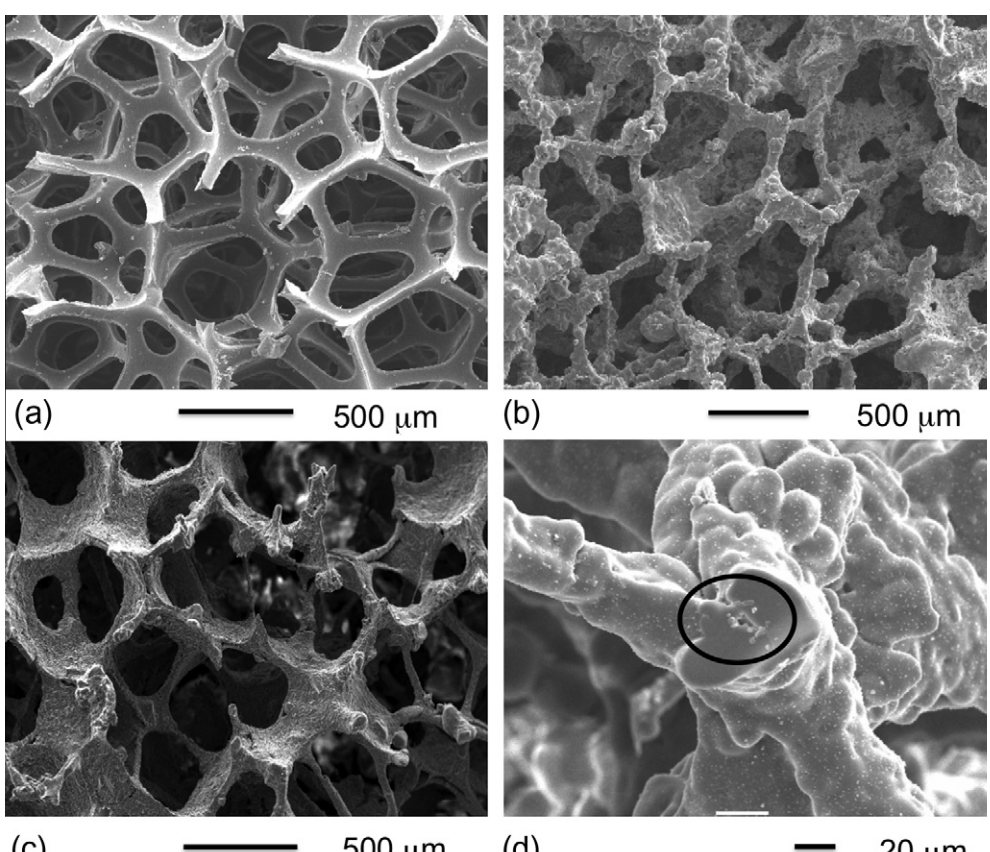

Fig. 12. SEM images of the polymer foam reticulation process. (a) Polyurethane foam template. (b) A porous glass foam after removal of the foam template and sintering. (c) A porous 45S5 glass–ceramic scaffold made by polymer foam reticulation (modified from Chen et al. [158]). (d) Cross-section of a hollow strut. (a, b, and d) courtesy of Xin Zhao.

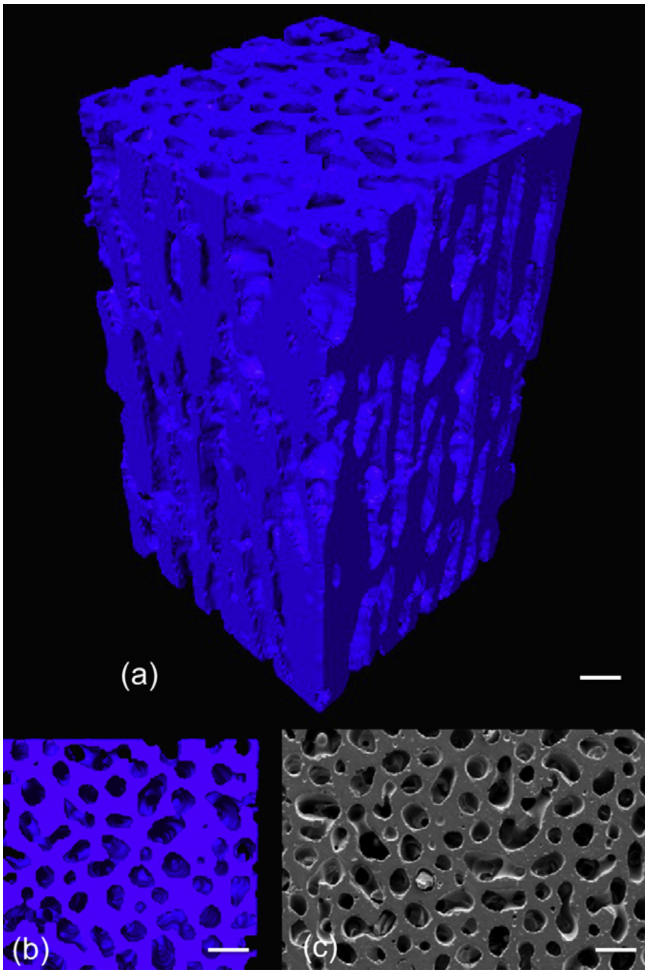

Fig. 13. Bioactive glass (13–93) scaffold produced by freeze-casting using camphene as the solvent. (a) 3-D μCT image of a scaffold. (b) 2-D μCT slice perpendicular to the freezing direction. (c) SEM image of cross-sections of columnar pore structures perpendicular to the freezing direction. Scale bar is 100 μm. Courtesy of Qiang Fu, Lawrence Berkeley National Laboratory, Berkeley, USA.

gave a porosity of 55% and a maximum pore width of 110 μm. This translated to a compressive strength of 25 MPa, which exceeds that of cancellous bone. Switching to camphene-based suspensions (10 vol.% particles) produced scaffolds with 60% porosity and pore diameters of up to 120 μm, with compressive strengths of 16 MPa (Fig. 13) [176]. Reducing porosity to 50% and pore diameter to 100 μm by adding a second stage to the process, where the scaffold is annealed near the softening point of the frozen mixture, increased compressive strength to 47 MPa [177,178]. The μCT images of the freeze-cast scaffolds (Fig. 13) show that there were also connections between the pores perpendicular to the freezing direction. It is not yet known whether the number and size of those connections are sufficient for good bone ingrowth and bone regeneration.

Interconnectivity can be improved using direct foaming techniques that use surfactants to stabilize bubbles created in a liquid (slurry or sol) by vigorous agitation. The bubbles must then be gelled to maintain the porous structure prior to sintering. The process is similar to what is used to produce Actifuse and is the latest technique for producing porous bioactive glasses with similar interconnected pore structures and mechanical strengths to cancellous bone. Melt-derived or sol–gel glasses can be used in direct foaming. Melt-derived glasses are foamed by the gel-cast foaming and sol–gel by the sol–gel foaming process. The processes have many similarities. In both techniques a solution or slurry is foamed under vigorous agitation with a surfactant to form bubbles. The bubbles are gelled and the viscous foam poured into moulds immediately prior to gelation. The main differences are that the gel-cast foaming process for melt-derived glass uses an in situ polymerization reaction to gel the bubbles. In the sol–gel foaming process, the silica network itself gels, which simplifies the process. Surfactants stabilize the bubbles in the slurry or sol by lowering the surface tension.

In the gel-cast foaming process for melt-derived glass, fine particles (<38 μm) of a sinterable composition, such as 13–93 or ICIE16 [179], are added to water to produce a slurry. The surfactant is then added and the slurry is foamed under vigorous agitation. For the in situ polymerization, monomer (usually acrylate) is added with its appropriate initiator and catalyst. As the polymerization reaction progresses, the viscosity increases until the glass is bound together in a polymer foam. Just prior to gelation, the foam is poured into a mould. To obtain an interconnected pore network, the bubbles must be large such that they are in contact with each other. On gelation, the bubbles become the pores and the surfactant films rupture, opening up spherical interconnects between the pores. After gelation, the foam is a composite of glass particles within the newly formed polymer matrix (Fig. 14a and b). Polymer removal and sintering occur in the same heat treatment procedure. The composite is usually held at ~300 °C to remove the polymer. After polymer removal, the particles are supported only by each other. As the temperature increases above T_g, the particles begin to sinter together. Fig. 14c and d shows images of the glass scaffold after sintering. Importantly, the struts of the foam are smooth and individual particles are not distinguishable, indicating efficient sintering. The struts are dense, which provides compressive strengths of 2 MPa for scaffolds with pore sizes in the range of 200–500 μm and modal interconnect diameters of 140 μm. As was the case for freeze casting, the amount of glass loading in the slurry is a critical factor: too little glass means the particles are not in contact with each other and the foam will slump before sintering can occur, and too much glass is difficult to foam.

Fig. 15 shows μCT images of Actifuse, a gel-cast foam scaffold and a sol–gel foam scaffold. Each of these scaffolds was produced by direct foaming, and the pore networks are similar to each other and to trabecular bone (Fig. 1).

8.2. Sol–gel-derived bioactive glass foam scaffolds

Before melt-derived compositions could be tailored to prevent glass crystallization during sintering, bioactive glass scaffolds were produced from the sol–gel process. As the silica network begins to form by room-temperature polymerization, T_g does not have to be surpassed to produce a foam scaffold. Porous scaffolds could therefore be produced using the simple binary and tertiary sol–gel compositions.

Figs. 8 and 9 illustrate the conventional sol–gel process for bioactive glass synthesis. A foaming step is added to produce scaffolds [180]. The process begins with conventional acid-catalysed preparation of a sol (Section 4), where TEOS is hydrolysed to form Si–OH species and condensation commences, initiating formation of the silica network. Nanoparticles of silica form and then coalesce before Si–O–Si bonds form between them. In the sol–gel foaming process, the gelation time is accelerated by adding hydrofluoric acid (HF) so that gelation occurs in a few minutes rather than the few days that are required in the conventional process. Surfactant and HF are added to the sol, which is then foamed by vigorous agitation. The viscosity increases and the foam is poured immediately prior to gelation. A hierarchical pore structure is produced with interconnected macropores [181] (Fig. 15c) and a textural nanoporosity (Fig. 7a) [182]. The surfactant-aided foaming process

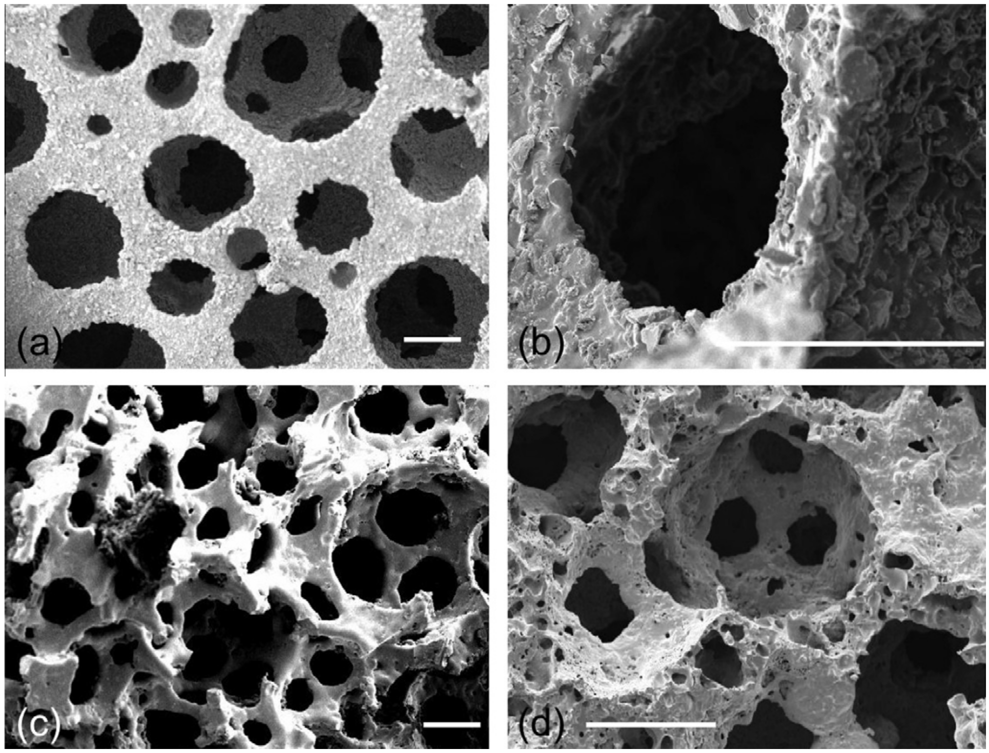

Fig. 14. SEM images from the gel-cast foaming process of a bioactive glass (ICIE16). (a and b) Glass particles within a polymer foam after polymerization of the monomer. (c and d) After polymer burn-out and sintering. Scale bars are 200 μm. Courtesy of Zoe Wu.

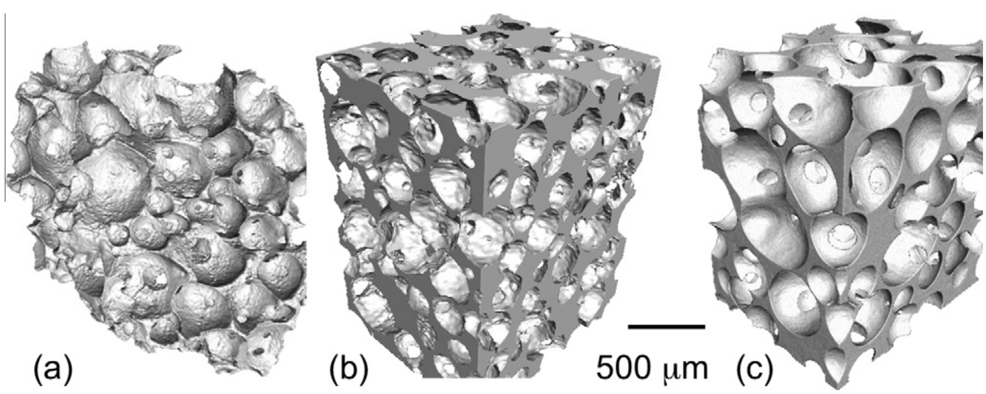

Fig. 15. μCT images of scaffolds made by foaming (a) Actifuse, (b) a gel-cast bioactive glass foam scaffold, and (c) a bioactive glass sol–gel foam scaffold. Courtesy of Sheng Yue.

produces interconnected macropores, and a nanoporous texture is inherent to the sol–gel process. There are many variables that affect the final morphology, of which surfactant concentration is key [152,183,184]. By sintering carefully, compressive strengths of 2.5 MPa can be achieved with a modal interconnect diameter of 100 μm between the larger spherical pores (diameter of 300–600 μm, 82% porosity) [185]. While it is difficult to produce crack-free sol–gel monoliths, foams several centimetres in diameter and height can be produced routinely because the open pore structure means that strut dimensions are of the order of millimetres or less, so the path for water evaporation through the nanopores is short.

The technique has been replicated by various groups [184,186–189]. Glass compositions are usually 58S or 70S30C, but the 45S5 composition has also been foamed. However, the 45S5 foam was sintered at 1000 °C, producing a glass–ceramic [190]. The calcium distribution throughout the struts of 70S30C foams at the micrometre scale was found to be homogeneous by elemental mapping from particle-induced X-ray emission (PIXE) associated with Rutherford backscattering spectroscopy (RBS) [191], but less so when foams were imaged with synchrotron X-ray microtomography [192].

Porous sol–gel foams have also been produced using the more traditional polymer foam reticulation [193] but the process offers little benefit over the sol–gel foaming method unless ordered mesoporosity is required. Ordered mesoporosity (5 nm) has been introduced into macroporous sol–gel bioactive glass foams by using non-ionic block copolymer P123 and polyurethane sponges as co-templates [194].

The sol can also be freeze-dried so that ice crystals are used as the template. Termed "ice-segregation-induced self-assembly" (ISISA), the sol (in its mould) is immersed into liquid nitrogen and hexagonal ice crystals form, pushing the sol to where the ice is absent. When the sol gels, ice is sublimed away, leaving thin struts and oriented pore channels. Although freezing rate can be used to control pore size, pores were no larger than 20 μm in diameter and, due to the thin struts, compressive strengths were less than 0.2 MPa [195].

8.3. Bioactive glass scaffolds from additive manufacturing techniques

Although direct foaming produces pore networks that mimic cancellous bone, control of pore size is limited to modal pore and interconnect sizes from the amount of surfactant used, the water content and agitation rate [152,183,196]. Pore morphology can be controlled more specifically using additive manufacturing techniques that can build scaffolds by depositing glass layer by layer [197]. The advantage of these techniques over foaming is that the scaffold pore structure is dictated by a computer-aided design (CAD) file. Recently, bioactive glass scaffolds were produced by a 3-D printing process called "robocasting" [198,199]. The scaffolds produced had thick struts (>50 μm) and pores in excess of 500 μm (Fig. 16). The alignment of the rows of struts was so accurate that compressive strengths of >150 MPa were achieved in the direction of the pore channels (50 MPa perpendicular to the pore channel directions), with 60% porosity. This is similar to the strength of cortical bone. The glass composition used was 6P53B (51.9 mol.% SiO_2, 9.8 mol.% Na_2O, 1.8 mol.% K_2O, 15.0 mol.% MgO, 19.0 mol.% CaO, 2.5 mol.% P_2O_5) with a particle size (D_{50}) of 1.2 μm. Inks were created by mixing 30 vol.% glass particles in 20 wt.% Pluronic F-127 solution. The inks were extruded through a 100 μm syringe nozzle and printed on an alumina substrate in a reservoir of non-wetting oil using a robotic deposition device. Viscosity of the ink is critical. After printing, the scaffolds were dried and sintered at 700 °C.

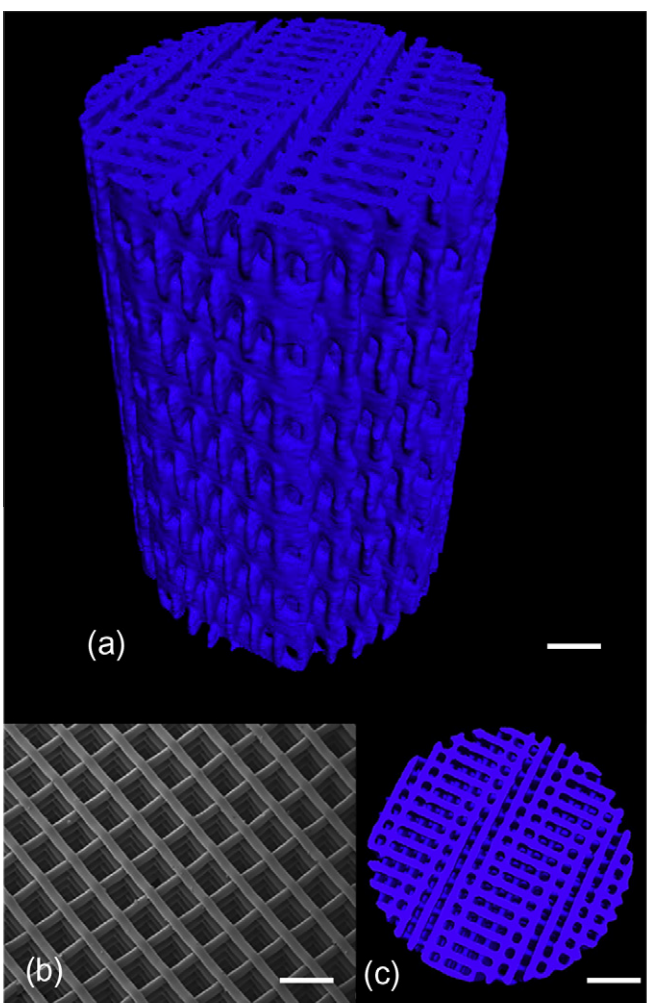

Fig. 16. Bioactive glass scaffolds produced by the robocasting solid freeform fabrication method. (a) 3-D μCT image; scale bar is 500 μm. (b) SEM image of cross-section; scale bar is 300 μm. (c) 2-D μCT image of cross-section; scale bar is 500 μm. Courtesy of Qiang Fu, Lawrence Berkeley National Laboratory, Berkeley, USA.

A similar method, termed "freeze extrusion fabrication" (FEF), combines extrusion printing with freeze-drying. FEF was used to make 13–93 glass scaffolds with 50% porosity and with pores and struts of equal size (300 μm), giving a compressive strength of 140 MPa [200,201]. A bioactive glass–polymer paste (particles <15 μm) was extruded and deposited layer by layer in a cold environment. Freeze-drying was used to remove the water that was in the paste before sintering at 700 °C. An alternative solid freeform fabrication method is selective laser sintering (SLS), where a laser is passed over a powder bed. An indirect SLS method was used to produce 13–93 scaffolds with pores in the range 300–800 μm with 50% porosity and compressive strength of ~20 MPa. Glass particles with a D_{50} of 42 μm were used [202] with a stearic acid binder. The CAD file dictates where the laser goes and therefore which regions are sintered. When the laser is focused on the particle–stearic acid mixture, the stearic acid melts and binds the particles as the laser moves on.

The high strengths obtained in additive manufacturing are a result of the ability to maintain highly interconnected channels (>300 μm) with high alignment at relatively low percentage porosity (50–60%). The scaffolds showed an elastic response during mechanical testing in compression, with an average compressive strength of 140 MPa and an elastic modulus of 5–6 GPa, comparable to the values for human cortical bone.

Bioactive sol–gel glasses can also be used in solid freeform fabrication. Sol–gel powders can be mixed with a binder, such as aqueous polyvinyl alcohol (PVA) and printed, after which the green body is sintered and the polymer burnt out [203]. Scaffolds with 60% porosity and pore sizes of 1 mm had compressive strengths of 16 MPa [203]. Owing to the nature of the sol–gel process, the sol can also be directly printed onto a substrate prior to gelation. An example is a scaffold that had three scales of porosity: large pores (up to 1 mm) from the solid freeform fabrication, ordered mesopores (~13 nm) from the use of a copolymer template (F127) and additional macropores (10–30 μm) from the use of a sacrificial methyl cellulose template. The sol containing the templates was extruded onto a heated substrate using a robotic deposition device. Critical to success was the viscosity of the sol, which was controlled by the methyl cellulose content [204,205].

Although bioactive glass scaffolds can mimic the porous structure of porous bone, with similar compressive strength (gel-cast [179] or sol–gel [185] foams), or can be made with strengths similar to cortical bone while having channels for tissue ingrowth (e.g. robocast glass [198]), they are still brittle and therefore not suitable for all grafting applications, such as sites that are under cyclic loads. Tougher scaffolds are required that still have all the bioactive properties of Bioglass 45S5. The obvious engineering solution is composite materials.

9. Bioactive glass composites

Tough conventional composites can be produced using a biodegradable polymer matrix with bioactive glass particles as the filler phase. The most common polymers used are polylactide (PLA) and polyglycolide (PGA) and their copolymers (PLGA), which have been used clinically for many years, mainly as degradable sutures [206].

Adding Bioglass 45S5 to polymers such as PLGA can increase the stiffness and compressive strength of the polymer. Composite scaffolds with 75 wt.% Bioglass 45S5 and 43% porosity, formed by fusing microspheres, had a Young's modulus (51 ± 6 MPa), which is double that of PLGA, but their compressive strength was similar to that of the polymer alone (0.42 ± 0.05 MPa) [207]. The compressive strength is too low even though the pores were small. In some cases, the addition of glass can be detrimental. For example, in composite rods of poly(DL-lactide) (PDLLA) and 13–93 bioactive glass particles (50–125 μm) produced using twin-screw extrusion, as the glass content is increased in the composite, the bending, torsional and shear strengths of the polymer decreased [208].

Perhaps the most promising Bioglass 45S5-containing composites for bone regeneration are the foams produced by thermally induced phase separation (TIPS, Fig. 17), which is a variation on freeze-drying [209]. The biodegradable polymer is dissolved in dimethylcarbonate and the glass fraction added (usually particles <5 μm). The mixture is quenched in liquid nitrogen before being stored at −10 °C. The solvent is then lyophilized. PDLLA foams containing 40 wt.% Bioglass 45S5 were produced with tubular pores (∼100 μm diameter) with interconnects of 10–50 μm and porosities of up to 97%. The thin pore walls allow the bioactive particles to be exposed. However, although the percentage porosity is high, the pore and interconnect sizes are less than ideal and the high percentage porosity (and thin pore walls) contribute to low mechanical properties. For example, a PLLA foam (94% porosity) with 15 vol.% Bioglass 45S5 had a stiffness of 1.2 MPa and a compressive strength of 0.08 MPa [210]. Sol–gel bioactive glass nanoparticles have also been introduced into freeze-cast gelatin–chitosan foams to give pore sizes in the range of 150–300 μm [211]. The low strength can be improved upon if the percentage porosity can be reduced. Bioactive glass–collagen–phosphatidylserine scaffolds (65 wt.% 58S sol–gel glass) with 75% porosity and pores of up to 300 μm were produced with a compressive strength of 1.5 MPa [212]. However, connectivity between pores was poor.

Polymer coatings have been applied to highly porous glass–ceramic foam scaffolds, of 90% porosity with pore diameter in the range of 500–700 μm, using PDLLA [213] or poly(3-hydroxybutyrate) (PHB) [214]. A very thin coating (1–5 μm on struts 100–200 μm thick) results in an improved work to fracture, but there was no change in compressive strength (0.3 MPa) [213]. There is also doubt over the effectiveness of polymer-coated scaffolds in terms of cellular response. The reason for using bioactive glass scaffolds is that they provide a bioactive surface. A polymer coating would mask that surface. The long-term effectiveness of the coating is also in doubt, as, once it degrades, only the brittle glass–ceramic scaffold will be left. These issues highlight general problems for all conventional composites: when bioactive glass particles are encased in a polymer matrix, the osteoprogenitor cells only encounter the polymer. Some particles will protrude from the surface, but the amount of particles protruding is difficult to control [208].

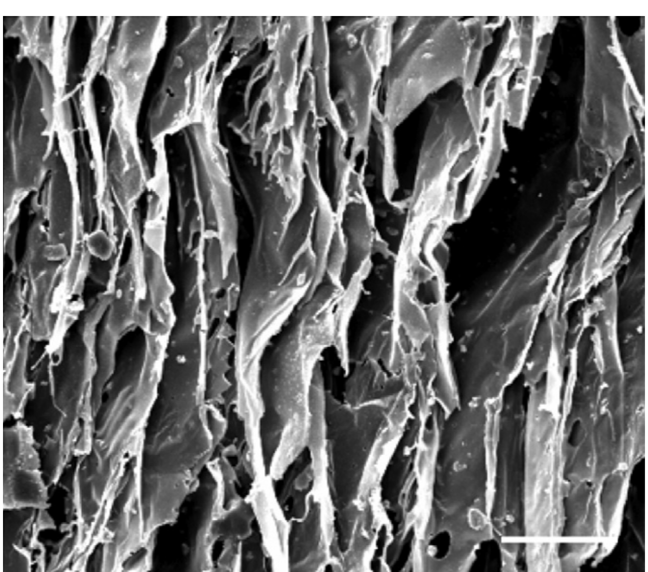

Fig. 17. An SEM image of a PLLA foam (94% porosity) containing 15 vol.% Bioglass 45S5 particles produced by the thermally induced phase separation (TIPS) process. Modified from Blaker et al. [210]. Scale bar is 100 μm.

Another concern is associated with the degradation rates of the two components of the composite. Ideally, the composite should maintain its mechanical properties as new bone grows. The two phases should degrade congruently and at a rate suitable for the application. However, in current bioactive glass–degradable polymer composites, the two phases degrade at different rates [215], which could cause instability of the scaffold and migration of the particles in vivo. It is difficult to match the degradation rate of a polymer to that of the glass and the difference can be worsened by the mechanism of degradation of the polymer. Polyesters are often chosen because they are approved by the US Food and Drug Administration (FDA). However, they degrade by hydrolytic chain scission. Each scission occurs by hydrolysis of an ester bond, which creates carboxylic acid groups, reducing the local pH. As pH moves from neutral, self-catalysis of the hydrolysis occurs [216]. Therefore, once degradation begins, it occurs rapidly, causing rapid loss in mechanical properties. The advantage of using bioactive glass as the filler phase compared to other bioceramics is that it releases cations on dissolution, which can locally buffer the acidic conditions that result from polyester degradation. However, adding bioactive glass to normally hydrophobic polyesters also increases the hydrophilicity of the composite, which increases water adsorption and therefore initiates polymer swelling and degradation [209,217,218]. Water can also penetrate the interfacial regions. Balancing these effects is difficult and does not remove the risk of non-homogeneous degradation and particle release. Another way to mitigate against autocatalytic degradation is to select different polymers, e.g. natural polymers such as gelatin (hydrolysed collagen) and chitosan (a polysaccharide). Many natural polymers can degrade by enzyme action, which results in a more linear degradation rate. The disadvantage is that it is more difficult to source reproducible natural polymers. Water uptake and swelling in gelatin–chitosan scaffolds containing sol–gel-derived bioactive glass particles decreased as the amount of glass increased [211]. However, the interface between the particles and the polymer was still weak.

In order to overcome the problems associated with conventional composites, materials must be developed that more closely resemble the hierarchical structure of bone, which is a nanocomposite consisting of an organic (collagen) and an inorganic (HCA) component [219]. The type of polymer used should also be reviewed in terms of degradation rate and mechanical polymers. Collagen has a natural triple-helix structure, which contributes to the high toughness of bone. It is also broken down by the natural bone remodelling process rather than by autocatalytic hydrolysis. Mechanical properties are further enhanced by the presence of chemical bonds at the interface of the HCA and collagen, where nanocrystals of HCA are thought to nucleate on the glutamic acid regions of collagen molecules during bone formation [220]. Creating covalent bonds between bioactive glass particles and a polymer is not trivial, and is an area that needs further research.

The production of nanocomposites with nanoparticles dispersed in a polymer matrix has the potential to improve interaction with host tissue/cells [218,221]. However, it is still difficult to match the degradation rate of the polymer with that of the glass. Mechanical properties are also not optimized if there is no interfacial bonding between the particles and the matrix. Part of the problem is the polymers used. Conventional polyesters degrade very rapidly once hydrolysis begins. Langer et al. have developed poly(polyol) sebacate, cross-linked elastomers [222], as alternative biodegradable polymers, but their hydrolysis can also yield toxic by-products. Composites have been produced using poly(glycerol sebacate) and Bioglass 45S5 fillers with ionic and covalent bonds between the components [223,224]. The poly(glycerol sebacate), was prepared by reacting a sebacic acid and glycerol. As the Bioglass 45S5 is added, it is thought to react with the –COOH groups of the sebacic acid, but the evidence for this is based on thermal analysis alone.

Dispersing nanoparticles homogeneously in a polymer matrix is a further challenge, which would be necessary to obtain a homogeneous composite. An alternative to conventional composites is hybrid materials.

10. Hybrid sol–gel materials

Inorganic–organic hybrid sol–gel materials are interpenetrating networks of inorganic and organic components that interact at the nanoscale [225]. The two components are indistinguishable above the nanoscale. This is different from nanocomposites, which have distinguishable components. However, synthesis of hybrids is complex and there are several chemistry challenges that must be overcome before hybrids will be successful in tissue regeneration [226].

Hybrids are synthesized introducing the polymer early in the sol–gel process, e.g. after hydrolysis of the TEOS, so that the inorganic (silica) network forms around the polymer molecules (Fig. 18), resulting in molecular-level interactions [226]. Of course, the thermal processing is modified from conventional sol–gel glass synthesis. Most hybrid systems are aged and dried below 100 °C. The hypothesis is that the fine-scale interactions between the organic and inorganic chains lead to the material behaving as a single phase, resulting in controlled congruent degradation and the potential for tailoring the mechanical properties [225]. The fine-scale dispersion of the two components means that cells are likely to attach to the hybrid surface as though it is one material, rather than bioactive particles dispersed in a polymer matrix. The aim is that a bioactive hybrid would have bioactivity similar to that of a bioactive glass, but have toughness and controlled congruent degradation.

Hybrids can be classified into two types depending on the interactions between the inorganic and organic chains. Class I hybrids contain molecular entanglements, hydrogen bonding and/or van der Waals forces. Class II hybrids also have covalent bonding between components [225] and are usually synthesized by first functionalizing the polymer with a coupling agent before it is introduced into the sol–gel process (Fig. 18).

As the polymer is usually added to the sol early, the sol–gel foaming process can be modified to produce porous scaffolds in a similar way to porous sol–gel glass foams [227]. However, there are many challenges that must be overcome to produce a successful hybrid [226,228]. The polymer must have a suitable degradation rate and be soluble in the sol–gel process. This eliminates most FDA-approved polyesters, as they are insoluble in water, unless they are functionalized to improve their solubility. A greater challenge is the incorporation of calcium into the hybrid. Calcium must be present if the material is to bond to bone and have the osteogenic properties of Bioglass 45S5. The final scaffold should also have controllable degradation, tailorable mechanical properties and a pore structure suitable for vascularized bone ingrowth. Once this has been achieved, the new materials have to be translated to product, which involves process up-scaling, FDA approval and eventually clinical trials.

In hybrid synthesis, the polymer is added to the sol during the condensation process. The chain-like structure of the silicate phase can entangle with the polymer chains. Under acidic catalysis, TEOS hydrolyses and then condensation continues, forming nanoparticles, which coalesce and then coordinate together to form a gel (Section 4) [74]. The gel is then dried.

The control of pH is important throughout the process, as it can affect the functionalization of the polymer and the gelation of the silica network. The longest gelation time is at the isoelectric point of silicic acid in water (pH ~ 2) [229]. The pH can also cause degradation of polymers during hybrid synthesis. Therefore, it may be necessary to raise the pH from less than 2 during sol preparation to close to 7 for polymer addition to maintain the molecular weight (M_w) and integrity of the desired polymer.

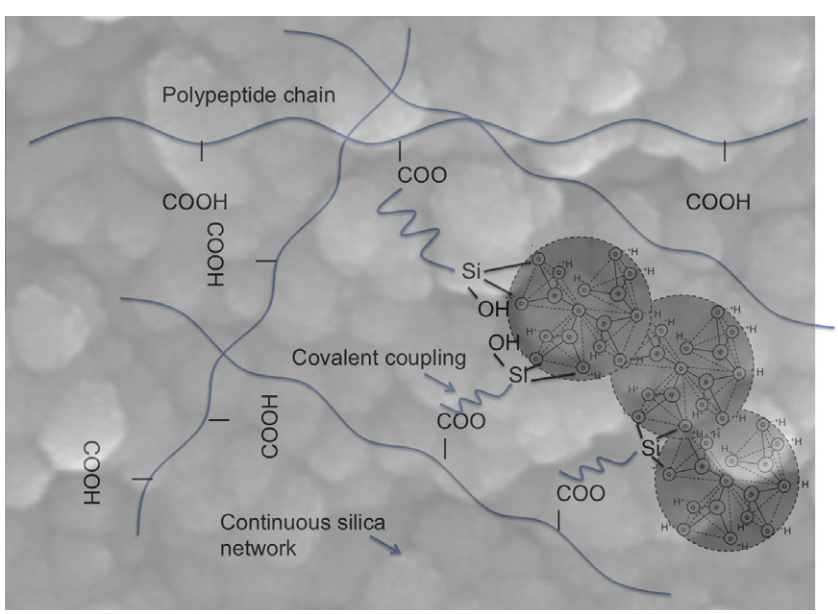

Fig. 18. Schematic of the interpenetrating inorganic and organic networks of a class II hybrid material. Three nanoparticles of the continuous silica network are highlighted. The polymer chains are linked to the silica network by a coupling agent (GPTMS). Carboxylic acid groups on the polymer act as nucleophiles to open the epoxy ring of the GPTMS and form a bond.

In class I hybrids, the polymer is mechanically entrapped in the silica network during condensation. The inorganic and organic chains are held together by mechanical and hydrogen bonding to the surface silanol (Si–OH) groups. Polycaprolactone (PCL)–silica hybrids have been produced using methyl ethyl ketone (MEK) as a solvent for the PCL, but there was no mention of how the solvent was removed (its boiling point is 80 °C and the hybrids were dried at 60 °C) and dissolution was not assessed [230]. Early sol–gel foam hybrids were produced by the incorporation of PVA into the foaming process prior to vigorous agitation [231]. PVA (M_w 16 kDa) was chosen because it is soluble and biocompatible. The low M_w was chosen so the polymer could be removed by the kidneys if it were used as an implant, as PVA is soluble rather than biodegradable. Porous foam scaffolds were successfully produced, and compression tests showed an improved strain to failure compared to bioactive glass foams and good response from MSCs [232]. However, as the PVA was not chemically linked to the silica, it was lost to solution rapidly in dissolution tests. Class II hybrids are needed.

There are two strategies for synthesizing class II hybrids: a coupling agent can be used to link the silica and the polymer; or a polymer can be used that already contains silane bonds. An example of a polymer that contains silane bonds is polydimethoxysilane (PDMS). PDMS has a silica backbone with organic side groups. When it is added to a sol, the terminal methyl groups hydrolyse to form silanol groups, which can condense with other silanol groups from hydrolysed TEOS, bonding the silica network to the PDMS [233–235]. The composition with 14 mol.% PDMS in TEOS had an elastic modulus of 106 ± 15 MPa and a bending strength of 4.5 ± 1.2 MPa. Although excellent coupling can be achieved, PDMS is not a degradable polymer, so it is not appropriate for a tissue scaffold.

A strategy for forming covalent bonds between a degradable polymer and the silicate network is the use of coupling agents. The polymer can be functionalized with a coupling agent before it is incorporated into the sol–gel process. The coupling agents are usually short-chain polymers containing three alkoxysilane groups on one end of a chain and a functional group that can attach to the polymer on the other end. The single functional group must react and bond to the polymer during the functionalization procedure. Polymers can be selected that contain nucleophilic groups such as –OH, –COOH or $–NH_2$ groups. An example of a coupling agent is glycidoxypropyltrimethoxysilane (GPTMS), which has an epoxy ring on one end that is susceptible to nucleophilic attack and three methoxysilane groups on the other end of the molecule [236]. A polymer containing nucleophilic groups can be functionalized with GPTMS as the nucleophilic groups open the epoxy ring. The functionalized polymer then has side chains with alkoxysilane groups and it is added to the sol–gel process [226,227]. The alkoxysilane groups on the polymer undergo hydrolysis and then condensation with the silanol bonds on the silica nanoparticle network that is forming in the sol, linking the two components (Fig. 18). Independent control of coupling and M_w of the polymer is important as both affect the mechanical properties and the degradation rate of the hybrid.

Functionalizing the polymer can increase its solubility. For example, functionalization of insoluble PCL with a coupling agent allows it to be used in hybrid synthesis. Poly(ε-caprolactone) diol was functionalized with isocyanatopropyl triethoxysilane (IPTS) [237,238]. The cyanate group of the coupling agent reacts with the terminal hydroxyl groups of the PCL chains, leaving short molecules with three ethoxysilane groups on each end of the PCL. Therefore, increasing the degree of coupling in this hybrid requires the M_w of the polymer to be reduced. Reducing M_w from ~2.3 kDa to ~6.6 kDa resulted in more rapid degradation despite the increased cross-linking. PCL hybrids with 60 wt.% PCL (M_w = 6693 Da) had a Young's modulus of 582 MPa and a tensile strength of 21 MPa. Further tailoring of the properties was limited by the coupling site, which was only at the ends of the polymer chains.

It is therefore more beneficial to use polymers with the functional groups as side groups of a chain, which allows control of the degree of cross-linking independent of molecular weight. This is not possible for conventional polyesters.

As one aim of using hybrids is to mimic the natural structure of bone, type I collagen is an obvious candidate polymer as it is 90% of the organic component of bone. Its excellent mechanical properties are due to its triple helix of polypeptide chains. The polypeptide chains are composed of amino acids, which contain many $–NH_2$ and –COOH groups that are available for functionalization. Collagen is remodelled by natural bone regeneration mechanisms, i.e. by specific enzymes (collagenase). However, the triple-helix structure makes processing collagen for scaffold synthesis difficult, as it is very insoluble. It can only be dissolved in acetic acid in low concentration. Low-density scaffolds can be produced by freeze-drying [239], but collagen is not suitable for hybrid synthesis.

An alternative is gelatin, which is hydrolysed collagen. It retains the functional groups along its chains but it is soluble in water. Class II silica–gelatin hybrid scaffolds have been produced using GPTMS to couple between a silica network derived from hydrolysed TEOS and the gelatin [227]. The coupling mechanism was confirmed by solid-state NMR. As the amount of covalent coupling increased, the amount of gelatin released unsurprisingly decreased. Importantly, the rate of silica release also decreased and followed a similar profile to the gelatin release. This implies that dissolution was congruent and it degraded as one material, a true hybrid. The compressive strength also increased as covalent coupling increased. Porous scaffolds were produced with up to 90% porosity and large open pores by the sol–gel foaming process with the addition of a freeze-drying step after gelation (Fig. 19). Scaffolds containing 60 wt.% organic component with low degrees of coupling had the flexibility of thermoplastic polymers. Doubling the inorganic–organic coupling caused a 360% increase in stiffness. Applying cellular solid theory indicated that scaffolds containing 53 wt.% gelatin with GPTMS/gelatin molar ratio of 750 and with a modal interconnect diameter of 100 μm would have a compressive strength of 2.6 MPa [227]. In early silica–gelatin hybrids, TEOS was not used; the silica network was formed from the GPTMS alone [236], where the hydrolysed GPTMS forms Si–O–Si bonds with other hydrolysed GPMTS molecules. A disadvantage is that the degree of coupling could not be controlled independently from polymer content and the mechanical properties were not reported.

A disadvantage of using a naturally derived polypeptide such as gelatin is that the amino acid chains are not necessarily uniform. So it is difficult to define exactly how many covalent links will form between the gelatin and silica, as it is not known how many functional groups each gelatin molecule will have.

Poly(γ-glutamic acid) (γPGA) is a simpler biopolymer produced by bacterial culture [240]. Each repeating unit contains a –COOH group. The polymer is found in the free acid form or in salt forms, including sodium and calcium salts, where cations associate with the –COOH group [241]. The salt forms of γPGA are very soluble in water [240] but the free acid form (γHPGA) has to be dissolved in dimethyl sulfoxide (DMSO) for hybrid synthesis, which must be removed after processing. Class II hybrid scaffolds have been produced using γHPGA functionalized with GPTMS in DMSO [242,243]. The mechanical properties are promising, but a potential barrier for regulatory approval of these promising scaffolds is whether the polymer produced by the fermentation process is reproducible in terms of molecular weight and racemic structure.

Freeze-drying is an alternative method to foaming and is particularly suitable for polysaccharides such as chitosan [244]. While high (e.g. 95%) porosity can be attained, the struts are often thin and form long angular pores, which can limit mechanical properties. The repeating unit of chitosan contains a ring structure with –OH and $-NH_2$ functional groups, and chitosan was successfully reacted with GPTMS (without TEOS) to form non-porous flexible membranes (thickness 70 μm) [245,246]. The mechanical properties were tailored with the amount of GPTMS. Increasing the GPTMS content from 9 to 33 mol.% caused the breaking stress to decrease from 95 MPa to 2.4 MPa while the Young's modulus increased from 2.7 MPa to 4.8 MPa, which is three orders of magnitude less than that of bone (18–20 GPa), making it unsuitable for a bone scaffold. When freeze-drying was used to produce scaffolds, pore diameters of up to 100 μm (90% porosity) were attained [247]. Pore morphologies were similar to other freeze-dried or TIPS scaffolds (Fig. 17) and mechanical properties were not reported.

Until now, most hybrids have not contained calcium. The calcium precursor in sol–gel glass synthesis is usually calcium nitrate tetrahydrate ($Ca(NO_3)_2{\cdot}4H_2O$), due to its high solubility, but the nitrate by-products are cytotoxic. This is fine in sol–gel glass processing, as the glasses are heated to 600 °C or higher to remove the nitrates [67]. This is not possible for hybrid synthesis. Recent studies also show that, when soluble calcium salts are used as calcium precursors, the calcium does not enter the silica network and become a network modifier until a temperature of 400 °C is reached [74,100,135]. The calcium salt remains dissolved in the sol throughout the formation of the silica network and in the condensation by-products until the gel has dried. The calcium only diffuses into the silica of 400 °C [74]. A different calcium source is required. To avoid the problem of nitrate toxicity, calcium chloride has been used as the calcium source to produce silica–calcium–PVA [249], silica–calcium–phosphate–PCL [230], silica–calcium–chitosan [246] and silica–calcium–γPGA [242,243] hybrids. Toxic by-products were avoided, but calcium was not incorporated into the bulk of the material, as calcium chloride recrystallized on the surface during drying because a maximum temperature of 60 °C was used [243,248]. New calcium precursors are needed if tough osteogenic scaffolds are to be produced. Calcium methoxyethoxide (CME) has been used in trials for bioactive glass processing [249]

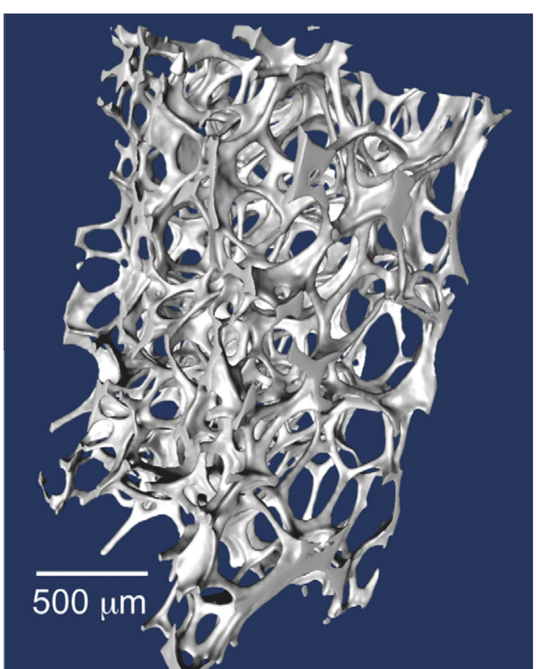

Fig. 19. X-ray microtomography image of a class II silica–gelatin (60 wt.% functionalized gelatin) hybrid scaffold. The hybrid has 90% porosity. Covalent coupling between silica and gelatin provided by functionalizing the gelatin with GPTMS (Fig. 18). Courtesy of Oliver Mahony and Sheng Yue.

but translation to hybrid processing is challenging due to its sensitivity to water [250,251]. One type of CME-based hybrid is "star gels", which are hybrids with an organic core surrounded by flexible arms terminated in alkoxysilane groups [252,253]. The alkoxysilanes form a silica-like network via hydrolysis and polycondensation. Monoliths had a Young's modulus of 1 GPa and compressive strength of 250 MPa. The fracture toughness of the material was measured at ~3 MPa $m^{1/2}$, which is in the range of that for cortical bone and three times higher than for conventional sol–gel bioactive glass. Also under cyclic fatigue tests the star gel outperformed a human femur by twice the number of cycles to failure. Unfortunately, the resorption characteristics and cytotoxicity were not reported. Electrospun silica–calcium–PLLA scaffolds (type I hybrids with only 20 wt.% silica) have been produced using CME through electrospinning [251]. But as CME is highly sensitive to water (it gels rapidly), it has not yet successfully been employed in the sol–gel foaming process, which requires water for the surfactant to operate. New calcium sources are still needed. Much work is also needed in translation of these materials from bench to clinical products.

11. Bioactive glasses and nanotechnology

11.1. Nanoparticles

Silica nanoparticles have great potential for various applications such as cell tracking and intracellular delivery of molecules, ranging from therapeutic agents to proteins and DNA [254]. Both melt and sol–gel glasses can be made in the form of nanoparticles.

Melt-derived (e.g. Bioglass 45S5) nanoparticles (20–80 nm) can be produced by flame synthesis, where the reagents, e.g. silica, sodium carbonate, calcium carbonate and phosphate, are fed into a flame reactor [255]. The reagents melt instantly in the flame and as they move away they quench to form a glass. The nature of the process means that it is possible to dope the glass, e.g. with radio-opaque agents [256].

The more common way to produce silica nanoparticles is through the sol–gel process. The Stöber process [72] uses ammonium hydroxide as the catalyst to increase the pH above the isoelectric point of soluble silica (silicic acid) [229]. The pH causes repulsion between the newly formed silica particles and terminates polycondensation. Therefore, after primary particles form due to hydrolysis (Fig. 8), some condensation occurs to form spherical secondary particles, but bonds do not form between the particles, so secondary particles remain as particles (Fig. 7b). The final size of the spherical silica powder can be controlled by pH, type of silicon alkoxide and reaction temperature. Small silica spheres have potential for cell labelling and drug delivery. This is because, if they are small enough to enter a cell and do not cause the cell to change behaviour, they can be used to carry therapeutic agents, e.g. small drug molecules. Of particular benefit are small particles that contain nanopores. Drugs and growth factors can then be loaded into the particles and the payload can be delivered into cells by the particles [78,257]. Mesoporous silica particles are also being designed to kill cancerous tumours. The challenge is to ensure that the payload reaches the tumour and only the tumour. Ordered pores are made by adding a surfactant micelle template to the sol (Fig. 20) [77]. Ashley et al. [254] have developed protocells that have mesoporous silica nanoparticles at their core but are surrounded by lipid bilayers that prevent premature release of payload, and by signalling molecules that target tumours and other molecules that trigger release of the payload once the particles reach their target.

Although producing spherical and monodisperse silica particles is now routine, synthesizing bioactive glass nanoparticles is not trivial. It is a challenge to incorporate calcium into the composition.

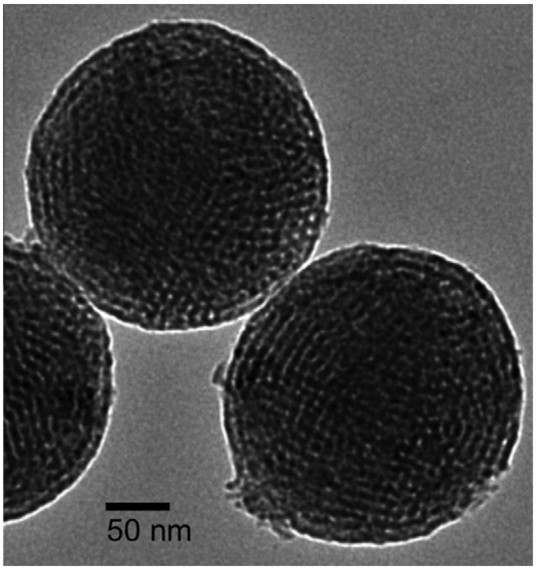

Fig. 20. Transmission electron microscope image of ordered mesoporous silica particles. Courtesy of Lijun Ji, Yangzhou University, China.

Adding calcium causes the particles to become irregular in morphology [73]. Calcium nitrate is usually used as the nitrate source, and, as discussed in Section 10, calcium is not incorporated into nanoparticles until they are heated to 400 °C [74]. Therefore, the amount of calcium that can enter the nanoparticles is dependent on the diffusion of calcium. When a polymer (or surfactant) is used to template the particles to improve dispersion and spherical shape, it can inhibit calcium diffusion, limiting the amount of calcium that can enter the glass [74]. Careful control of pH [211,258,259] and the use of aerosol techniques [260] may help to increase the calcium content, but unfortunately compositions of the particles made by these methods are rarely documented in the literature, or only non-quantitative *energy-dispersive X-ray* spectroscopy (EDX) data are provided. An alternative strategy is to produce a gel by conventional sol–gel methods and to grind the gel after drying and prior to stabilization [212,261,262]. Particles of 100 nm and below can be produced this way due to the nanoporosity of the glass making grinding easy, but the particles are less spherical and of broader distribution than those produced by Stöber-like processes.

Bioactive nanoparticles with ordered mesopores have been produced through surfactant templating [263] and through aerosol processes [260,264]. Adding calcium affected pore morphology and particle size [263]. Silica particles exhibited a hexagonal arrangement of mesopores, but when 16 mol.% of calcium oxide was added to the composition, the pores were in a wormhole-like arrangement and the mean particle size decreased from 160 nm to 30 nm. High calcium contents were again not reported. Adding phosphate to the composition did not change the particle size or the pore network.

Bioactive mesoporous particles have also been found to have haemostatic (blood clotting) properties and have emerged as a potential rapid clotting agent for large wounds such as battlefield injuries [264]. More conventional wound healing materials tend to be in the form of fibre mats or textiles, and glasses can now also be made in that form.

11.2. Nanofibres

Thin glass fibres can be highly flexible. However, the narrow sintering window of Bioglass 45S5 makes it difficult to produce fibres by conventional melt-spinning methods without the glass crystallizing. One of the benefits of the 13–93 composition is that fibres can be drawn from the melt, but this method yields micrometre-scale diameter fibres [265]. Nanofibres are of interest in regenerative medicine as they have the potential to mimic the natural morphology of collagenous extracellular matrix, which may provide beneficial cellular response in certain applications [266]. Only the novel laser spinning approach has produced amorphous Bioglass 45S5 fibres (Fig. 21a). Nanofibres were produced by concentrating a laser on a Bioglass 45S5 monolith. The laser created a small pool of molten glass, which was spun using a high-velocity gas jet from a supersonic nozzle [84]. The rapid rate of cooling suppressed crystallization and produced a non-woven 3-D fibre ball. However, owing to the small diameters of the fibres and their highly bioactive composition, the fibres rapidly dissolved in SBF, leaving HCA tubules (Fig. 21b) [84]. This is similar to what was observed for Bioglass 45S5 particles (e.g. Biogran) in certain in vivo studies [18].

Electrospinning is a popular technique for producing nanofibres in mesh or fibre mat morphology that uses an electric field to send fine streams of solution to an earthed collector [267–269]. The first electrospun bioactive silcate glass was the sol–gel 70 mol.% SiO_2, 25 mol.% CaO, 5 mol.% P_2O_5 composition with mean fibre diameter of 84 nm [269]. Viscosity is critical in electrospinning, so a small amount of polymer (polyvinylbutyral in ethanol) was added to the sol prior to spinning. Submicrometre bioactive glass 70S30C fibres were also electrospun with the addition of PVA to the sol [269]. Hollow mesoporous bioactive glass fibres (~600 nm in

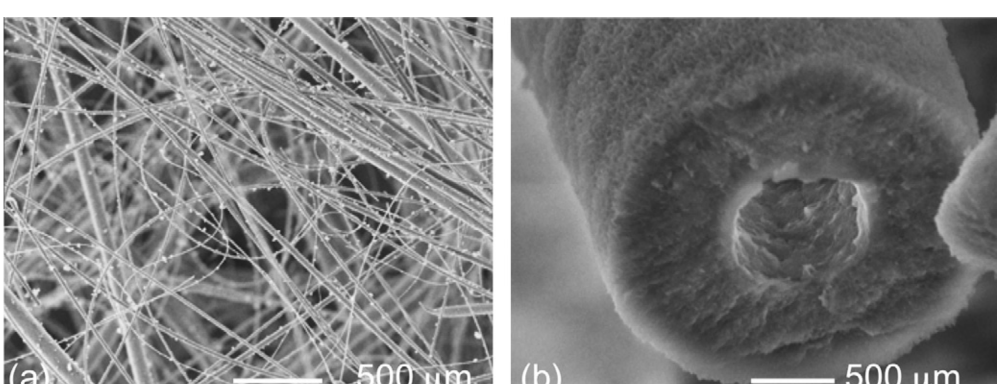

Fig. 21. SEM images of Bioglass 45S5 nanofibres produced by the laser spinning method. (a) The as-produced fibres. (b) After 48 h in simulated body fluid a fibre has become a tube of HCA. Modified from Quintero et al. [84].

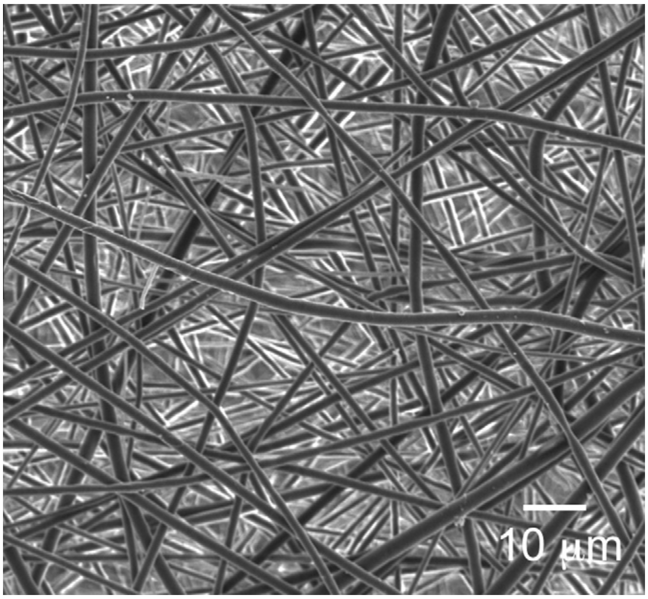

Fig. 22. SEM image of an electrospun sol–gel hybrid fiber mat of silica–calcium–PLLA (20 wt.% silica). Courtesy of Gowsihan Poologasundarampillai.

diameter) were also produced using high-M_w poly(ethylene oxide) as a phase separation agent [270]. In these examples, the polymer was burnt out during stabilization to leave glass fibre meshes. More recently, hybrid scaffolds have been successfully electrospun. An example is a fibre mat of 40 wt.% silica in PCL [271]. The fibre mat had fibre diameters of ~400 nm and was much less hydrophobic than PCL, but the silica dissolution was too rapid (80% of soluble silica had resorbed within 3 days). A similar reduction in hydrophobicity was seen for silica–PLLA hybrids with silica contents up to 20 wt.% [251]. However, in this case only 20% of the total silica in the sample was released in 7 days. Kim and Rhee electrospun PLGA/silica hybrids containing calcium chloride but did not report on the proportion of inorganic to organic [272]. As calcium was added as calcium chloride, it would have remained in the form of calcium chloride in the fibres. Calcium was successfully incorporated into the silica–PLLA hybrid materials using calcium methoxyethoxide (CME) to produce the first electrospun hybrid fibres of bioactive compositions [252]. Owing to the sensitivity of CME to water, a twin syringe system had to be developed to feed the sol to the needle. The sol containing some PLLA was mixed with more PLLA containing some CME in a mixing zone immediately prior to the needle tip. Fig. 22 shows electrospun silica–calcium–PLLA fibres (20 wt.% silica) with diameters in the range from 700 nm to 4 μm. The resulting fibres showed sustained (rather than burst) silica and calcium release in dissolution.

12. Angiogenesis

The ability of bioactive glasses to stimulate bone matrix has already been discussed, but, for the regeneration of large defects, blood vessels must enter the defect, otherwise any new bone formed will die, as it will be starved of nutrients. When a porous scaffold is used, transport of oxygen and nutrients is initially dependent on diffusion, which is limited to a few hundred micrometres from vessels, so new vessels must be produced and they must penetrate the porous scaffold [273]. Whether bioactive glasses take an active role in stimulating angiogenesis is a topic of much discussion [274].

Angiogenesis can be stimulated through the delivery of angiogenic growth factors such as vascular endothelial growth factor (VEGF) [275]. However, growth factors do not have to be delivered in a drug delivery approach – the scaffold can stimulate cells to secrete the growth factors. In vitro studies suggest that bioactive glass dissolution products can stimulate fibroblasts to secrete VEGF and endothelial cells to proliferate [276,277]. Importantly, the increase was not due to an increase in cell number. Similarly to osteoblast response to bioactive glasses, VEGF expression was dose-dependent [278]. Media containing the VEGF from fibroblasts can then stimulate endothelial cells to form vascular networks [277].

Mitogenic stimulation of endothelial cells occurred when they were cultured on tissue culture plastic in the presence of Bioglass 45S5-coated (slurry dipping) PLGA scaffolds (in trans-wells), compared to uncoated PLGA scaffolds. When VEGF was incorporated into the polymer, the mitogenic stimulation increased, but it increased further when the PLGA/VEGF scaffold was coated with the glass [279]. Endothelial cells cultured on tissue culture plastic in the presence of collagen sponges containing Bioglass 45S5 (0.6, 1.2 and 6 mg) enhanced proliferation and endothelial tube formation in a dose-dependent manner, with the greatest effect occurring on the sponges containing 1.2 mg of Bioglass 45S5 [280]. As a result, the cells exposed to 1.2 mg of Bioglass 45S5 produced higher quantities of VEGF mRNA. It is not clear which specific bioactive glass dissolution ions caused increased VEGF production. It could be an increase in extracellular calcium ions that is responsible for this effect [281].

There are in vivo data (subcutaneous implantation in rats) to support the in vitro results, but not every experiment showed the same positive results. In some experiments, angiogenesis was enhanced in PGA scaffolds coated in Bioglass 45S5 compared to uncoated scaffolds [276,282]. Collagen–Bioglass 45S5 composites in rat calvaria also stimulated more neovascularization in 2 weeks than collagen alone [283]. However, other similar experiments, such as Bioglass 45S5-coated PLGA scaffolds in mice [284] and polyethylene containing Bioglass 45S5 in orbital implants in rabbits [285], showed little difference from the polymers without the glass. It could be that the relative doses of glass were higher in the implants that showed enhancement, e.g. the same concentration of glass was implanted into the mouse and the rat. Dose-dependent effects were observed in vitro. Whatever the reasons for the discrepancy, it seems to be difficult to control the amount of angiogenic stimulation using conventional bioactive glasses alone.

An alternative is the tissue engineering or cell therapy approach, where cells are seeded on the scaffold prior to implantation. Seeding 13–93 bioactive glass scaffolds with rat-bone-marrow-derived MSCs enhanced (3×) tissue infiltration into bioactive glass scaffolds [176] in subcutaneous sites in rats over 4 weeks compared to unseeded scaffolds. This can even be taken a step further where vessels can be grown inside scaffolds in vitro and the construct implanted such that the vessels connect to the host's blood vessels [286]. Questions remain over tissue engineering approaches. For example, how practical are they for a patient and surgeon, as cells have to be harvested, shipped to a laboratory, expanded and seeded on a scaffold and cultured? The tissue engineered construct then has to be returned to the clinic. Having the material alone stimulate angiogenesis would be of much greater benefit.

A recent strategy has been to design bioactive glass scaffolds that can trick the body into thinking that the bone defect site is hypoxic (low oxygen pressure). When hypoxia occurs, a cascade of processes is initiated that results in the production of new blood vessels. A successful hypoxia-mimicking material would stimulate natural blood vessel growth. The strategy involves doping glass compositions so they will release ions, such as cobalt, that can simulate hypoxia. The hypothesis is that under normal oxygen pressure the hypoxia inducing factor 1a (HIF-1a) transcription factor is degraded via proteasome but under hypoxic conditions HIF-1a degradation is inhibited [287]. When HIF-1a is not broken down, it initiates the expression of many genes associated with tissue regeneration. Cobalt ions can stabilize HIF-1a, preventing its breakdown and thereby simulating hypoxia [288]. A bioactive glass containing small amounts of CoO (<5 mol.%) is likely to be an efficient delivery vehicle for cobalt ions [289]. In terms of glass formation, the cobalt behaves in a similar manner to magnesium in that it can act as a network former and a network modifier, so its addition reduces glass dissolution rate and HCA layer formation. If the glass is wanted for wound healing or other soft tissue applications, magnesium can be added to prevent HCA formation while still allowing cobalt release [289]. Cobalt has also been incorporated (5 wt.% using $CoCl_2$) into sol–gel scaffolds with large pores (300–500 μm) and ordered mesopores (5 nm), which enhanced not only bone-related gene expression of bone-marrow-derived MSCs, but also VEGF protein secretion and HIF-1a expression compared to cobalt-free scaffolds [290]. Perhaps the most surprising piece of data from this study was the cobalt release rate. As cobalt levels were low, as Co^{2+} ions might be expected to fill the same sites as Ca^{2+}, and as Ca^{2+} release from sol–gel glasses is rapid, all the cobalt might be expected to be released within the first few hours of exposure to solution. However, sustained cobalt release into culture media was observed over 7 days. A question that needs answering is how long should there be the presence of cobalt and a simulation of hypoxia in a bone defect for ideal bone regeneration? Systemic effects of cobalt ions should also be considered, although levels are low. Further research is needed in this intriguing area.

13. Antibacterial properties

Bioactive glass can kill microbes due to the pH rise caused by cation release during dissolution [291]. As an example, S53P4 was shown to kill pathogens connected with enamel caries (*Streptococcus mutans*), root caries (*Actinomyces naeslundii*, *S. mutans*) and periodontitis (e.g. *Actinobacillus actinomycetemcomitas*) in vitro. When S53P4, 13–93 and other compositions were added to broth cultures of 16 different bacteria, concentrations of 50 mg ml^{-1} (<45 μm particles) or higher showed antibacterial properties, which were attributed to the pH increase [292,293]. Unfortunately, cell culture with other cell types was not performed to show whether these pH conditions were toxic to other cell types. Bactericidal properties due to pH increase may be relevant in vivo, as the in vivo environment is in sink conditions, so the pH may not increase to the same levels in vivo.

Silver ions are known to be antimicrobial and they can be introduced into a glass easily (e.g. substituting Na for Ag). The Ag ions are then released during dissolution. The first silver-containing antibacterial glass was a sol–gel-derived composition: 76 wt.% SiO_2, 19 wt.% CaO, 2 wt.% P_2O_5 and 3 wt.% Ag_2O [294]. In these studies, only 1, 0.5 and 0.5 mg ml^{-1} of glass in culture was needed to kill bacteria *Escherichia coli*, *Pseudomonas aeruginosa* and *Staphylococcus aureus*, respectively, compared to 50 mg ml^{-1} of glass that was needed for the silver-free glasses to be bactericidal (and perhaps toxic) [295]. Importantly, the low concentrations of the sol–gel glass that was bactericidal were not toxic to human osteoblasts, and 45S5 was not found to have antibacterial properties under the conditions tested [296]. Silver-doped bioactive glass nanospheres that provide sustained silver release can also be synthesized by adding silver nitrate into the modified Stöber process [296].

In other studies, nanoparticles of 45S5 have been shown to kill *Enterococcus faecalis*, a micro-organism associated with failed root canal treatments [297]. This again could be a pH affect. The disadvantage for the synthesis of sol–gel glasses that contain silver is that they must be synthesized under infrared lighting and stored in the dark to prevent the silver nitrate precursor and Ag_2O in the glass reducing to silver metal. This increases the cost of commercialization and complicates potential surgical procedures. Silver has also been incorporated into melt-derived glasses, which showed improved bactericidal properties compared to silver-free equivalent glasses [298].

Whether adding zinc to a bioactive glass is beneficial or detrimental is not quite clear [299]. It is thought to have antibacterial properties [300] and some studies report beneficial cellular response [301,302], but it can also cause toxicity [303].

14. Strontium doping

Strontium ions have been shown to be beneficial to patients suffering from osteoporosis, as they inhibit osteoclast activity [304]. Therefore, strontium incorporation in bioactive glasses may be an effective way to deliver a steady supply of strontium ions to a bone defect site for osteoporotic patients [305]. However, too much osteoclast inhibition may inhibit long-term bone regeneration, as the remodelling process may also be inhibited. The effect of strontium substitution into the Bioglass 45S5 composition on glass properties and osteoblast and osteoclast response was investigated by replacing 0–100% of the calcium with strontium. Metabolic activity of osteoblasts and osteoclast activity inhibited in the presence of dissolution products from the glasses as strontium substitution increased. Alkaline phosphatase activity of osteoblasts cultured on the glasses also increased with increased strontium substitution [305–307]. Increasing strontium substitution also decreased the T_g of the glass, but left $T_{c,onset}$ unchanged, widening the sintering window. The sintering window increased from 140 °C to 190 °C as strontium content increased from 0% to 100% [149]. Molecular dynamics simulations [308] and solid-state NMR data [149,306,307] agree that the network connectivity did not change. Therefore, strontium-containing compositions may be useful for scaffold processing.

Other studies have also been carried out on strontium-containing melt-derived glasses, including in vitro and in vivo studies [309], but unfortunately substitutions were performed in wt.%. As strontium has higher mass than calcium, replacing calcium with an equivalent weight of strontium means that there would be less strontium atoms in the glass than there were calcium atoms. This would increase the network connectivity and therefore reduces the bioactivity of the glass, making comparison between glasses difficult [310].

Strontium can also be incorporated into the sol–gel process using strontium nitrate as the precursor [311]. In glasses with a base composition of 61 mol.% SiO_2, 31 mol.% CaO and 5 mol.% P_2O_5, calcium was replaced with up to 10 mol.% strontium. Increasing strontium retarded HCA layer formation in SBF. Rat cranial osteoblast proliferation and their alkaline phosphatase activity were dose-dependent, with 5 mol.% of Sr optimal [312]. Unfortunately, osteoclasts were not investigated. The dissolution rate was also seen to decrease with strontium content in binary and other ternary sol–gel glasses, but the substitutions were made in wt.% [313]. However, HCA layer formation rate increased. Mouse osteoblasts cultured in the presence of bioactive sol–gel glass particles containing 5 wt.% SrO showed a significant up-regulation of Runx2, Osterix, Dlx5, collagen I, ALP, bone sialoprotein (BSP) and OC mRNA levels on day 12, which was associated with an increase of ALP activity on day 6 and OC secretion on day 12 compared to glasses with less or zero strontium [314]. Strontium doping therefore remains of interest for synthetic bone grafts, especially for patients with osteoporosis.

15. Summary and outlook

Clinical and in vivo studies on commercially available bioactive glass particulates show that bioactive glasses can perform better than other bioceramic particles but not as well as autograft bone. Porous granules of silicon-doped HA are the market-leading synthetic bone graft. One reason is that the commercially available (and FDA-approved) bioactive glass particles cannot be made into porous scaffolds without them crystallizing during sintering. Now, through understanding how atomic structure and network connectivity relate to sintering and bioactivity, new compositions have been developed that can be sintered without crystallizing, and new techniques such as gel-cast foaming, sol–gel foaming and solid freeform fabrication can be used to make structures that mimic porous bone or that have large channels and compressive strengths larger than porous bone. Translation of these new products is necessary for them to be used in the clinic, i.e. up-scaling with good manufacturing practice and clinical trials. However, these porous scaffolds can only be used in sites where there is little load or only compressive load. Autograft still has better toughness. Scaffolds are still needed that have all the properties of the porous bioactive glasses but can also be pressed into defects, be cut to shape by surgeons and share cyclic loads with the host bone. If the scaffolds can take load, bone regeneration will be of higher quality, as good bone remodelling requires load.

Conventional composites do not seem to be able to mimic the hierarchical structure of bone. A class of materials that has potential to mimic the nanostructure of bone and have tailorable mechanical properties and degradation rates are inorganic–organic hybrids. However, the synthesis chemistry is challenging and perhaps the ideal polymers have not yet been used or even synthesized. Biomaterials is an area that would really benefit from more synthetic polymer chemistry. The biodegradable polymers that are used at present are great for certain applications, such as sutures, but their degradation profiles are not ideal for structural scaffolds.

Optimizing these new biomaterials requires understanding their structures and properties. The fields of bioactive glasses and hybrids are really pushing the boundaries of materials characterization. Interconnected porous networks can now be non-destructively imaged and quantified by μCT imaging and image analysis [182,315]; and the atomic structure of glasses and hybrids can be understood through NMR, X-ray and neutron diffraction [135] and particle-induced X-ray emission (PIXE) [191]. The information can be related to cellular response and fed back into materials design.

Once new materials have been developed, we need to understand if they will work. Academics are working on new ISO standards for bioactivity testing and cell culture screening. Academics should also agree on the best animal models to use to test materials and allow comparison between them. If new materials are to reach the clinic, medical device companies and the regulatory bodies also need to be open to adapt to new materials and techniques.

Disclaimer

The author is not employed by any of the companies mentioned in this paper.

Acknowledgements

The author thanks the UK Engineering and Physical Sciences Research Council (EPSRC) for funding (EP/I020861/1).

Appendix A. Figures with essential colour discrimination

Certain figures in this article, particularly Figs. 1, 2, 4, 6, 8, 9, 10, 13, 16, 18, and 19, are difficult to interpret in black and white. The full colour images can be found in the on-line version, at http://dx.doi.org/10.1016/j.actbio.2012.08.023.

References

[1] Hench LL. The story of Bioglass®. J Mater Sci – Mater Med 2006;17:967–78.
[2] Hench LL, Splinter RJ, Allen WC, Greenlee TK. Bonding mechanisms at the interface of ceramic prosthetic materials. J Biomed Mater Res Symp 1971;334:117–41.
[3] Kokubo T. Bioactive glass-ceramics – properties and applications. Biomaterials 1991;12:155–63.
[4] LeGeros RZ. Properties of osteoconductive biomaterials: calcium phosphates. Clin Orthop Relat Res 2002;395:81–98.
[5] Hench LL, Polak JM. Third-generation biomedical materials. Science 2002;295:1014–7.
[6] Rahaman MN, Day DE, Bal BS, Fu Q, Jung SB, Bonewald LF, et al. Bioactive glass in tissue engineering. Acta Biomater 2011;7:2355–73.
[7] Jung SB, Day DE, Day T, Stoecker W, Taylor P. Treatment of non-healing diabetic venous stasis ulcers with bioactive glass nanofibers. Wound Repair Regen 2011;19:A30.
[8] Abou Neel EA, Pickup DM, Valappil SP, Newport RJ, Knowles JC. Bioactive functional materials: a perspective on phosphate-based glasses. J Mater Chem 2009;19:690–701.
[9] Kucera T, Urban K, Ragkou S. Healing of cavitary bone defects. Eur J Orthop Surg Traumatol 2012;22:123–8.
[10] Moutos FT, Freed LE, Guilak F. A biomimetic three-dimensional woven composite scaffold for functional tissue engineering of cartilage. Nat Mater 2007;6:162–7.
[11] Hench LL. Bioactive materials for gene control. In: Hench LL, Jones JR, Fenn MB, editors. New materials and technologies for healthcare. Singapore: World Scientific; 2011. p. 25–48.
[12] Rust KR, Singleton GT, Wilson J, Antonelli PJ. Bioglass middle ear prosthesis: long-term results. Am J Otolaryngol 1996;17:371–4.
[13] Stanley HR, Hall MB, Clark AE, King CJ, Hench LL, Berte JJ. Using 45S5 bioglass cones as endosseous ridge maintenance implants to prevent alveolar ridge resorption: a 5-year evaluation. Int J Oral Maxillofac Implants 1997;12:95–105.
[14] Thompson ID. Clinical applications of bioactive glasses for maxillofacial repair. In: Hench LL, Fenn MB, Jones JR, editors. New materials and technologies for healthcare. Singapore: World Scientific; 2011. p. 77–96.
[15] Kinnunen I, Aitasalo K, Pollonen M, Varpula M. Reconstruction of orbital floor fractures using bioactive glass. J Craniofac-Maxillofac Surg 2000;28:229–34.
[16] Fetner AE, Low SB, Wilson J, Hench LL. Histologic evaluation of bioglass particulates in gingival tissue. J Dent Res 1987;66:298–398.
[17] Wilson J, Low SB. Bioactive ceramics for periodontal treatment – comparative studies in the *Patus* monkey. J Appl Biomater 1992;3:123–9.
[18] Schepers EJG, Ducheyne P. Bioactive glass particles of narrow size range for the treatment of oral bone defects: a 1–24 months experiment with several materials and particle sizes and size ranges. J Oral Rehabil 1997;24:171–81.
[19] Low SB, King CJ, Krieger J. An evaluation of bioactive ceramic in the treatment of periodontal osseous defects. Int J Periodontol Rest, Dent 1997;17:359–67.
[20] Lovelace TB, Mellonig JT, Meffert RM, Jones AA, Nummikoski PV, Cochran DL. Clinical evaluation of bioactive glass in the treatment of periodontal osseous defects in humans. J Periodontol 1998;69:1027–35.
[21] Rosenberg ES, Cho SC, Elian N, Jalbout ZN, Froum S, Evian CI. A comparison of characteristics of implant failure and survival in periodontally compromised and periodontally healthy patients: a clinical report. Int J Oral Maxillofac Implants 2004;19:873–9.
[22] Anderegg CR, Alexander DC, Freidman M. A bioactive glass particulate in the treatment of molar furcation invasions. J Periodontol 1999;70:384–7.
[23] Yukna RA, Evans GH, Aichelmann-Reidy MB, Mayer ET. Clinical comparison of bioactive glass bone replacement graft material and expanded polytetrafluoroethylene barrier membrane in treating human mandibular molar Class II furcations. J Periodontol 2001;72:125–33.
[24] Park JS, Suh JJ, Choi SH, Moon IS, Cho KS, Kim CK, Chai JK. Effects of pretreatment clinical parameters on bioactive glass implantation in intrabony periodontal defects. J Periodontol 2001;72:730–40.
[25] Norton MR, Wilson J. Dental implants placed in extraction sites implanted with bioactive glass: human histology and clinical outcome. Int J Oral Maxillofac Implants 2002;17:249–57.
[26] Sculean A, Barbe G, Chiantella GC, Arweiler NB, Berakdar M, Brecx M. Clinical evaluation of an enamel matrix protein derivative combined with a bioactive glass for the treatment of intrabony periodontal defects in humans. J Periodontol 2002;73:401–8.
[27] Mengel R, Soffner M, Flores-De-Jacoby L. Bioabsorbable membrane and bioactive glass in the treatment of intrabony defects in patients with generalized aggressive periodontitis: results of a 12-month clinical and radiological study. J Periodontol 2003;74:899–908.

[28] Froum SJ, Weinberg MA, Tarnow D. Comparison of bioactive glass synthetic bone graft particles and open debridement in the treatment of human periodontal defects. A clinical study. J Periodontol 1998;69:698–709.

[29] Shapoff CA, Alexander DC, Clark AE. Clinical use of a bioactive glass particulate in the treatment of human osseous defects. Compend Contin Educ Dent (Jamesburg, NJ: 1995) 1997;18:352–58.

[30] Zamet JS, Darbar UR, Griffiths GS, Bulman JS, Bragger U, Burgin W, et al. Particulate Bioglass® as a grafting material in the treatment of periodontal intrabony defects. J Clin Periodontol 1997;24:410–8.

[31] Zamet JS, Darbar UR, Griffiths GS, Burgin W, Newman HN. Particulate bioglass (Perioglas®) in the treatment of periodontal intrabony defects. J Dent Res 1997;76:2219–3219.

[32] AboElsaad NS, Soory M, Gadalla LMA, Ragab LI, Dunne S, Zalata KR, et al. Effect of soft laser and bioactive glass on bone regeneration in the treatment of infra-bony defects (a clinical study). Lasers Med Sci 2009;24:387–95.

[33] Yadav VS, Narula SC, Sharma RK, Tewari S, Yadav R. Clinical evaluation of guided tissue regeneration combined with autogenous bone or autogenous bone mixed with bioactive glass in intrabony defects. J Oral Sci 2011;53:481–8.

[34] Waltimo T, Mohn D, Paque F, Brunner TJ, Stark WJ, Imfeld T, Schaetzle M, Zehnder M. Fine-tuning of bioactive glass for root canal disinfection. J Dent Res 2009;88:235–38.

[35] Ilharreborde B, Morel E, Fitoussi F, Presedo A, Souchet P, Pennecot G-F, et al. Bioactive glass as a bone substitute for spinal fusion in adolescent idiopathic scoliosis a comparative study with iliac crest autograft. J Pediatr Orthop 2008;28:347–51.

[36] Turunen T, Peltola J, Yli-Urpo A, Happonen RP. Bioactive glass granules as a bone adjunctive material in maxillary sinus floor augmentation. Clin Oral Implants Res 2004;15:135–41.

[37] Peltola M, Aitasalo K, Suonpaa J, Varpula M, Yli-Urpo A. Bioactive glass S53P4 in frontal sinus obliteration: a long-term clinical experience. Head Neck 2006;28:834–41.

[38] Frantzen J, Rantakokko J, Aro HT, Heinanen J, Kajander S, Gullichsen E, et al. Instrumented spondylodesis in degenerative spondylolisthesis with bioactive glass and autologous bone: a prospective 11-year follow-up. J Spinal Disord Tech 2011;24:455–61.

[39] Lindfors NC, Hyvonen P, Nyyssonen M, Kirjavainen M, Kankare J, Gullichsen E, et al. Bioactive glass S53P4 as bone graft substitute in treatment of osteomyelitis. Bone 2010;47:212–8.

[40] Rantakokko J, Frantzen JP, Heinanen J, Kajander S, Kotilainen E, Gullichsen E, et al. Posterolateral spondylodesis using bioactive glass S53P4 and autogenous bone in instrumented unstable lumbar spine burst fractures. Scand J Surg 2012;101:66–71.

[41] Pernaa K, Koski I, Mattila K, Gullichsen E, Heikkila J, Aho A, et al. Bioactive glass S53P4 and autograft bone in treatment of depressed tibial plateau fractures – a prospective randomized 11-year follow-up. J Long-term Eff Med Implants 2011;21:139–48.

[42] Heikkila JT, Kukkonen J, Aho AJ, Moisander S, Kyyronen T, Mattila K. Bioactive glass granules: a suitable bone substitute material in the operative treatment of depressed lateral tibial plateau fractures: a prospective, randomized 1 year follow-up study. J Mater Sci – Mater Med 2011;22:1073–80.

[43] Lindfors NC, Koski I, Heikkila JT, Mattila K, Aho AJ. A prospective randomized 14-year follow-up study of bioactive glass and autogenous bone as bone graft substitutes in benign bone tumors. J Biomed Mater Res Part B 2010;94B:157–64.

[44] Lindfors NC, Heikkila JT, Koski I, Mattila K, Aho AJ. Bioactive glass and autogenous bone as bone graft substitutes in benign bone tumors. J Biomed Mater Res Part B 2009;90B:131–6.

[45] Lindfors NC, Heikkila JT, Aho AJ. Long-term evaluation of blood silicon and ostecalcin in operatively treated patients with benign bone tumors using bioactive glass and autogenous bone. J Biomed Mater Res Part B 2008;87B:73–6.

[46] Stoor P, Pulkkinen J, Grenman R. Bioactive glass S53P4 in the filling of cavities in the mastoid cell area in surgery for chronic otitis media. Ann Otolaryngol Rhinol Laryngol 2010;119:377–82.

[47] Gillam DG, Tang JY, Mordan NJ, Newman HN. The effects of a novel Bioglass® dentifrice on dentine sensitivity: a scanning electron microscopy investigation. J Oral Rehabil 2002;29:305–13.

[48] Tai BJ, Bian Z, Jiang H, Greenspan DC, Zhong J, Clark AE, et al. Anti-gingivitis effect of a dentifrice containing bioactive glass (NovaMin®) particulate. J Clin Periodontol 2006;33:86–91.

[49] Pradeep AR, Sharma A. Comparison of clinical efficacy of a dentifrice containing calcium sodium phosphosilicate to a dentifrice containing potassium nitrate and to a placebo on dentinal hypersensitivity: a randomized clinical trial. J Periodontol 2010;81:1167–73.

[50] Earl JS, Leary RK, Muller KH, Langford RM, Greenspan DC. Physical and chemical characterization of dentin surface, following treatment with NovaMin® technology. J Clin Dent 2011;22:2–67.

[51] Mitchell JC, Musanje L, Ferracane JL. Biomimetic dentin desensitizer based on nano-structured bioactive glass. Dent Mater 2011;27:386–93.

[52] Mneimne M, Hill RG, Bushby AJ, Brauer DS. High phosphate content significantly increases apatite formation of fluoride-containing bioactive glasses. Acta Biomater 2011;7:1827–34.

[53] Lusvardi G, Malavasi G, Menabue L, Aina V, Morterra C. Fluoride-containing bioactive glasses: surface reactivity in simulated body fluids solutions. Acta Biomater 2009;5:3548–62.

[54] Brauer DS, Mneimne M, Hill RG. Fluoride-containing bioactive glasses: fluoride loss during melting and ion release in tris buffer solution. J Non-Cryst Solids 2011;357:3328–33.

[55] Banerjee A, Hajatdoost-Sani M, Farrell S, Thompson I. A clinical evaluation and comparison of bioactive glass and sodium bicarbonate air-polishing powders. J Dentistry 2010;38:475–9.

[56] Gomez-Vega JM, Saiz E, Tomsia AP, Oku T, Suganuma K, Marshall GW, et al. Novel bioactive functionally graded coatings on Ti_6Al_4V. Adv Mater 2000;12:894–8.

[57] Gomez-Vega JM, Hozumi A, Saiz E, Tomsia AP, Sugimura H, Takai O. Bioactive glass-mesoporous silica coatings on Ti_6Al_4V through enameling and triblock-copolymer-templated sol–gel processing. J Biomed Mater Res 2001;56:382–9.

[58] Gomez-Vega JM, Saiz E, Tomsia AP. Glass-based coatings for titanium implant alloys. J Biomed Mater Res 1999;46:549–59.

[59] Gomez-Vega JM, Saiz E, Tomsia AP, Marshall GW, Marshall SJ. Bioactive glass coatings with hydroxyapatite and Bioglass® particles on Ti-based implants. 1. Processing. Biomaterials 2000;21:105–11.

[60] Lopez-Esteban S, Saiz E, Fujino S, Oku T, Suganuma K, Tomsia AP. Bioactive glass coatings for orthopedic metallic implants. J Eur Ceram Soc 2003;23:2921–30.

[61] Pavon J, Jimenez-Pique E, Anglada M, Saiz E, Tomsia AP. Delamination under Hertzian cyclic loading of a glass coating on Ti_6Al_4V for implants. J Mater Sci 2006;41:5134–45.

[62] Pazo A, Saiz E, Tomsia AP. Silicate glass coatings on Ti-based implants. Acta Mater 1998;46:2551–8.

[63] Moritz N, Rossi S, Vedel E, Tirri T, Ylanen H, Aro H, et al. Implants coated with bioactive glass by CO_2-laser, an in vivo study. J Mater Sci – Mater Med 2004;15:795–802.

[64] Mistry S, Kundu D, Datta S, Basu D. Comparison of bioactive glass coated and hydroxyapatite coated titanium dental implants in the human jaw bone. Aust Dent J 2011;56:68–75.

[65] Hench LL, West JK. The sol–gel process. Chem Rev 1990;90:33–72.

[66] Li R, Clark AE, Hench LL. An investigation of bioactive glass powders by sol–gel processing. J Appl Biomater 1991;2:231–9.

[67] Saravanapavan P, Jones JR, Pryce RS, Hench LL. Bioactivity of gel-glass powders in the CaO-SiO_2 system: a comparison with ternary (CaO–P_2O_5–SiO_2) and quaternary glasses (SiO_2–CaO–P_2O_5–Na_2O). J Biomed Mater Res Part A 2003;66A:110–9.

[68] Brinker J, Scherer GW. Sol–gel science: the physics and chemistry of sol–gel processing. Boston, MA: Academic Press; 1990.

[69] Sepulveda P, Jones JR, Hench LL. Characterization of melt-derived 45S5 and sol–gel-derived 58S bioactive glasses. J Biomed Mater Res 2001;58:734–40.

[70] Lei B, Chen XF, Wang YJ, Zhao NR, Du C, Fang LM. Surface nanoscale patterning of bioactive glass to support cellular growth and differentiation. J Biomed Mater Res Part A 2010;94A:1091–9.

[71] Siqueira RL, Peitl O, Zanotto ED. Gel-derived SiO_2–CaO–Na_2O–P_2O_5 bioactive powders: synthesis and in vitro bioactivity. Mater Sci Eng, C 2011;31:983–91.

[72] Stöber W. Controlled growth of monodisperse silica spheres in micron size range. J Colloid Interf Sci 1968;26:62.

[73] Labbaf S, Tsigkou O, Mueller KH, Stevens MM, Porter AE, Jones JR. Spherical bioactive glass particles and their interaction with human mesenchymal stem cells in vitro. Biomaterials 2011;32:1010–8.

[74] Lin S, Ionescu C, Pike KJ, Smith ME, Jones JR. Nanostructure evolution and calcium distribution in sol–gel derived bioactive glass. J Mater Chem 2009;19:1276–82.

[75] Valliant EM, Turdean-Ionescu CA, Hanna JV, Smith ME, Jones JR. Role of pH and temperature on silica network formation and calcium incorporation into sol–gel derived bioactive glasses. J Mater Chem 2012;22:1613–9.

[76] Saravanapavan P, Hench LL. Mesoporous calcium silicate glasses. II. Textural characterisation. J Non-Cryst Solids 2003;318:14–26.

[77] Brinker CJ, Lu YF, Sellinger A, Fan HY. Evaporation-induced self-assembly: nanostructures made easy. Adv Mater 1999;11:579–85.

[78] Vallet-Regi M, Izquierdo-Barba I, Colilla M. Structure and functionalization of mesoporous bioceramics for bone tissue regeneration and local drug delivery. Philos Trans R Soc A 2012;370:1400–21.

[79] Hench LL, Pantano CG, Buscemi PJ, Greenspan DC. Analysis of Bioglass fixation of hip prostheses. J Biomed Mater Res 1977;11:267–82.

[80] Oonishi H, Hench LL, Wilson J, Sugihara F, Tsuji E, Matsuura M, et al. Quantitative comparison of bone growth behavior in granules of Bioglass®, A-W glass-ceramic, and hydroxyapatite. J Biomed Mater Res 2000;51: 37–46.

[81] Oonishi H, Kushitani S, Yasukawa E, Iwaki H, Hench LL, Wilson J, Tsuji EI, Sugihara T. Particulate bioglass compared with hydroxyapatite as a bone graft substitute. Clin Orthop Relat Res 1997;316–25.

[82] Oonishi H, Hench LL, Wilson J, Sugihara F, Tsuji E, Kushitani S, et al. Comparative bone growth behavior in granules of bioceramic materials of various sizes. J Biomed Mater Res 1999;44:31–43.

[83] Wheeler DL, Eschbach EJ, Hoellrich RG, Montfort MJ, Chamberland DL. Assessment of resorbable bioactive material for grafting of critical-size cancellous defects. J Orthop Res 2000;18:140–8.

[84] Quintero F, Pou J, Comesana R, Lusquinos F, Riveiro A, Mann AB, et al. Laser spinning of bioactive glass nanofibers. Adv Funct Mater 2009;19:3084–90.

[85] Wheeler DL, Stokes KE, Hoellrich RG, Chamberland DL, McLoughlin SW. Effect of bioactive glass particle size on osseous regeneration of cancellous defects. J Biomed Mater Res 1998;41:527–33.

[86] Wang Z, Lu B, Chen L, Chang JA. Evaluation of an osteostimulative putty in the sheep spine. J Mater Sci – Mater Med 2011;22:185–91.
[87] Kobayashi H, Turner AS, Seim HB, Kawamoto T, Bauer TW. Evaluation of a silica-containing bone graft substitute in a vertebral defect model. J Biomed Mater Res Part A 2010;92A:596–603.
[88] Fujibayashi S, Neo M, Kim HM, Kokubo T, Nakamura T. A comparative study between in vivo bone ingrowth and in vitro apatite formation on Na_2O-CaO-SiO_2 glasses. Biomaterials 2003;24:1349–56.
[89] Vogel M, Voigt C, Gross UM, Muller-Mai CM. In vivo comparison of bioactive glass particles in rabbits. Biomaterials 2001;22:357–62.
[90] Vogel M, Voigt C, Knabe C, Radlanski RJ, Gross UM, Muller-Mai CM. Development of multinuclear giant cells during the degradation of Bioglass® particles in rabbits. J Biomed Mater Res Part A 2004;70A:370–9.
[91] Hupa L, Karlsson KH, Hupa M, Aro HT. Comparison of bioactive glasses in vitro and in vivo. Glass Technol – Eur J Glass Sci Technol Part A 2010;51:89–92.
[92] Lai W, Garino J, Ducheyne P. Silicon excretion from bioactive glass implanted in rabbit bone. Biomaterials 2002;23:213–7.
[93] Lai W, Garino J, Flaitz C, Ducheyne P. Excretion of resorption products from bioactive glass implanted in rabbit muscle. J Biomed Mater Res Part A 2005;75A:398–407.
[94] Li H, Chen SY, Wu Y, Jiang J, Ge YS, Gao K, et al. Enhancement of the osseointegration of a polyethylene terephthalate artificial ligament graft in a bone tunnel using 58S bioglass. Int Orthop 2012;36:191–7.
[95] Conejero JA, Lee JA, Ascherman JA. Cranial defect reconstruction in an experimental model using different mixtures of bioglass and autologous bone. J Craniofac Surg 2007;18:1290–5.
[96] Hench LL, Paschall HA. Direct chemical bonding of bioactive glass-ceramic materials and bone. J Biomed Mater Res Symp 1973;4:25–42.
[97] Sanders DM, Hench LL. Mechanisms of glass corrosion. J Am Ceram Soc 1973;56:373–7.
[98] Clark AE, Pantano CG, Hench LL. Auger spectroscopic analysis of Bioglass corrosion films. J Am Ceram Soc 1976;59:37–9.
[99] Hench LL. Bioceramics – from concept to clinic. J Am Ceram Soc 1991;74:1487–510.
[100] Skipper LJ, Sowrey FE, Pickup DM, Drake KO, Smith ME, Saravanapavan P, et al. The structure of a bioactive calcia-silica sol–gel glass. J Mater Chem 2005;15:2369–74.
[101] Martin RA, Twyman H, Qiu D, Knowles JC, Newport RJ. A study of the formation of amorphous calcium phosphate and hydroxyapatite on melt quenched Bioglass® using surface sensitive shallow angle X-ray diffraction. J Mater Sci – Mater Med 2009;20:883–8.
[102] Li PJ, Zhang FP. The electrochemistry of a glass-surface and its application to bioactive glass in solution. J Non-Cryst Solids 1990;119:112–8.
[103] Doostmohammadi A, Monshi A, Fathi MH, Braissant O. A comparative physico-chemical study of bioactive glass and bone-derived hydroxyapatite. Ceram Int 2011;37:1601–7.
[104] Karlsson KH, Froberg K, Ringbom T. A structural approach to bone adhering of bioactive glasses. J Non-Cryst Solids 1989;112:69–72.
[105] FitzGerald V, Pickup DM, Greenspan D, Wetherall KM, Moss RM, Jones JR, et al. An atomic scale comparison of the reaction of Bioglass® in two types of simulated body fluid. Phys Chem Glasses – Eur J Glass Sci Technol Part B 2009;50:137–43.
[106] FitzGerald V, Martin RA, Jones JR, Qiu D, Wetherall KM, Moss RM, et al. Bioactive glass sol–gel foam scaffolds: evolution of nanoporosity during processing and in situ monitoring of apatite layer formation using small- and wide-angle X-ray scattering. J Biomed Mater Res Part A 2009;91A:76–83.
[107] Arcos D, Greenspan DC, Vallet-Regi M. A new quantitative method to evaluate the in vitro bioactivity of melt and sol–gel-derived silicate glasses. J Biomed Mater Res Part A 2003;65A:344–51.
[108] Greenspan DC, Hench LL. Chemical and mechanical behavior of Bioglass-coated alumina. J Biomed Mater Res 1976;10:503–9.
[109] Gross UM, Strunz V. The anchoring of glass-ceramics of different solubility in the femur of the rat. J Biomed Mater Res 1980;14:607–18.
[110] Vallet-Regi M, Ragel CV, Salinas AJ. Glasses with medical applications. Eur J, Inorg Chem 2003;1029–42.
[111] Hench LL, Thompson I. Twenty-first century challenges for biomaterials. J R Soc Interf 2010;7:S379–91.
[112] Gough JE, Jones JR, Hench LL. Nodule formation and mineralisation of human primary osteoblasts cultured on a porous bioactive glass scaffold. Biomaterials 2004;25:2039–46.
[113] Kaufmann E, Ducheyne P, Shapiro IM. Evaluation of osteoblast response to porous bioactive glass (45S5) substrates by RT-PCR analysis. Tissue Eng 2000;6:19–28.
[114] Bosetti M, Cannas M. The effect of bioactive glasses on bone marrow stromal cells differentiation. Biomaterials 2005;26:3873–9.
[115] Jones JR, Tsigkou O, Coates EE, Stevens MM, Polak JM, Hench LL. Extracellular matrix formation and mineralization of on a phosphate-free porous bioactive glass scaffold using primary human osteoblast (HOB) cells. Biomaterials 2007;28:1653–63.
[116] Silver IA, Deas J, Erecinska M. Interactions of bioactive glasses with osteoblasts in vitro: effects of 45S5 Bioglass®, and 58S and 77S bioactive glasses on metabolism, intracellular ion concentrations and cell viability. Biomaterials 2001;22:175–85.
[117] Xynos ID, Edgar AJ, Buttery LDK, Hench LL, Polak JM. Gene-expression profiling of human osteoblasts following treatment with the ionic products of Bioglass® 45S5 dissolution. J Biomed Mater Res 2001;55:151–7.
[118] Xynos ID, Edgar AJ, Buttery LDK, Hench LL, Polak JM. Ionic products of bioactive glass dissolution increase proliferation of human osteoblasts and induce insulin-like growth factor II mRNA expression and protein synthesis. Biochem Biophys Res Commun 2000;276:461–5.
[119] Xynos ID, Hukkanen MVJ, Batten JJ, Buttery LD, Hench LL, Polak JM. Bioglass® 45S5 stimulates osteoblast turnover and enhances bone formation in vitro: implications and applications for bone tissue engineering. Calcified Tissue Int 2000;6:321–9.
[120] Hench LL. Genetic design of bioactive glass. J Eur Ceram Soc 2009;29:1257–65.
[121] Hench LL, Polak JM, Xynos ID, Buttery LDK. Bioactive materials to control cell cycle. Mater Res Innovations 2000;3:313–23.
[122] Marie PJ. The calcium-sensing receptor in bone cells: a potential therapeutic target in osteoporosis. Bone 2010;46:571–6.
[123] Maeno S, Niki Y, Matsumoto H, Morioka H, Yatabe T, Funayama A, et al. The effect of calcium ion concentration on osteoblast viability, proliferation and differentiation in monolayer and 3D culture. Biomaterials 2005;26:4847–55.
[124] Valerio P, Pereira MM, Goes AM, Leite MF. Effects of extracellular calcium concentration on the glutamate release by bioactive glass (BG60S) preincubated osteoblasts. Biomed Mater 2009;4:045011.
[125] Reffitt DM, Ogston N, Jugdaohsingh R, Cheung HFJ, Evans BAJ, Thompson RPH, et al. Orthosilicic acid stimulates collagen type 1 synthesis and osteoblastic differentiation in human osteoblast-like cells in vitro. Bone 2003;32:127–35.
[126] Hoppe A, Gueldal NS, Boccaccini AR. A review of the biological response to ionic dissolution products from bioactive glasses and glass-ceramics. Biomaterials 2011;32:2757–74.
[127] Jell G, Notingher I, Tsigkou O, Notingher P, Polak JM, Hench LL, et al. Bioactive glass-induced osteoblast differentiation: a noninvasive spectroscopic study. J Biomed Mater Res Part A 2008;86A:31–40.
[128] Tsigkou O, Jones JR, Polak JM, Stevens MM. Differentiation of fetal osteoblasts and formation of mineralized bone nodules by 45S5 Bioglass® conditioned medium in the absence of osteogenic supplements. Biomaterials 2009;30:3542–50.
[129] Reilly GC, Radin S, Chen AT, Ducheyne P. Differential alkaline phosphatase responses of rat and human bone marrow derived mesenchymal stem cells to 45S5 bioactive glass. Biomaterials 2007;28:4091–7.
[130] Karpov M, Laczka M, Leboy PS, Osyczka AM. Sol–gel bioactive glasses support both osteoblast and osteoclast formation from human bone marrow cells. J Biomed Mater Res Part A 2008;84A:718–26.
[131] Bielby RC, Pryce RS, Hench LL, Polak JM. Enhanced derivation of osteogenic cells from murine embryonic stem cells after treatment with ionic dissolution products of 58S bioactive sol–gel glass. Tissue Eng 2005;11:479–88.
[132] Haimi S, Moimas L, Pirhonen E, Lindroos B, Huhtala H, Raty S, et al. Calcium phosphate surface treatment of bioactive glass causes a delay in early osteogenic differentiation of adipose stem cells. J Biomed Mater Res Part A 2009;91A:540–7.
[133] Wilson T, Parikka V, Holmbom J, Ylanen H, Penttinen R. Intact surface of bioactive glass S53P4 is resistant to osteoclastic activity. J Biomed Mater Res Part A 2006;77A:67–74.
[134] Hamadouche M, Meunier A, Greenspan DC, Blanchat C, Zhong JPP, La Torre GP, et al. Long-term in vivo bioactivity and degradability of bulk sol–gel bioactive glasses. J Biomed Mater Res 2001;54:560–6.
[135] Martin RA, Yue S, Hanna JV, Lee PD, Newport RJ, Smith ME, et al. Characterizing the hierarchical structures of bioactive sol–gel silicate glass and hybrid scaffolds for bone regeneration. Philos Trans R Soc A 2012;370:1422–43.
[136] Cormack AN. The structure of bioactive glasses and their surfaces. In: Jones JR, Clare AG, editors. Bio-glasses: an introduction. Chichester: Wiley; 2012. p. 65–74.
[137] FitzGerald V, Pickup DM, Greenspan D, Sarkar G, Fitzgerald JJ, Wetherall KM, et al. A neutron and X-ray diffraction study of bioglass with reverse Monte Carlo modelling. Adv Funct Mater 2007;17:3746–53.
[138] Elgayar I, Aliev AE, Boccaccini AR, Hill RG. Structural analysis of bioactive glasses. J Non-Cryst Solids 2005;351:173–83.
[139] Pedone A, Charpentier T, Malavasi G, Menziani MC. New insights into the atomic structure of 45S5 bioglass by means of solid-state NMR spectroscopy and accurate first-principles simulations. Chem Mater 2010;22:5644–52.
[140] Cerruti M, Bianchi CL, Bonino F, Damin A, Perardi A, Morterra C. Surface modifications of bioglass immersed in TRIS-buffered solution. A multitechnical spectroscopic study. J Phys Chem B 2005;109:14496–505.
[141] Sepulveda P, Jones JR, Hench LL. In vitro dissolution of melt-derived 45S5 and sol–gel derived 58S bioactive glasses. J Biomed Mater Res 2002;61: 301–11.
[142] Galliano PG, Lopez JMP, Varetti EL, Sobrados I, Sanz. Analysis by nuclear-magnetic-resonance and Raman spectroscopies of the structure of bioactive alkaline-earth silicophosphate glasses. J Mater Res Bull 1994;24:1297–306.
[143] Hill RG, Brauer DS. Predicting the bioactivity of glasses using the network connectivity or split network models. J Non-Cryst Solids 2011;357:3884–7.
[144] Li A, Wang D, Xiang J, Newport RJ, Reinholdt MX, Mutin PH, et al. Insights into new calcium phosphosilicate xerogels using an advanced characterization methodology. J Non-Cryst Solids 2011;357:3548–55.
[145] Tilocca A, Cormack AN, de Leeuw NH. The structure of bioactive silicate glasses: new insight from molecular dynamics simulations. Chem Mater 2007;19:95–103.

[146] Mercier C, Follet-Houttemane C, Pardini A, Revel B. Influence of P_2O_5 content on the structure of SiO_2–Na_2O–CaO–P_2O_5 bioglasses by ^{29}Si and ^{31}P MAS-NMR. J Non-Cryst Solids 2011;357:3901–9.
[147] Hill R. An alternative view of the degradation of bioglass. J Mater Sci Lett 1996;15:1122–5.
[148] O'Donnell MD, Candarlioglu PL, Miller CA, Gentleman E, Stevens MM. Materials characterisation and cytotoxic assessment of strontium-substituted bioactive glasses for bone regeneration. J Mater Chem 2010;20:8934–41.
[149] Eden M. The split network analysis for exploring composition–structure correlations in multi-component glasses: I. Rationalizing bioactivity–composition trends of bioglasses. J Non-Cryst Solids 2011;357:1595–602.
[150] Ottermann CR, Bange K, Wagner W, Laube M, Rauch F. Correlation of hydrogen content with properties of oxidic thin-films. Surf Interf Anal 1992;19:435–8.
[151] Pereira MM, Clark AE, Hench LL. Effect of texture on the rate of hydroxyapatite formation on gel-silica surface. J Am Ceram Soc 1995;78:2463–8.
[152] Jones JR, Hench LL. Effect of surfactant concentration and composition on the structure and properties of sol–gel-derived bioactive glass foam scaffolds for tissue engineering. J Mater Sci 2003;38:3783–90.
[153] Soulie J, Nedelec JM, Jallot E. Influence of Mg doping on the early steps of physico-chemical reactivity of sol–gel derived bioactive glasses in biological medium. Phys Chem Chem Phys 2009;11:10473–83.
[154] Ma J, Chen CZ, Wang DG, Hu JH. Synthesis, characterization and in vitro bioactivity of magnesium-doped sol–gel glass and glass-ceramics. Ceram Int 2011;37:1637–44.
[155] Ma J, Chen CZ, Wang DG, Jiao Y, Shi JZ. Effect of magnesia on the degradability and bioactivity of sol–gel derived SiO_2–CaO–MgO–P_2O_5 system glasses. Colloids Surf B – Biointerfaces 2010;81:87–95.
[156] Mead RN, Mountjoy G. Modeling the local atomic structure of bioactive sol–gel-derived calcium silicates. Chem Mater 2006;18:3956–64.
[157] Chen QZ, Thompson ID, Boccaccini AR. 45S5 Bioglass®-derived glass-ceramic scaffolds for bone tissue engineering. Biomaterials 2006;27:2414–25.
[158] Bellucci D, Cannillo V, Sola A, Chiellini F, Gazzarri M, Migone C. Macroporous Bioglass®-derived scaffolds for bone tissue regeneration. Ceram Int 2011;37:1575–85.
[159] Deb S, Mandegaran R, Di Silvio L. A porous scaffold for bone tissue engineering/45S5 Bioglass® derived porous scaffolds for co-culturing osteoblasts and endothelial cells. J Mater Sci – Mater Med 2010;21:893–905.
[160] Chen QZ, Mohn D, Stark WJ. Optimization of Bioglass® scaffold fabrication process. J Am Ceram Soc 2011;94:4184–90.
[161] Peitl O, LaTorre GP, Hench LL. Effect of crystallization on apatite-layer formation of bioactive glass 45S5. J Biomed Mater Res 1996;30:509–14.
[162] Massera J, Fagerlund S, Hupa L, Hupa M. Crystallization mechanism of the bioactive glasses, 45S5 and S53P4. J Am Ceram Soc 2012;95:607–13.
[163] Brink M. The influence of alkali and alkaline earths on the working range for bioactive glasses. J Biomed Mater Res 1997;36:109–17.
[164] Brink M, Turunen T, Happonen RP, YliUrpo A. Compositional dependence of bioactivity of glasses in the system Na_2O–K_2O–MgO–CaO–B_2O_3–P_2O_5–SiO_2. J Biomed Mater Res 1997;37:114–21.
[165] Vedel E, Zhang D, Arstila H, Hupa L, Hupa M. Predicting physical and chemical properties of bioactive glasses from chemical composition. Part 4: Tailoring compositions with desired properties. Glass Technol – Eur J Glass Sci Technol Part A 2009;50:9–16.
[166] Oudadesse H, Dietrich E, Gal YL, Pellen P, Bureau B, Mostafa AA, Cathelineau G. Apatite forming ability and cytocompatibility of pure and Zn-doped bioactive glasses. Biomed Mater 2011;6. http://dx.doi.org/10.1088/1748-6041/6/3/035006.
[167] Watts SJ, Hill RG, O'Donnell MD, Law RV. Influence of magnesia on the structure and properties of bioactive glasses. J Non-Cryst Solids 2010;356:517–24.
[168] Moimas L, Biasotto M, Di Lenarda R, Olivo A, Schmid C. Rabbit pilot study on the resorbability of three-dimensional bioactive glass fibre scaffolds. Acta Biomater 2006;2:191–9.
[169] Bellucci D, Cannillo V, Sola A. A new potassium-based bioactive glass: sintering behaviour and possible applications for bioceramic scaffolds. Ceram Int 2011;37:145–57.
[170] Cannillo V, Sola A. Potassium-based composition for a bioactive glass. Ceram Int 2009;35:3389–93.
[171] Bellucci D, Cannillo V, Sola A. Calcium and potassium addition to facilitate the sintering of bioactive glasses. Mater Lett 2011;65:1825–7.
[172] Wallace KE, Hill RG, Pembroke JT, Brown CJ, Hatton PV. Influence of sodium oxide content on bioactive glass properties. J Mater Sci – Mater Med 1999;10:697–701.
[173] Jayabalan P, Tan AR, Rahaman MN, Bal BS, Hung CT, Cook JL. Bioactive glass 13–93 as a subchondral substrate for tissue-engineered osteochondral constructs: a pilot study. Clin Orthop Relat Res 2011;469:2754–63.
[174] Deville S, Saiz E, Nalla RK, Tomsia AP. Freezing as a path to build complex composites. Science 2006;311:515–8.
[175] Fu Q, Rahaman MN, Bal BS, Bonewald LF, Kuroki K, Brown RF. Silicate, borosilicate, and borate bioactive glass scaffolds with controllable degradation rate for bone tissue engineering applications. II. In vitro and in vivo biological evaluation. J Biomed Mater Res Part A 2010;95A:172–79.
[176] Fu Q, Rahaman MN, Bal BS, Kuroki K, Brown RF. In vivo evaluation of 13–93 bioactive glass scaffolds with trabecular and oriented microstructures in a subcutaneous rat implantation model. J Biomed Mater Res Part A 2010;95A:235–44.
[177] Liu X, Rahaman MN, Fu Q, Tomsia AP. Porous and strong bioactive glass (13–93) scaffolds prepared by unidirectional freezing of camphene-based suspensions. Acta Biomater 2012;8:415–23.
[178] Liu X, Rahaman MN, Fu QA. Oriented bioactive glass (13–93) scaffolds with controllable pore size by unidirectional freezing of camphene-based suspensions: microstructure and mechanical response. Acta Biomater 2011;7:406–16.
[179] Wu ZY, Hill RG, Yue S, Nightingale D, Lee PD, Jones JR. Melt-derived bioactive glass scaffolds produced by a gel-cast foaming technique. Acta Biomater 2011;7:1807–16.
[180] Sepulveda P, Jones JR, Hench LL. Bioactive sol–gel foams for tissue repair. J Biomed Mater Res 2002;59:340–8.
[181] Jones JR, Poologasundarampillai G, Atwood RC, Bernard D, Lee PD. Non-destructive quantitative 3D analysis for the optimisation of tissue scaffolds. Biomaterials 2007;28:1404–13.
[182] Jones JR, Lin S, Yue S, Lee PD, Hanna JV, Smith ME, et al. Bioactive glass scaffolds for bone regeneration and their hierarchical characterisation. Proc Inst Mech Eng H – J Eng Med 2010;224:1373–87.
[183] Jones JR, Hench LL. Factors affecting the structure and properties of bioactive foam scaffolds for tissue engineering. J Biomed Mater Res Part B 2004;68B:36–44.
[184] Coelho MD, Pereira MM. Sol–gel synthesis of bioactive glass scaffolds for tissue engineering: effect of surfactant type and concentration. J Biomed Mater Res Part B 2005;75B:451–6.
[185] Jones JR, Ehrenfried LM, Hench LL. Optimising bioactive glass scaffolds for bone tissue engineering. Biomaterials 2006;27:964–73.
[186] Wang S, Falk MM, Rashad A, Saad MM, Marques AC, Almeida RM, et al. Evaluation of 3D nano-macro porous bioactive glass scaffold for hard tissue engineering. J Mater Sci – Mater Med 2011;22:1195–203.
[187] Almeida RM, Gama A, Vueva Y. Bioactive sol–gel scaffolds with dual porosity for tissue engineering. J Sol–Gel Sci Technol 2011;57:336–42.
[188] Marques AC, Almeida RM, Thiema A, Wang S, Falk MM, Jain H. Sol–gel-derived glass scaffold with high pore interconnectivity and enhanced bioactivity. J Mater Res 2009;24:3495–502.
[189] Valerio P, Guimaraes MHR, Pereira MM, Leite MF, Goes AM. Primary osteoblast cell response to sol–gel derived bioactive glass foams. J Mater Sci – Mater Med 2005;16:851–6.
[190] Chen Q-Z, Thouas GA. Fabrication and characterization of sol–gel derived 45S5 Bioglass®-ceramic scaffolds. Acta Biomater 2011;7:3616–26.
[191] Jallot E, Lao J, John L, Soulie J, Moretto P, Nedelec JM. Imaging physicochemical reactions occurring at the pore surface in binary bioactive glass foams by micro ion beam analysis. ACS Appl Mater Interf 2010;2:1737–42.
[192] Yue S, Lee PD, Poologasundarampillai G, Yao ZZ, Rockett P, Devlin AH, et al. Synchrotron X-ray microtomography for assessment of bone tissue scaffolds. J Mater Sci – Mater Med 2010;21:847–53.
[193] Wang S, Jain H. High surface area nanomacroporous bioactive glass scaffold for hard tissue engineering. J Am Ceram Soc 2010;93:3002–5.
[194] Wang X, Li X, Ito A, Sogo Y. Synthesis and characterization of hierarchically macroporous and mesoporous CaO–MO–SiO_2–P_2O_5 (M = Mg, Zn, Sr) bioactive glass scaffolds. Acta Biomater 2011;7:3638–44.
[195] Minaberry Y, Jobbagy M. Macroporous bioglass scaffolds prepared by coupling sol–gel with freeze drying. Chem Mater 2011;23:2327–32.
[196] Jones JR, Ahir S, Hench LL. Large-scale production of 3D bioactive glass macroporous scaffolds for tissue engineering. J Sol–Gel Sci Technol 2004;29:179–88.
[197] Fu Q, Saiz E, Rahaman MN, Tomsia AP. Bioactive glass scaffolds for bone tissue engineering: state of the art and future perspectives. Mater Sci Eng, C 2011;31:1245–56.
[198] Fu Q, Saiz E, Tomsia AP. Bioinspired strong and highly porous glass scaffolds. Adv Funct Mater 2011;21:1058–63.
[199] Fu Q, Saiz E, Tomsia AP. Direct ink writing of highly porous and strong glass scaffolds for load-bearing bone defects repair and regeneration. Acta Biomater 2011;7:3547–54.
[200] Doiphode ND, Huang T, Leu MC, Rahaman MN, Day DE. Freeze extrusion fabrication of 13–93 bioactive glass scaffolds for bone repair. J Mater Sci – Mater Med 2011;22:515–23.
[201] Huang TS, Rahaman MN, Doiphode ND, Leu MC, Bal BS, Day DE, et al. Porous and strong bioactive glass (13–93) scaffolds fabricated by freeze extrusion technique. Mater Sci Eng, C 2011;31:1482–9.
[202] Kolan KCR, Leu MC, Hilmas GE, Brown RF, Velez M. Fabrication of 13–93 bioactive glass scaffolds for bone tissue engineering using indirect selective laser sintering. Biofabrication 2011;3:025004.
[203] Wu C, Luo Y, Cuniberti G, Xiao Y, Gelinsky M. Three-dimensional printing of hierarchical and tough mesoporous bioactive glass scaffolds with a controllable pore architecture, excellent mechanical strength and mineralization ability. Acta Biomater 2011;7:2644–50.
[204] Yun HS, Kim SE, Hyeon YT. Design and preparation of bioactive glasses with hierarchical pore networks. Chem Commun 2007;2139–41.
[205] Garcia A, Izquierdo-Barba I, Colilla M, de Laorden CL, Vallet-Regi M. Preparation of 3-D scaffolds in the SiO_2–P_2O_5 system with tailored hierarchical meso-macroporosity. Acta Biomater 2011;7:1265–73.
[206] Rezwan K, Chen QZ, Blaker JJ, Boccaccini AR. Biodegradable and bioactive porous polymer/inorganic composite scaffolds for bone tissue engineering. Biomaterials 2006;27:3413–31.

[207] Lu HH, El-Amin SF, Scott KD, Laurencin CT. Three-dimensional, bioactive, biodegradable, polymer-bioactive glass composite scaffolds with improved mechanical properties support collagen synthesis and mineralization of human osteoblast-like cells in vitro. J Biomed Mater Res Part A 2003;64A:465–74.
[208] Niemela T, Niiranen H, Kellomaki M, Tormala P. Self-reinforced composites of bioabsorbable polymer and bioactive glass with different bloactive glass contents. Part 1: Initial mechanical properties and bioactivity. Acta Biomater 2005;1:235–42.
[209] Maquet V, Boccaccini AR, Pravata L, Notingher I, Jerome R. Porous poly(alpha-hydroxyacid)/Bioglass® composite scaffolds for bone tissue engineering. I: Preparation and in vitro characterisation. Biomaterials 2004;25:4185–94.
[210] Blaker JJ, Maquet V, Jerome R, Boccaccini AR, Nazhat SN. Mechanical properties of highly porous PDLLA/Bioglass® composite foams as scaffolds for bone tissue engineering. Acta Biomater 2005;1:643–52.
[211] Peter M, Binulal NS, Nair SV, Selvamurugan N, Tamura H, Jayakumar R. Novel biodegradable chitosan-gelatin/nano-bioactive glass ceramic composite scaffolds for alveolar bone tissue engineering. Chem Eng J 2010;158:353–61.
[212] Xu C, Su P, Chen X, Meng Y, Yu W, Xiang AP, et al. Biocompatibility and osteogenesis of biomimetic Bioglass-collagen-phosphatidylserine composite scaffolds for bone tissue engineering. Biomaterials 2011;32:1051–8.
[213] Chen QZ, Boccaccini AR. Poly(D,L-lactic acid) coated 45S5 Bioglass®-based scaffolds: processing and characterization. J Biomed Mater Res Part A 2006;77A:445–57.
[214] Bretcanu O, Chen Q, Misra SK, Boccaccini AR, Roy I, Verne E, et al. Biodegradable polymer coated 45S5 Bioglass-derived glass-ceramic scaffolds for bone tissue engineering. Glass Technol – Eur J Glass Sci Technol Part A 2007;48:227–34.
[215] Blaker JJ, Bismarck A, Boccaccini AR, Young AM, Nazhat SN. Premature degradation of poly(alpha-hydroxyesters) during thermal processing of Bioglass®-containing composites. Acta Biomater 2010;6:756–62.
[216] Eglin D, Mortisen D, Alini M. Degradation of synthetic polymeric scaffolds for bone and cartilage tissue repairs. Soft Matter 2009;5:938–47.
[217] Maquet V, Boccaccini AR, Pravata L, Notingher I, Jerome R. Preparation, characterization, and in vitro degradation of bioresorbable and bioactive composites based on Bioglass®-filled polylactide foams. J Biomed Mater Res Part A 2003;66A:335–46.
[218] Misra SK, Ansari T, Mohn D, Valappil SP, Brunner TJ, Stark WJ, et al. Effect of nanoparticulate bioactive glass particles on bioactivity and cytocompatibility of poly(3-hydroxybutyrate) composites. J R Soc Interf 2010;7:453–65.
[219] Fantner GE, Rabinovych O, Schitter G, Thurner P, Kindt JH, Finch MM, et al. Hierarchical interconnections in the nano-composite material bone: fibrillar cross-links resist fracture on several length scales. Compos Sci Technol 2006;66:1205–11.
[220] Hunter GK, Goldberg HA. Modulation of crystal-formation by bone phosphoproteins – role of glutamic acid-rich sequences in the nucleation of hydroxyapatite by bone sialoprotein. Biochem J 1994;302:175–9.
[221] Marelli B, Ghezzi CE, Mohn D, Stark WJ, Barralet JE, Boccaccini AR, et al. Accelerated mineralization of dense collagen-nano bioactive glass hybrid gels increases scaffold stiffness and regulates osteoblastic function. Biomaterials 2011;32:8915–26.
[222] Bruggeman JP, de Bruin BJ, Bettinger CJ, Langer R. Biodegradable poly(polyol sebacate) polymers. Biomaterials 2008;29:4726–35.
[223] Liang SL, Cook WD, Chen QZ. Physical characterization of poly(glycerol sebacate)/Bioglass® composites. Polymer Int 2012;61:17–22.
[224] Liang XH, Yang DJ, Hu J, Hao XM, Gao JR, Maoi ZY. Hypoxia inducible factor-1alpha expression correlates with vascular endothelial growth factor-C expression and lymphangiogenesis/angiogenesis in oral squamous cell carcinoma. Anticancer Res 2008;28:1659–66.
[225] Novak BM. Hybrid nanocomposite materials – between inorganic glasses and organic polymers. Adv Mater 1993;5:422–33.
[226] Valliant EM, Jones JR. Softening bioactive glass for bone regeneration: sol–gel hybrid materials. Soft Matter 2011;7:5083–95.
[227] Mahony O, Tsigkou O, Ionescu C, Minelli C, Hanly R, Ling L, et al. Silica-gelatin hybrids with tailorable degradation and mechanical properties for tissue regeneration. Adv Funct Mater 2010;20:3835–45.
[228] Jones JR. New trends in bioactive scaffolds: the importance of nanostructure. J Eur Ceram Soc 2009;29:1275–81.
[229] Iler RK. The chemistry of silica: solubility, polymerization, colloid and surface properties and biochemistry of silica. New York: Wiley-Interscience; 1979.
[230] Allo BA, Rizkalla AS, Mequanint K. Synthesis and electrospinning of epsilon-polycaprolactone-bioactive glass hybrid biomaterials via a sol–gel process. Langmuir 2010;26:18340–8.
[231] Pereira MM, Jones JR, Orefice RL, Hench LL. Preparation of bioactive glass-polyvinyl alcohol hybrid foams by the sol–gel method. J Mater Sci – Mater Med 2005;16:1045–50.
[232] Gomide VS, Zonari A, Ocarino NM, Goes AM, Serakides R, Pereira MM. In vitro and in vivo osteogenic potential of bioactive glass-PVA hybrid scaffolds colonized by mesenchymal stem cells. Biomed Mater 2012;7. http://dx.doi.org/10.1088/1748-6041/7/1/015004.
[233] Tsuru K, Aburatani Y, Yabuta T, Hayakawa S, Ohtsuki C, Osaka A. Synthesis and in vitro behavior of organically modified silicate containing Ca ions. J Sol–Gel Sci Technol 2001;21:89–96.
[234] Tsuru K, Hayakawa S, Osaka A. Synthesis of bioactive and porous organic–inorganic hybrids for biomedical applications. J Sol–Gel Sci Technol 2004;32:201–5.
[235] Yabuta T, Bescher EP, Mackenzie JD, Tsuru K, Hayakawa S, Osaka A. Synthesis of PDMS-based porous materials for biomedical applications. J Sol–Gel Sci Technol 2003;26:1219–22.
[236] Ren L, Tsuru K, Hayakawa S, Osaka A. Novel approach to fabricate porous gelatin-siloxane hybrids for bone tissue engineering. Biomaterials 2002;23:4765–73.
[237] Rhee SH, Choi JY, Kim HM. Preparation of a bioactive and degradable poly(epsilon-caprolactone)/silica hybrid through a sol–gel method. Biomaterials 2002;23:4915–21.
[238] Rhee SH, Lee YK, Lim BS. Evaluation of a novel poly(epsilon-caprolactone)-organosiloxane hybrid material for the potential application as a bioactive and degradable bone substitute. Biomacromolecules 2004;5:1575–9.
[239] O'Brien FJ, Harley BA, Yannas IV, Gibson L. Influence of freezing rate on pore structure in freeze-dried collagen-GAG scaffolds. Biomaterials 2004;25:1077–86.
[240] Richard A, Margaritis A. Poly(glutamic acid) for biomedical applications. Crit Rev Biotechnol 2001;21:219–32.
[241] Shih IL, Van YT, Yeh LC, Lin HG, Chang YN. Production of a biopolymer flocculant from *Bacillus licheniformis* and its flocculation properties. Bioresour Technol 2001;78:267–72.
[242] Poologasundarampillai G, Ionescu C, Tsigkou O, Murugesan M, Hill RG, Stevens MM, et al. Synthesis of bioactive class II poly(gamma-glutamic acid)/silica hybrids for bone regeneration. J Mater Chem 2010;20:8952–61.
[243] Poologasundarampillai G, Yu B, Tsigkou O, Valliant EM, Yue S, Lee PD, et al. Bioactive silica–poly(γ-glutamic acid) hybrids for bone regeneration: effect of covalent coupling on dissolution and mechanical properties and fabrication of porous scaffolds. Soft Matter 2012;8:4822–32.
[244] Yang B, Li XY, Shi SA, Kong XY, Guo G, Huang MJ, et al. Preparation and characterization of a novel chitosan scaffold. Carbohydr Polym 2010;80:860–5.
[245] Shirosaki Y, Tsuru K, Hayakawa S, Osaka A, Lopes MA, Santos JD, et al. Physical, chemical and in vitro biological profile of chitosan hybrid membrane as a function of organosiloxane concentration. Acta Biomater 2009;5:346–55.
[246] Shirosaki Y, Tsuru K, Hayakawa S, Osaka A, Lopes MA, Santos JD, et al. In vitro cytocompatibility of MG63 cells on chitosan-organosiloxane hybrid membranes. Biomaterials 2005;26:485–93.
[247] Shirosaki Y, Okayama T, Tsuru K, Hayakawa S, Osaka A. Synthesis and cytocompatibility of porous chitosan-silicate hybrids for tissue engineering scaffold application. Chem Eng J 2008;137:122–8.
[248] Pereira MM, Jones JR, Hench LL. Bioactive glass and hybrid scaffolds prepared by sol–gel method for bone tissue engineering. Adv Appl Ceram 2005;104:35–42.
[249] Pereira MM, Clark AE, Hench LL. Calcium-phosphate formation on sol–gel-derived bioactive glasses in-vitro. J Biomed Mater Res 1994;28:693–8.
[250] Ramila A, Balas F, Vallet-Regi M. Synthesis routes for bioactive sol–gel glasses: alkoxides versus nitrates. Chem Mater 2002;14:542–8.
[251] Poologasundarampillai G, Yu B, Jones JR, Kasuga T. Electrospun silica/PLLA hybrid materials for skeletal regeneration. Soft Matter 2011;7:10241–51.
[252] Manzano M, Arcos D, Delgado MR, Ruiz E, Gil FJ, Vallet-Regi M. Bioactive star gels. Chem Mater 2006;18:5696–703.
[253] Vallet-Regi M, Salinas AJ, Arcos D. From the bioactive glasses to the star gels. J Mater Sci – Mater Med 2006;17:1011–7.
[254] Ashley CE, Carnes EC, Phillips GK, Padilla D, Durfee PN, Brown PA, et al. The targeted delivery of multicomponent cargos to cancer cells by nanoporous particle-supported lipid bilayers. Nat Mater 2011;10:389–97.
[255] Brunner TJ, Grass RN, Stark WJ. Glass and bioglass nanopowders by flame synthesis. Chem Commun 2006;13:1384–86.
[256] Mohn D, Zehnder M, Imfeld T, Stark WJ. Radio-opaque nanosized bioactive glass for potential root canal application: evaluation of radiopacity, bioactivity and alkaline capacity. Int Endodont J 2010;43:210–7.
[257] Vallet-Regi M, Balas F, Arcos D. Mesoporous materials for drug delivery. Angew Chem – Int Ed 2007;46:7548–58.
[258] Hong Z, Luz GM, Hampel PJ, Jin M, Liu A, Chen X, et al. Mono-dispersed bioactive glass nanospheres: preparation and effects on biomechanics of mammalian cells. J Biomed Mater Res Part A 2010;95A:747–54.
[259] Luz GM, Mano JF. Preparation and characterization of bioactive glass nanoparticles prepared by sol–gel for biomedical applications. Nanotechnology 2011;22:494014.
[260] Curtis AR, West NX, Su B. Synthesis of nanobioglass and formation of apatite rods to occlude exposed dentine tubules and eliminate hypersensitivity. Acta Biomater 2010;6:3740–6.
[261] Roohani-Esfahani SI, Nouri-Khorasani S, Lu ZF, Appleyard RC, Zreiqat H. Effects of bioactive glass nanoparticles on the mechanical and biological behavior of composite coated scaffolds. Acta Biomater 2011;7:1307–18.
[262] Doostmohammadi A, Monshi A, Salehi R, Fathi MH, Golniya Z, Daniels AU. Bioactive glass nanoparticles with negative zeta potential. Ceram Int 2011;37:2311–6.
[263] Yun HS, Kim SH, Lee S, Song IH. Synthesis of high surface area mesoporous bioactive glass nanospheres. Mater Lett 2010;64:1850–3.
[264] Ostomel TA, Shi QH, Tsung CK, Liang HJ, Stucky GD. Spherical bioactive glass with enhanced rates of hydroxyapatite deposition and hemostatic activity. Small 2006;2:1261–5.
[265] Pirhonen E, Niiranen H, Niemela T, Brink M, Tormala P. Manufacturing, mechanical characterization, and in vitro performance of bioactive glass 13–93 fibers. J Biomed Mater Res Part B 2006;77B:227–33.

[266] Stevens MM, George JH. Exploring and engineering the cell surface interface. Science 2005;310:1135–8.
[267] Doshi J, Reneker DH. Electrospinning process applications of electrospun fibers. J Electrostat 1995;35:151–60.
[268] Reneker DH, Chun I. Nanometre diameter fibres of polymer, produced by electrospinning. Nanotechnology 1996;7:216–23.
[269] Lu H, Zhang T, Wang XP, Fang QF. Electrospun submicron bioactive glass fibers for bone tissue scaffold. J Mater Sci – Mater Med 2009;20:793–8.
[270] Hong YL, Chen XS, Jing XB, Fan HS, Gu ZW, Zhang XD. Fabrication and drug delivery of ultrathin mesoporous bioactive glass hollow fibers. Adv Funct Mater 2010;20:1501–10.
[271] Lee E-J, Teng S-H, Jang T-S, Wang P, Yook S-W, Kim H-E, et al. Nanostructured poly(epsilon-caprolactone)-silica xerogel fibrous membrane for guided bone regeneration. Acta Biomater 2010;6:3557–65.
[272] Kim IA, Rhee S-H. Effects of poly(lactic-co-glycolic acid) (PLGA) degradability on the apatite-forming capacity of electrospun PLGA/SiO_2-CaO nonwoven composite fabrics. J Biomed Mater Res Part B 2010;93B:218–26.
[273] Lovett M, Lee K, Edwards A, Kaplan DL. Vascularization strategies for tissue engineering. Tissue Eng Part B 2009;15:353–70.
[274] Gorustovich AA, Roether JA, Boccaccini AR. Effect of bioactive glasses on angiogenesis: a review of in vitro and in vivo evidences. Tissue Eng Part B 2010;16:199–207.
[275] Grunewald M, Avraham I, Dor Y, Bachar-Lustig E, Itin A, Yung S, et al. VEGF-induced adult neovascularization: recruitment, retention, and role of accessory cells. Cell 2006;124:175–89.
[276] Day RM, Boccaccini AR, Shurey S, Roether JA, Forbes A, Hench LL, et al. Assessment of polyglycolic acid mesh and bioactive glass for soft-tissue engineering scaffolds. Biomaterials 2004;25:5857–66.
[277] Day RM. Bioactive glass stimulates the secretion of angiogenic growth factors and angiogenesis in vitro. Tissue Eng 2005;11:768–77.
[278] Keshaw H, Forbes A, Day RM. Release of angiogenic growth factors from cells encapsulated in alginate beads with bioactive glass. Biomaterials 2005;26:4171–9.
[279] Leach JK, Kaigler D, Wang Z, Krebsbach PH, Mooney DJ. Coating of VEGF-releasing scaffolds with bioactive glass for angiogenesis and bone regeneration. Biomaterials 2006;27:3249–55.
[280] Leu A, Leach JK. Proangiogenic potential of a collagen/bioactive glass substrate. Pharmaceutical Res 2008;25:1222–9.
[281] Aguirre A, Gonzalez A, Planell JA, Engel E. Extracellular calcium modulates in vitro bone marrow-derived Flk-1(+) CD34(+) progenitor cell chemotaxis and differentiation through a calcium-sensing receptor. Biochem Biophys Res Commun 2010;393:156–61.
[282] Gerhardt L-C, Widdows KL, Erol MM, Burch CW, Sanz-Herrera JA, Ochoa I, et al. The pro-angiogenic properties of multi-functional bioactive glass composite scaffolds. Biomaterials 2011;32:4096–108.
[283] Leu A, Stieger SM, Dayton P, Ferrara KW, Leach JK. Angiogenic response to bioactive glass promotes bone healing in an irradiated calvarial defect. Tissue Eng Part A 2009;15:877–85.
[284] Day RM, Maquet V, Boccaccini AR, Jerome R, Forbes A. In vitro and in vivo analysis of macroporous biodegradable poly(D,L-lactide-co-glycolide) scaffolds containing bioactive glass. J Biomed Mater Res Part A 2005;75A:778–87.
[285] Choi HY, Lee JE, Park HJ, Oum BS. Effect of synthetic bone glass particulate on the fibrovascularization of porous polyethylene orbital implants. Ophthalmic Plastic Recon Surg 2006;22:121–5.
[286] Tsigkou O, Pomerantseva I, Spencer JA, Redondo PA, Hart AR, O'Doherty E, et al. Engineered vascularized bone grafts. PNAS 2010;107:3311–6.
[287] Semenza GL. Life with oxygen. Science 2007;318:62–4.
[288] Peters K, Schmidt H, Unger RE, Kamp G, Prols F, Berger BJ, et al. Paradoxical effects of hypoxia-mimicking divalent cobalt ions in human endothelial cells in vitro. Mol Cell Biochem 2005;270:157–66.
[289] Azevedo MM, Jell G, O'Donnell MD, Law RV, Hill RG, Stevens MM. Synthesis and characterization of hypoxia-mimicking bioactive glasses for skeletal regeneration. J Mater Chem 2010;20:8854–64.
[290] Wu C, Zhou Y, Fan W, Han P, Chang J, Yuen J, et al. Hypoxia-mimicking mesoporous bioactive glass scaffolds with controllable cobalt ion release for bone tissue engineering. Biomaterials 2012;33:2076–85.
[291] Stoor P, Soderling E, Salonen JI. Antibacterial effects of a bioactive glass paste on oral microorganisms. Acta Odontol Scand 1998;56:161–5.
[292] Munukka E, Lepparanta O, Korkeamaki M, Vaahtio M, Peltola T, Zhang D, et al. Bactericidal effects of bioactive glasses on clinically important aerobic bacteria. J Mater Sci – Mater Med 2008;19:27–32.
[293] Zhang D, Lepparanta O, Munukka E, Ylanen H, Viljanen MK, Eerola E, et al. Antibacterial effects and dissolution behavior of six bioactive glasses. J Biomed Mater Res Part A 2010;93A:475–83.
[294] Bellantone M, Coleman NJ, Hench LL. Bacteriostatic action of a novel four-component bioactive glass. J Biomed Mater Res 2000;51:484–90.
[295] Bellantone M, Williams HD, Hench LL. Broad-spectrum bactericidal activity of Ag_2O-doped bioactive glass. Antimicrob Agents Chemother 2002;46:1940–5.
[296] El-Kady AM, Ali AF, Rizk RA, Ahmed MM. Synthesis, characterization and microbiological response of silver doped bioactive glass nanoparticles. Ceram Int 2012;38:177–88.
[297] Waltimo T, Brunner TJ, Vollenweider M, Stark WJ, Zehnder M. Antimicrobial effect of nanometric bioactive glass 45S5. J Dent Res 2007;86:754–7.
[298] Ahmed AA, Ali AA, Mahmoud DAR, El-Fiqi AM. Preparation and characterization of antibacterial P_2O_5–CaO–Na_2O–Ag_2O glasses. J Biomed Mater Res Part A 2011;98A:132–42.
[299] Oki A, Parveen B, Hossain S, Adeniji S, Donahue H. Preparation and in vitro bioactivity of zinc containing sol–gel-derived bioglass materials. J Biomed Mater Res Part A 2004;69A:216–21.
[300] Boyd D, Carroll G, Towler MR, Freeman C, Farthing P, Brook IM. Preliminary investigation of novel bone graft substitutes based on strontium-calcium-zinc-silicate glasses. J Mater Sci – Mater Med 2009;20:413–20.
[301] Saino E, Grandi S, Quartarone E, Maliardi V, Galli D, Bloise N, et al. In vitro calcified matrix deposition by human osteoblasts onto a zinc-containing bioactive glass. Eur Cells Mater 2011;21:59–72.
[302] Oh S-A, Kim S-H, Won J-E, Kim J-J, Shin US, Kim H-W. Effects on growth and osteogenic differentiation of mesenchymal stem cells by the zinc-added sol–gel bioactive glass granules. J Tissue Eng 2011;2010:475260.
[303] Aina V, Perardi A, Bergandi L, Malavasi G, Menabue L, Morterra C, et al. Cytotoxicity of zinc-containing bioactive glasses in contact with human osteoblasts. Chem-Biol Interact 2007;167:207–18.
[304] Bonnelye E, Chabadel A, Saltel F, Jurdic P. Dual effect of strontium ranelate: stimulation of osteoblast differentiation and inhibition of osteoclast formation and resorption in vitro. Bone 2008;42:129–38.
[305] Gentleman E, Fredholm YC, Jell G, Lotfibakhshaiesh N, O'Donnell MD, Hill RG, et al. The effects of strontium-substituted bioactive glasses on osteoblasts and osteoclasts in vitro. Biomaterials 2010;31:3949–56.
[306] Fredholm YC, Karpukhina N, Brauer DS, Jones JR, Law RV, Hill RG. Influence of strontium for calcium substitution in bioactive glasses on degradation, ion release and apatite formation. J R Soc Interf 2012;9:880–9.
[307] Fredholm YC, Karpukhina N, Law RV, Hill RG. Strontium containing bioactive glasses: glass structure and physical properties. J Non-Cryst Solids 2010;356:2546–51.
[308] Xiang Y, Du JC. Effect of strontium substitution on the structure of 45S5 Bioglasses. Chem Mater 2011;23:2703–17.
[309] Gorustovich AA, Steimetz T, Cabrini RL, Lopez JMP. Osteoconductivity of strontium-doped bioactive glass particles: a histomorphometric study in rats. J Biomed Mater Res Part A 2010;92A:232–37.
[310] O'Donnell MD, Hill RG. Influence of strontium and the importance of glass chemistry and structure when designing bioactive glasses for bone regeneration. Acta Biomater 2010;6:2382–5.
[311] Lao J, Jallot E, Nedelec J-M. Strontium-delivering glasses with enhanced bioactivity: a new biomaterial for antiosteoporotic applications? Chem Mater 2008;20:4969–73.
[312] Hesaraki S, Gholami M, Vazehrad S, Shahrabi S. The effect of Sr concentration on bioactivity and biocompatibility of sol–gel derived glasses based on CaO–SrO–SiO_2–P_2O_5 quaternary system. Mater Sci Eng, C 2010;30:383–90.
[313] Lao J, Nedelec JM, Jallot E. New strontium-based bioactive glasses: physicochemical reactivity and delivering capability of biologically active dissolution products. J Mater Chem 2009;19:2940–9.
[314] Isaac J, Nohra J, Lao J, Jallot E, Nedelec JM, Berdal A, et al. Effects of strontium-doped bioactive glass on the differentiation of cultured osteogenic cells. Eur Cells Mater 2011;21:130–43.
[315] Yue S, Lee PD, Poologasundarampillai G, Jones JR. Evaluation of 3-D bioactive glass scaffolds dissolution in a perfusion flow system with X-ray microtomography. Acta Biomater 2011;7:2637–43.